AN ULTRACENTRIFUGE STUDY OF SELF-ASSOCIATING PROTEIN SYSTEMS

by

David John Fennell, B.Sc.

Thesis presented for the degree of
Doctor of Philosophy

in the Department of Physical and Inorganic Chemistry
University of Adelaide

1971

CONTENTS

SUMMARY

A study has been made, at alkaline pH, of α-chymotrypsin and zinc-free insulin using ultracentrifuge methods. The initial aim of this research was to test the various theories available for the analysis of the concentration dependent molecular weight curves of self-associating protein systems.

The results of a preliminary sedimentation velocity study of α-chymotrypsin are reported. The $S^{o}_{20,w}$ value, obtained by extrapolation of the corrected sedimentation coefficients to zero concentration, was used to compare the empirical equations of Atassi and Gandhi[75] with those of Halsall[76]. The subsequent sedimentation equilibrium experiments using 3mm solution columns did not give interlacing molecular weight versus concentration curve segments. It is shown that the non-interlacing was not due to curve fitting methods applied to the data. A simple photometric attachment for facilitating measurement of interference fringe photographs and specifically designed to eliminate personal bias was developed. The construction and operation of this device is reported.

Sedimentation equilibrium experiments using 1mm columns of α-chymotrypsin were carried out at $5^{o}C$ and $20^{o}C$, each experiment yielding a single molecular weight. The molecular weight versus concentration data were analyzed by the methods of Steiner[17,18] and of Adams[20-27].

Anhydro-α-chymotrypsin was prepared in order to overcome autolysis which was suspected as a possible cause for non-interlacing. Experiments with α-chymotrypsin were discontinued when molecular weight curve segments obtained from sedimentation equilibrium experiments on 3mm columns of anhydro-α-chymotrypsin failed to interlace.

The results of sedimentation equilibrium experiments on 3mm columns of zinc-free insulin are reported. The molecular weight curve segments did not interlace. Since interlacing of molecular weight curve segments is essential for the application of the analytical theories for simple self-association, the aim of this thesis was altered towards finding an explanation of the non-interlacing.

The control experiments and methods used to test for possible optical and mechanical effects are reported. The effect of change of concentration by adsorption of the protein on cell walls and other surfaces is discussed. Sedimentation velocity and equilibrium experiments were performed to test for a pressure dependent self-association. The results clearly show that no such effect operates for zinc-free insulin under the conditions used. Precautions were taken to prevent leaching of heavy metal ions from glassware and cell walls.

It was concluded that the non-interlacing was due to a complex self-association and the results for zinc-free insulin were analyzed for the specific type of complex system to which the Haschemeyer and Bowers[124] theory applies. Application of

the theory, which is specific for self-associating systems containing some incompetent material but having at least one fully competent species, indicated that the zinc-free insulin system was not of this type. Other types of complex self-associations are discussed.

This thesis contains no material previously submitted for a degree or diploma in any University and, as far as the author is aware, contains no material written by another person, except when due reference is made in the text.

ACKNOWLEDGEMENTS

I wish to thank Dr. J. H. Coates for the interest he has shown in this work and for many helpful discussions.

I am grateful to the Commonwealth of Australia and the University of Adelaide for financial assistance.

I wish to thank Lorraine Howlett for her care in typing this thesis.

Finally I wish to acknowledge with thanks the encouragement and the sacrifices of my parents which made everything possible.

D.J.F.

Department of Physical and Inorganic Chemistry,
The University of Adelaide.

September, 1971.

Chapter 1

INTRODUCTION

A wide variety of substances undergo reversible association reactions which do not involve the formation of covalent bonds. Possibly the largest class of reactions of this type are the self-association reactions in which molecules of the same compound interact to form dimers, trimers and higher polymers. Self-association reactions may be further broken down into (i) dimerisation reactions as observed for carboxylic acids and nucleosides[1], (ii) association to a larger definite n-mer involving multiple equilibria with different association constants and (iii) association of an indefinite number of monomers involving equilibria with equal association constants as in the case of micelle formation[2] or the stacking of planar molecules such as dyes[3], purine bases and pyrimidine bases[4].

The recognition that many biologically important materials undergo self-association aroused much speculation as to the implications that could be drawn about the mode of action in living cells. In particular, protein chemists were interested in the relative biological activities of the monomeric and polymeric species since, if the polymeric species had reduced or zero activity, this effect could supply a simple method of control of reactions in vivo[5,6]. That the explanation is not necessarily so simple was shown by the findings that urease was more active as

the monomer[7] whereas beef liver L-glutamate dehydrogenase was more active as the tetramer[8] and that even crystalline ribonuclease retains some activity[9]. More recently the research of Monod and co-workers[10,11] demonstrated that many aspects of cellular control mechanisms and the regulation of enzymic activity could operate on a molecular level by allosteric inhibition. This type of reaction, however, belongs to the class of reactions involving association between an enzyme and a small molecule effector, the enzyme always being composed of several subunits.

In the broad study of the biological implications of self-association it is necessary to consider the type of bonding which occurs between the associating molecules and the conditions which promote the associations. It is known that most protein self-association reactions are dependent on such conditions as pH, ionic strength, temperature and specific nature of the medium (e.g. presence of urea or detergents) as well as the concentration of the protein itself[12]. The type of bonds postulated to account for the association include hydrogen bonds, hydrophobic bonds and electrostatic bonds[12]. In addition, the covalent disulphide bond has also been invoked to explain some associations. In order to determine the type of forces which promote association it is necessary to collate information about the thermodynamics of the reaction in different media. Since one of the manifestations of association is a change in weight average properties, such as molecular weight, as a function of concentration[13], a study of such changes

provides one method of approach to the understanding of the problem of association.

The more commonly used methods for determination of molecular weights of proteins (e.g. osmometry and light scattering) have the disadvantage that only a single value of molecular weight is determined at a single concentration in each experiment. For this reason it is rapidly becoming routine procedure to use the sedimentation equilibrium technique, since the molecular weight may be determined over a range of concentrations in each experiment. Also the method stands up to rigorous thermodynamic requirements[14]. Prior to 1960 the ultracentrifuge was used mainly for sedimentation velocity experiments and, although the theory of the method lacked the thermodynamic basis of the sedimentation equilibrium technique, important information could be obtained about the relative rates of association and dissociation and about the mode of association. This was possible due to the theoretical work of Gilbert[15,16,71] who applied chromatographic principles to the problem of mass transport in a centrifugal field. The theory is qualitative rather than quantitative due to the number of assumptions required. Used in conjunction, however, the two ultracentrifuge techniques provide a powerful means of studying self-association reactions.

At the commencement of the study reported in this thesis the only method of analysis of molecular weight data for

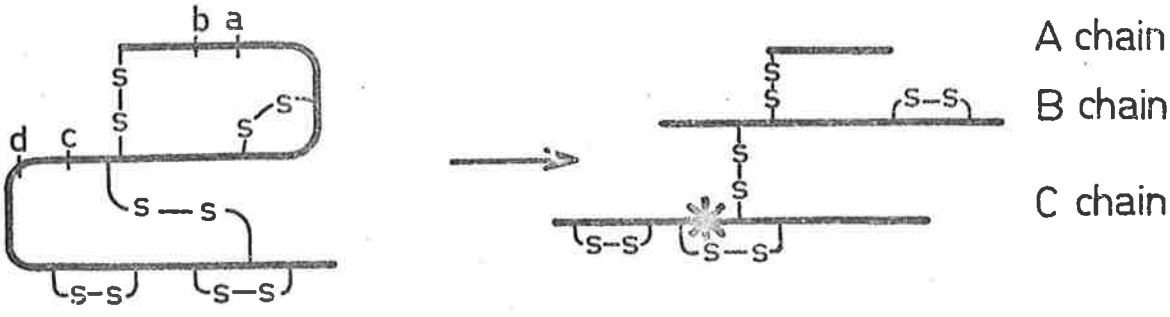

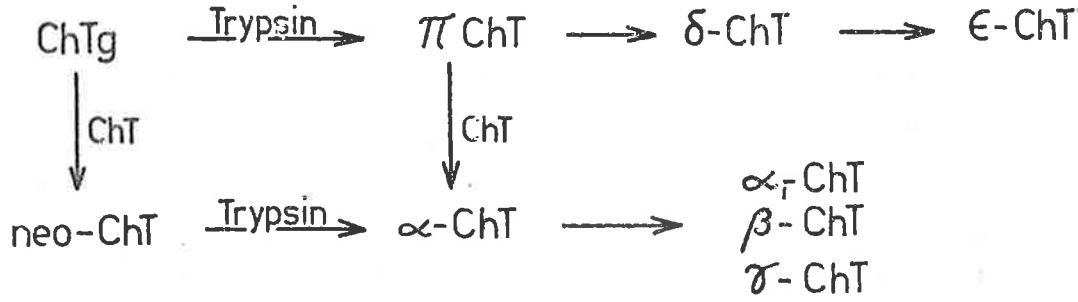

Cleavage	Enzyme	Enzyme Product
a	Trypsin	π- ChT
a + b	ChT (b)	δ - ChT
a,b,c + d	ChT (b,c,d)	α- ChT
c &/or d	ChT	neo-ChT

Fig. 1.1 Activation of Chrymotrypsinogen A
* marks the serine residue which participates in the active site.

equilibrium constants was that due to Steiner[17,18] and only Jeffrey[19] and Adams[20] had used this theory in conjunction with the sedimentation equilibrium technique. The Steiner method could only be applied to ideal solutions which could be assumed for most cases where dilute, isoelectric protein solutions were used. The theory of Adams and co-workers[21-27] provided a general approach since it included a non-ideality factor. This thesis reports the application of ultracentrifuge techniques, and available theoretical treatments of the data, to the self-association of the proteins α-chymotrypsin and insulin.

α-Chymotrypsin is one of a family of proteolytic enzymes that arise from the activation of the pancreatic zymogen chymotrypsinogen A. The zymogen appears to be a single chain polypeptide cross-linked by five disulphide bridges [28,29] and is activated according to the scheme shown in Fig. 1.1 . α-Chymotrypsin is formed by elimination of two dipeptides and is therefore unusual in that it consists of three polypeptide chains linked by disulphide bridges.

There is evidence[30] that the serine residue marked in Fig. 1.1 is involved in the active site and that catalysis depends on the acylation of this group[31]. A large number of papers have been published on the catalytic action of α-chymotrypsin and the relation of this evidence to the active site has been reviewed by many authors (see for example Knowles[31]

and Niemann[32]). The role of the active site in self-association is not clear as evidence both for and against participation of the active site has been published.[33-36]

Evidence for the self-association of α-chymotrypsin has come from ultracentrifugation,[37-45] electrophoresis,[42,47] light scattering,[44,46] depolarization of fluorescence,[43] viscometry and diffusion.[29] In each case the experimental data show a concentration dependence consistent with an increase in molecular weight with increase in concentration from zero to 1 gm/100 mls (1%). Rao and Kegeles[45] concluded that, since no other isoelectric proteins displayed a similar concentration dependence of molecular weight, the trend in the data was due to self-association. Most of the ultracentrifuge experiments[37-46] employed the sedimentation velocity technique and showed that in the concentration range 0-1% the molecular weight increased as the pH decreased from the isoelectric point and as the ionic strength decreased. Since these trends are opposite to those shown by insulin[48,49] it is likely that the mechanism of self-association is different in these two cases. Rao and Kegeles[47] used the Archibald approach to equilibrium method, obtaining results consistent with the presence of monomers, dimers and trimers in equilibrium, whereas previous experiments had only implied the monomer-dimer equilibrium.

Insulin is a pancreatic protein hormone which plays a vital role in the control of glucose concentration in the bloodstream.

Because of its importance in the treatment of diabetes, insulin has been widely studied and in particular the amino acid sequence[50] and three dimensional structure[61] have been determined. Insulin consists of two polypeptide chains, the shorter A chain, of 21 amino acid units, and the longer B chain, of 30 amino acid units. There is an intrachain disulphide link between the A6 and A11 units and interchain links between A7 and B7 and between A20 and B19. The molecular weight of this molecule is 5733 a.w.u.

For some time there was uncertainty about the monomer molecular weight of insulin in acid solution; some workers obtained a value of approximately 12,000 from such techniques as sedimentation velocity,[51] light scattering[17] and osmotic pressure[52] whereas other workers obtained a value of 6,000 from the same techniques.[53,54,55] There was also uncertainty about the number and nature of species present, three different workers proposing different self-association schemes.[56,57,17] However, Jeffrey and Coates[49] demonstrated that these uncertainties could be overcome by use of the sedimentation equilibrium technique with analysis of the data by Steiner's[17,18] method.

No similar study had been carried out on insulin in alkaline solution. This system is complicated by the strong binding of zinc above pH 6[58] and the greatly enhanced association in the presence of zinc. The association was shown[59] by sedimentation velocity measurements to be increased by increasing zinc content

over the range of zinc content 0-1%. Fredericq[59] and Marcker[52] had worked with zinc-free insulin and had found the self-association behaviour to be different from that of zinc insulin but no quantitative analysis of the data was presented. Kakiuchi[60] showed that analysis of sedimentation equilibrium data for α-amylase dimerisation, in which zinc played a stoichiometric part, was complex and required knowledge of the stoichiometry of the reaction. Thus it was considered that the self-association of zinc-free insulin in basic solution would not only be simpler to study but would be more readily compared with Jeffrey's results with zinc-free insulin in acid solution.

Chapter 2

THEORY REVIEW

Goldberg[14] laid the foundation of the sedimentation equilibrium technique as a powerful analytical method when he provided a rigorous thermodynamic treatment of a system at sedimentation equilibrium. The system was treated in terms of a continuous sequence of phases of fixed volume and infinitesimal depth in the direction of the centrifugal field and, by application of the condition that the total potential of a component is uniform throughout the system at thermodynamic equilibrium, he was able to derive the equation

$$M_i(1 - \bar{v}_i^{(x)}\rho^{(x)})\,\omega^2 x\,dx = \sum_{k=1}^{r}\left(\frac{\partial \mu_i}{\partial c_k}\right)_{T,P,c_{j\neq k}}^{(x)} dc_k^{(x)} \qquad 2(1)$$

$$i = 0,\ 1,\ \ldots\ldots\ r$$

where component i has the molecular weight M_i, chemical potential μ_i and partial specific volume $\bar{v}_i$, x is the distance from the axis of rotation, ω is the angular velocity and ρ is the density of the solution. The subscripts i = 1,2,.....r refer to the solute species and the superscript (x) refers to the value of the designated quantity at a distance x from the axis of rotation. The concentration c_i is on a weight per volume scale.

For a non-ideal system 2(1) becomes

$$M_i(1 - \bar{v}_i^{(x)}\rho^{(x)})\omega^2 x dx = RT\, d\ln c_i^{(x)}$$

$$+ RT \sum_{k=1}^{r} \left(\frac{\partial \ln \gamma_i}{\partial c_k}\right)_{T,P,c_j}^{(x)} dc_k^{(x)} \qquad 2(2)$$

If ρ and $\bar{v}_i$ are assumed to be independent of x and it is assumed that $\bar{v}$ is the same for all solutes, then equation 2(2) can be summed over all solutes to give

$$\frac{(1 - \bar{v}\rho)\omega^2}{2RT} \cdot \frac{d(x^2)}{d\ln c^{(x)}} = \frac{1}{M_w^{(x)}}$$

$$+ \frac{c^{(x)}}{M_w^{(x)}} \sum_{i,k=1}^{r} \frac{c_i^{(x)}}{c} \left(\frac{\partial \ln \gamma_i}{\partial c_k}\right)_{T,P,c_j}^{(x)} \frac{dc_k^{(x)}}{dc}$$

where $c = \sum_{i=1}^{r} c_i$ and $M_w^{(x)} = \dfrac{\sum_{i=1}^{r} c_i^{(x)} M_i}{\sum_{i=1}^{r} c_i^{(x)}}$ .....2(3)

This can be expressed in the form

$$\frac{1}{M_{w\ app}^{(x)}} = \frac{1}{M_w^{(x)}} + Bc^{(x)} \qquad 2(4)$$

where $M_{w\ app}^{(x)} = \dfrac{2RT}{(1 - \bar{v}\rho)\omega^2} \cdot \dfrac{d\ln c^{(x)}}{d(x^2)}$ 2(5)

and the subscript "app" refers to the fact that it is an apparent molecular weight because it contains a non-ideality contribution. Since the weight average molecular weight M_w is a function of the total concentration c in a self-associating system (none of the species can be varied independently), equation 2(4) implies that $M_{w\ app}$ is a unique function of c (i.e. there is a 1:1 correspondence between $M_{w\ app}$ and c). Under certain conditions[24], however, this may not be true.

A Rayleigh interference pattern at sedimentation equilibrium gives the refractive index j as a function of the distance x from the axis of rotation and by suitable mathematical treatment $\frac{d\ln j}{d(x^2)}$ can be obtained as a function of x. For most proteins it is found empirically that the refractive index is directly proportional to the concentration expressed on a weight per volume scale[62]. This was assumed to be the case for α-chymotrypsin and insulin so that it was possible to write

$$\frac{d\ln j^{(x)}}{d(x^2)} = \frac{d\ln c^{(x)}}{d(x^2)}$$

Thus equation 2(5) becomes

$$M^{(x)}_{w\ app} = \frac{2RT}{(1 - \bar{v}\rho)\omega^2} \cdot \frac{d\ln j^{(x)}}{d(x^2)} \qquad 2(6)$$

and from this relation the apparent molecular weight, as a function of concentration, is obtained.

For an ideal, homogeneous, non-associating system the graph of lnj against x^2 is a straight line and the molecular weight is obtained from the slope. In the case of a non-ideal self-associating system the graph of lnj against x^2 is curved, depending on the extent of deviation from ideal character and degree of self-association. A graph which is concave upwards indicates polydispersity whereas one which is concave downwards indicates non-ideality[63]. In order to derive an expression for $\frac{d\ln j}{d(x^2)}$ as a function of x^2, the dependence of lnj upon x^2 ($x^2 = \bar{x}$) is usually expressed as a series expansion

$$\ln j = a + b\bar{x} + c\bar{x}^2$$

The method used to obtain this relationship and $\frac{d\ln j}{d(x^2)}$ is described in Chapter 5.

During sedimentation equilibrium the initially homogeneous (with respect to concentration) solution is redistributed under the influence of sedimentation and diffusion so that at equilibrium there is only one point in the cell where the concentration is unchanged. If this point is known, then $\frac{d\ln j}{d(x^2)}$ can be measured at this point and the molecular weight evaluated at the initial protein concentration without the need to measure the whole j versus x distribution. Van Holde and Baldwin[64] showed that the position at which the concentration (c) equalled the initial concentration (c_0) could be approximated if

the experimental conditions were arranged so that there was only a slight redistribution of protein. They showed that the error in setting $c = c_o$ at position $x' = [\frac{1}{2}(x_m^2 + x_b^2)]^{\frac{1}{2}}$ was within 0.2% when $H < 0.1$ where x_m and x_b are the distances from the axis of rotation of the solution column meniscus and bottom respectively and $H = \frac{M(1 - \bar{v}\rho)\omega^2}{2RT} \cdot \frac{b^2 - a^2}{2}$. The correct speed can then be calculated provided an approximate molecular weight is known. This method was used in the investigation of the α-chymotrypsin self-association described in Chapter 3.

The first theoretical treatment of the sedimentation equilibrium of self-associating systems was reported by Tiselius[65] but he did not show how the data could be analyzed. It was Steiner[17,18] who first developed a method of treatment of molecular weight versus concentration data which yielded equilibrium constants. This procedure which was developed for an ideal, uncharged system is outlined below.

If the molar concentration of species i is denoted by $[A_i]$ then the various self-association reactions which may occur (up to the tetramer) are

$$2[A_1] \underset{}{\overset{k_2}{\rightleftharpoons}} [A_2]$$

$$[A_1] + [A_2] \overset{k_3}{\rightleftharpoons} [A_3]$$

$$[A_1] + [A_3] \overset{k_4}{\rightleftharpoons} [A_4]$$

$$2[A_2] \overset{k_4'}{\rightleftharpoons} [A_4]$$

The equilibrium constants (k_i) for the reactions and the $[A_i]$ in terms of k_i and $[A_1]$ can then be written as

$$k_2 = \frac{[A_2]}{[A_1]^2} \quad , \quad [A_2] = k_2[A_1]^2$$

$$k_3 = \frac{[A_3]}{[A_2]\,[A_1]} \quad , \quad [A_3] = k_2k_3[A_1]^3$$

$$k_4 = \frac{[A_4]}{[A_3]\,[A_1]} \quad ,$$

$$[A_4] = k_2k_3k_4[A_1]^4$$

$$k_4' = \frac{[A_4]}{[A_2]^2} \quad ,$$

The weight average molecular weight which is defined by

$$M_w = \frac{\sum_i n_i M_i^2}{\sum_i n_i M_i}$$

can be rewritten as

$$M_w = \frac{[A_1]M_1^2 + 4[A_2]M_1^2 + 9[A_3]M_1^2 + 16[A_4]M_1^2}{c} \qquad 2(7)$$

where M_1 is the monomer molecular weight and c is the total weight concentration of all species. Substitution of expressions for $[A_i]$, i 1 in 2(7) and division by M_1 gives

$$\frac{M_w}{M_1} = \alpha = \frac{1}{c/M_1}\left([A_1] + 4k_2[A_1]^2 + 9k_2k_3[A_1]^3 + 16k_2k_3k_4[A_1]^4\right)$$

..... 2(8)

The weight fraction of monomer is defined as

$$f = \frac{c_1}{c} = \frac{M_1[A_1]}{c}$$

and substitution for $[A_1]$ in 2(8) yields

$$\alpha = \frac{1}{c/M_1}\left[\left(\frac{fc}{M_1}\right) + 4k_2\left(\frac{fc}{M_1}\right)^2 + 9k_2k_3\left(\frac{fc}{M_1}\right)^3 + 16k_2k_3k_4\left(\frac{fc}{M_1}\right)^4\right] \quad \ldots\ldots\ldots 2(9)$$

But

$$\frac{c}{M_1} = \left[\left(\frac{fc}{M_1}\right) + 2k_2\left(\frac{fc}{M_1}\right)^2 + 3k_2k_3\left(\frac{fc}{M_1}\right)^3 + 4k_2k_3k_4\left(\frac{fc}{M_1}\right)^4\right]$$

and therefore

$$\alpha = \left(\frac{fc}{M_1}\right) \cdot \frac{d\left(\frac{c}{M_1}\right)}{d\left(\frac{fc}{M_1}\right)} \cdot \frac{1}{c/M_1} = f\,\frac{dc}{d(fc)}$$

$$\therefore \quad \alpha^{-1} - 1 = \frac{d\ln f}{d\ln c}$$

which on integration gives

$$\ln\left(\frac{f}{f_0}\right) = \int_{c_0}^{c} \frac{\alpha^{-1}-1}{c}\,dc \qquad 2(10)$$

where f and f_0 are the weight fractions of monomer at concentrations $c = c$ and $c = c_0$ respectively. When $c_0 = 0$, $f_0 = 1$ and it is possible to get an accurate function of f versus c by numerical integration of 2(10) since $\alpha = \frac{M_w}{M_1}$ is

obtained experimentally as a function of c.

Rearrangement of 2(9) gives

$$\varepsilon = 1 + 4k_2\gamma + 9k_2k_3\gamma^2 + 16k_2k_3k_4\gamma^3 \qquad 2(11)$$

where $\varepsilon = \frac{\alpha}{f}$ and $\gamma = \frac{fc}{M_1} = [A_1]$. Thus in 2(11) the only unknowns are the equilibrium constants k_i. Steiner put forward a graphical method of solution of equation 2(11) which was used until the general availability of modern high-speed computers permitted the application of curve fitting methods which provided more accurate solutions with less time and labour. The way in which a computer was used to solve equations of this type is discussed in Chapter 3.

In an ideal non-associating system the apparent molecular weight is unchanged with change in concentration. If non-ideality occurs it is manifest as a decreasing apparent molecular weight with increasing concentration. On the other hand, in an ideal self-associating system, apparent molecular weight increases with increasing concentration, and non-ideality appears as an initial increase to a maximum apparent molecular weight with a subsequent decrease at higher concentrations. While the Steiner method of analysis is suitable for the many self-associating protein systems which behave ideally it is not adequate for the systems which behave non-ideally. It was not until 1963 that Adams and co-workers[21-27] in a series of

publications developed a satisfactory method of analysis of non-ideal self-associating systems. The method can be applied to discrete self-association (limited to four or five species) or with modifications to indefinite self-association where all equilibrium constants are equal. An outline of the Adams procedure for discrete monomer-dimer-trimer association is given below.

The Adams procedure requires an estimate of the degree of association that is present, then for n species, n + 1 equations are written down, one for each species present plus one for the non-ideal behaviour. Combination of the equations in a suitable manner enables the elimination of the equilibrium constants so that an equation in one unknown, the virial coefficient B, is obtained. The equation is solved by successive approximations and all other unknowns can then be calculated.

The basic starting equation is obtained by multiplication of equation 2(4) by M_1 to give

$$\frac{M_1}{M_{w\ app}} = \frac{M_1}{M_w} + BM_1c \qquad 2(12)$$

This form of the equation is used because it is assumed initially, that the activity coefficient for each species y_i can be represented by

$$\ln y_i = iBM_1c + O(c^2) \qquad i = 2,3 \ldots \qquad 2(13)$$

where $O(c^2)$ indicates that terms of the order c^2 and higher are negligible. It follows from 2(13) that

$$c_j = K_j c_1^{\,j} \qquad j = 2,3,.... \qquad 2(14)$$

and since $c = \sum_{i=1}^{n} c_i$ application of 2(14) in the case of monomer-dimer-trimer association gives

$$c = c_1 + K_2 c_1^{\,2} + K_3 c_1^{\,3} \qquad 2(15)$$

Since the Adams equations are developed using a weight per volume scale of concentration (rather than molar) as well as overall equilibrium constants $(K_i = \prod_{j=2}^{i} k_j)$ the Steiner equation 2(8) becomes

$$\frac{cM_w}{M_1} = (c_1 + 2K_2 c_1^{\,2} + 3K_3 c_1^{\,3}) \qquad 2(16)$$

Furthermore the weight fraction of monomer calculated is an apparent value (f_a) since the apparent weight average molecular weight is used in the calculation

$$\ln f_a = \int_0^c \left(\frac{M_1}{M_{w\ app}} - 1\right) \frac{dc}{c} = \ln f + BM_1 c \qquad 2(17)$$

This equation on rearrangement gives

$$c_1 = \alpha \exp(-BM_1 c) \qquad 2(18)$$

where $\alpha = f_a c$. It is also possible to show that

$$\frac{cM_1}{M_{n\ app}} = \int_0^c \frac{M_1}{M_{w\ app}}\,dc = c_1 + \frac{K_2 c_1^2}{2} + \frac{K_3 c_1^3}{3} + \frac{BM_1 c^2}{2} \qquad 2(19)$$

where the number average molecular weight, M_n, is defined by

$$M_n = \frac{\sum_i n_i M_i}{\sum_i n_i} = \frac{c}{\sum_i c_i / M_i}$$

and the apparent number average molecular weight, $M_{n\ app}$, is given by

$$\frac{1}{M_{n\ app}} = \frac{1}{M_n} + BM_1 c$$

Rearrangement of equation 2(12) and comparison with 2(16) gives

$$\frac{cM_w}{M_1} = \frac{1}{\frac{M_1}{cM_{w\ app}} - BM_1} = c_1 + 2K_2 c_1^2 + 3K_3 c_1^3 \qquad 2(20)$$

It is possible, by combination of equations 2(15) and 2(20) and equations 2(15) and 2(19), to obtain two equations in which the $K_3 c_1^3$ term has been eliminated and which, in turn can be combined to give an equation in which the $K_2 c_1^2$ term has been eliminated. This final equation contains only one unknown (BM_1)

$$\frac{6cM_1}{M_{n\ app}} - 5c = 2\alpha \exp(-BM_1 c) + 3BM_1 c^2 - \frac{1}{\frac{M_1}{cM_{w\ app}} - BM_1} \qquad 2(21)$$

The method of successive approximations is then used to choose a value of BM_1 such that the left and right hand sides of equation 2(21) are equal. The manner in which this procedure was modified and applied is shown in Chapter 3. A similar approach to the above is used for the case of monomer-dimer-trimer-tetramer association except that an extra equation is required.

The Steiner theory is limited to ideal systems but a more critical limitation is the graphical procedure for determination of equilibrium constants since this involved the drawing of limiting slopes. The latter difficulty has been overcome by application of computerised curve fitting techniques. One advantage of the theory is that it can be used with number or weight average molecular weights, thus allowing determination of equilibrium constants by independent methods e.g. osmotic pressure (M_n) and light scattering (M_w).

The Adams theory provides a unified theory applicable to ideal and non-ideal systems. At the same time it establishes a functional relationship between M_n and M_w (see equation 2(19)) and provides equations to distinguish between discrete and indefinite self-associations. There are, however, some limitations. The theory requires integration and differentiation of fitted curves and the integrals and differentials depend to some extent on the manner of fitting the curves. An initial guess at the form of the self-association is required in order to choose which equation to solve for BM_1. The analysis of

discrete self-associations is limited to systems with a maximum of five species since n + 1 equations are required for a system with n species. It is possible that the theory in the form presented will be insufficient to differentiate between discrete and indefinite self-associations[27]. This may be due to the use of one virial coefficient in equation 2(13) which may be modified to include two virial coefficients.

$$\ln y_i = iB_1M_1c + iB_2M_1c^2 + O(c^3) \qquad 2(22)$$

Such an extension to the theory has been made[23] and applied with success[66]. In spite of the disadvantages listed above the Adams theory is probably the most widely applied theory in use.

More recently two different approaches to the treatment of self-associating systems have been advanced by Derechin[67], and by Roark and Yphantis[68] with modifications by Chun and Kim[69]. The latter treatment first suggested by Roark and Yphantis is a graphical method which is applicable only when two or three species are present and may be applied whether or not the species are in self-association equilibrium. Thus this method is severely limited in the range of systems to which it may be applied and it appears that the main area in which it will find use is in analysis of non-associating mixtures of two or three proteins.

The theory proposed by Derechin, however, is an elegant, general method based on the multinomial theorem. The initial

approach to the problem is similar to that of Adams except that the function F(c), defined by

$$F(c) = \frac{M_1 c}{M_n} = \int_0^c \frac{M_1}{M_w}\, dc = \sum_{i=1}^{m} \frac{K_i}{i}\, c_1^{\,i}$$

is expanded in powers of c by Maclaurin's theorem to give

$$F(c) = \sum_{r=0}^{\alpha} \frac{1}{r} \left(\frac{d^{(r)}F}{dc^r} \right)_{c=0} \left[\sum_{i=1}^{m} K_i c_1^{\,i} \right]^r = \sum_{i=1}^{m} \frac{K_i}{i}\, c_1^{\,i}$$

The power term $\left[\sum_{i=1}^{m} K_i c_1^{\,i} \right]^r$ is then evaluated using the multinomial theorem and expressions for the equilibrium constants are obtained in terms of $\frac{M_1}{M_w}$ and c only. Thus there is no need to calculate the weight fraction of monomer as in the Steiner and Adams theories. Another advantage is the generality of the thenry since it can be applied equally as well to number average as to weight average molecular weight data. No iteration is required for the solution of the expressions for K_i which are equally valid for indefinite and discrete self-associating systems. The theory has also been extended to cope with non-ideality but it is necessary to assume the absence ofa particular species to solve for the non-ideality coefficient (i.e. $K_i = 0$ if species i is absent and the equation for K_i can be solved for the unknown BM_1).

The most serious disadvantage is the requirement of very accurate values of $\frac{M_1}{M_w}$ versus c at near zero concentrations since the expressions in K_i use the limiting slopes

$$\frac{d\left(\frac{M_1}{M_w}\right)}{dc}, \quad \frac{d^{(2)}\left(\frac{M_1}{M_w}\right)}{dc^2} \quad \text{etc.} \quad \text{at zero concentration.}$$

The multinomial theory may become more widely used as the accuracy of molecular weight data at low concentrations is improved but the Steiner and particularly the Adams theories supply the most generally applicable analyses of self-associating systems.

See Addenda p. 136.

Chapter 3

EXPERIMENTS WITH α-CHYMOTRYPSIN

I SEDIMENTATION VELOCITY STUDY

It is possible to detect reversible self-association of a protein in solution from the variation of sedimentation coefficient (S) with concentration (c). For non-associating proteins S values are usually linearly dependent on c such that the lines, which have a negative slope, can be described by equations of the form

$$S = S^{o}(1 - kc) \qquad \text{or} \qquad S = \frac{S^{o}}{1 + kc}$$

where S^{o} is the sedimentation coefficient at zero protein concentration and k is a positive constant. The dependence of sedimentation coefficient on concentration is governed by the viscosity and density of the solution and by the backward flow of the solvent[70]. In dilute solution of systems which undergo self-association reactions of the type

$$nP \rightleftharpoons P_n$$

one often observes weight average sedimentation coefficients which increase with concentration. The increase of S at low concentrations is presumed to be due to readjustment of the equilibrium to give rise to higher molecular weight species as concentration increases. Since (where the second moment

method is used) it is a weight average sedimentation coefficient that is measured, a greater proportion of higher molecular weight species causes an increased rate of sedimentation.

If adjustment of the equilibrium is slow compared with the rate of separation by sedimentation, separation of the n-mer from the monomer can be expected and two boundaries will be visible in the sedimentation pattern. In the case of rapid reversible equilibrium Gilbert's[71] theory predicts a single boundary for $n = 2$ but a bimodal boundary for all $n > 2$ regardless of the rate of adjustment of equilibrium. Cox[72] has shown by computer simulation techniques that the bimodal boundary is not apparent at low values of the equilibrium constant for the association and that the sedimentation boundary is asymmetric in all cases. For systems where there are more than two species in equilibrium e.g.

$$2P \rightleftharpoons P_2$$

$$P_2 + P \rightleftharpoons P_3 \qquad \text{etc.}$$

the situation is more complex. However, if the equilibria are rapid only a single boundary is usually observed[71].

Thus, whilst the sedimentation coefficients at different concentrations provide a simple test for association, little can be deduced about the form of the association from the boundary shapes. Thus sedimentation velocity should be considered only as a preliminary technique in the investigation of self-association.

Sedimentation velocity experiments on α-chymotrypsin were performed in 0.2 ionic strength, pH 6.2 phosphate buffer, also used by Rao and Kegeles. This buffer, in which the protein is isoelectric, was chosen in order to avoid complications due to charge effects. Sedimentation coefficients at 13 different concentrations of α-chymotrypsin were evaluated from the slopes of log x versus time plots in accordance with equation 5(2a). The slope used was that obtained by fitting a straight line to the points by the method of least squares. The sedimentation coefficients were converted to standard conditions, by use of equation 5(2b) and correspond to sedimentation in a solvent with the viscosity and density of water at 20^{o}C.

The corrected sedimentation coefficients ($S_{20,w}$), at various concentrations, are shown in Fig. 3.1 . The error bars were determined from the gradients of the lines which could be drawn with maximum and minimum slope through the log x versus t plots at each concentration. A smooth curve was drawn through the $S_{20,w}$ values to give, on extrapolation to zero concentration, a value of $S^{o}_{20,w}$ of 2.6 S in agreement with values quoted by other authors (Schwert[37,38] 2.4 S, Smith and Brown[40] 2.56 S, Massey et. al.[43] 2.9 S and Tinoco[44] 2.2 S).

Comparison of the experimental curve in Fig. 3.1 with curves obtained by other workers is difficult because of the dependence of the self-association on ionic strength and on pH. The variation of the isoelectric pH with the type of buffer

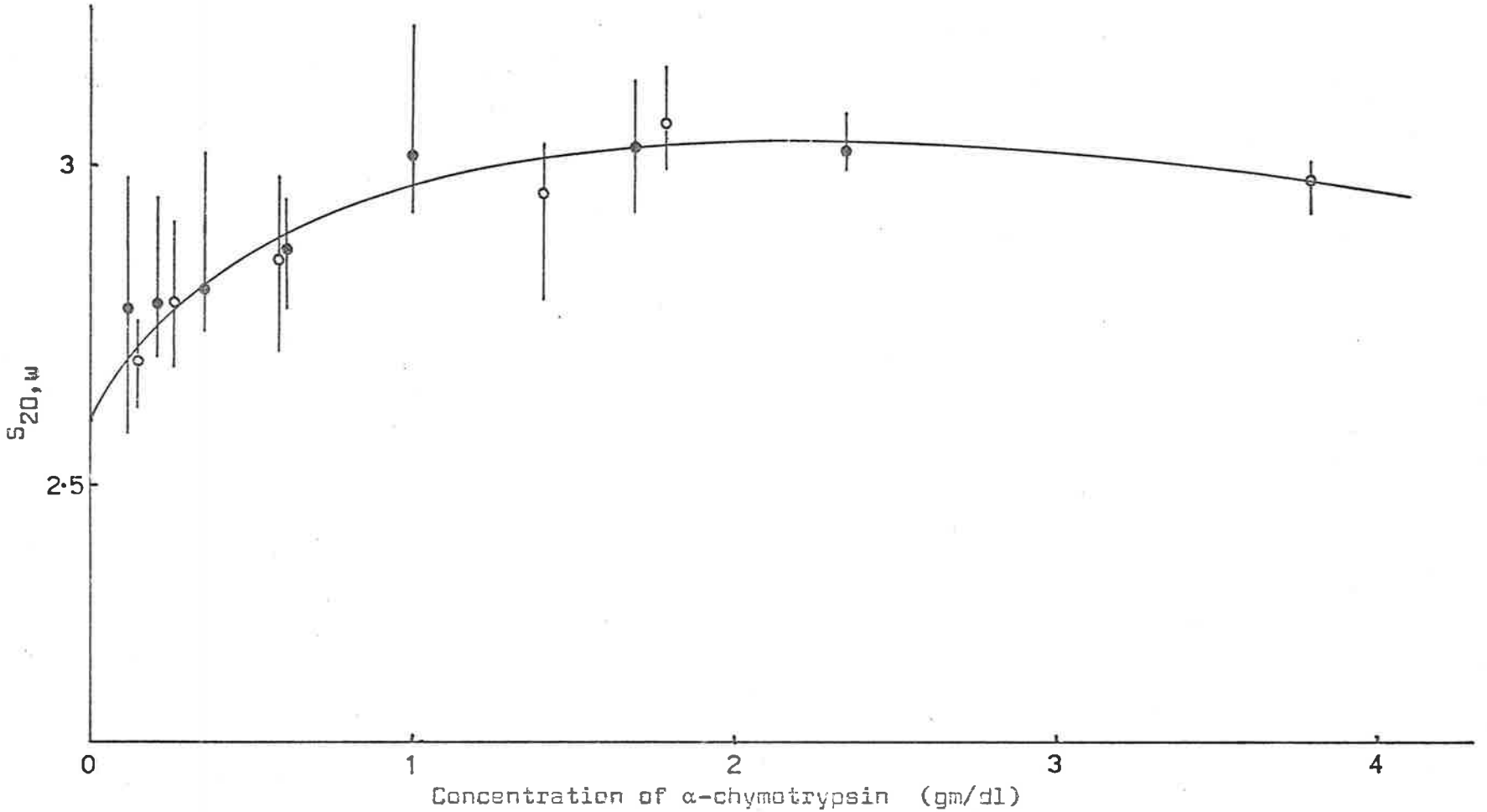

Fig. 3.1 : The corrected sedimentation coefficient of α-chymotrypsin as a function of concentration in phosphate buffer pH 6.2, I = 0.2 . The filled and open circles represent dilutions of two different stock solutions and the error bars were calculated as described in the text.

used is a further complication; for phosphate buffer at 0.2 ionic strength the isoelectric pH is 6.20[13] whereas with univalent buffer salts the isoelectric pH ranges from 8.6 at 0.01 ionic strength to 8.1 at 0.1 ionic strength[73]. The buffer used in experiments reported in Fig. 3.1 was similar to that of Schwert[37] who used a phosphate-sodium chloride buffer pH6.20 at 0.2 ionic strength. Schwert's graph of $S_{20,w}$ versus concentration showed an increase of $S_{20,w}$ in dilute solutions with a maximum at about 20 gm/litre, above which concentration the $S_{20,w}$ values decreased with increasing concentration. It is probable that the small differences between Schwert's curve and that shown in Fig. 3.1 is due to a combination of experimental error and charge effects since Schwert's system would not necessarily be at the isoelectric pH in the buffer used. The absence of a maximum in the $S_{20,w}$ curves reported by other workers is probably due to the greater association of α-chymotrypsin at the lower ionic strengths which they used.

The curve shown in Fig. 3.1 is typical of that expected for a relatively simple self-association, showing an increase in $S_{20,w}$ values at low concentrations and reaching a maximum (at about 18 gm/litre) after which the $S_{20,w}$ values slowly decrease. The decrease of $S_{20,w}$ values at high concentrations can be explained in terms of solution viscosity and density, and backward flow of the solvent retarding the sedimentation of the species which predominate at the higher concentrations[70].

A typical schlieren photograph is shown in Fig. 3.2 . As expected for an associating system the boundary is not symmetrical but no bimodal nature is apparent. The self-association then, is probably not between protein monomer and n-mer with $n > 2$, and although the shape of the $S_{20,w}$ versus c curve is consistent with that expected for a monomer-dimer self-association, it is not possible to rule out monomer-dimer-trimer or monomer-dimer-trimer-tetramer self-associations. It was felt that the asymmetry of the boundary was not great enough to warrant the location and use of the second moment of the refractive index gradient curve in the calculation of the sedimentation coefficient, thus in all cases the maximum ordinate was used. Fig. 3.2 also illustrates the difference in schlieren patterns obtained at different concentrations and it is obvious, from the width of the peak at the lower concentration, why the errors associated with $S_{20,w}$ values are greatest in dilute solutions.

In general it is possible to obtain the monomer molecular weight of a protein from the $S^{o}_{20,w}$ value if the corresponding diffusion coefficient is known, these quantities being related by the Svedberg equation

$$M = \frac{RTS}{D(1 - \bar{v}\rho)}$$

However, in the case of globular proteins, which includes

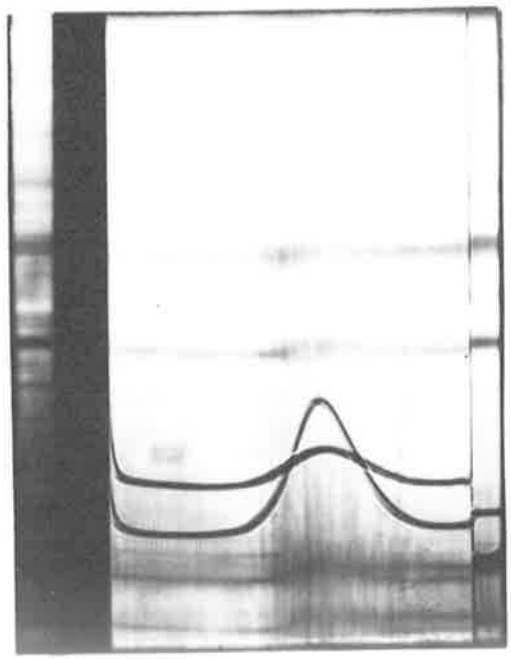

(a)

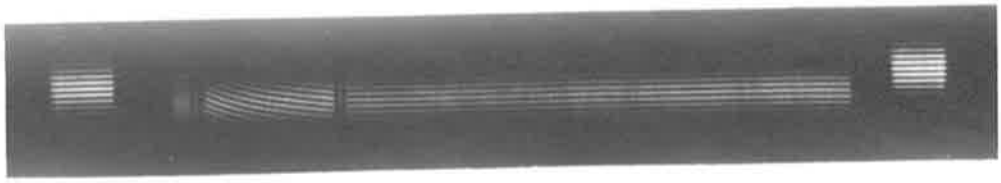

Reference fringes Solution fringes Reference fringes

(b)

Fig. 3.2 : (a) A typical schlieren photograph
(b) A typical Rayleigh interference

In both cases the centrifugal direction is from right to left.

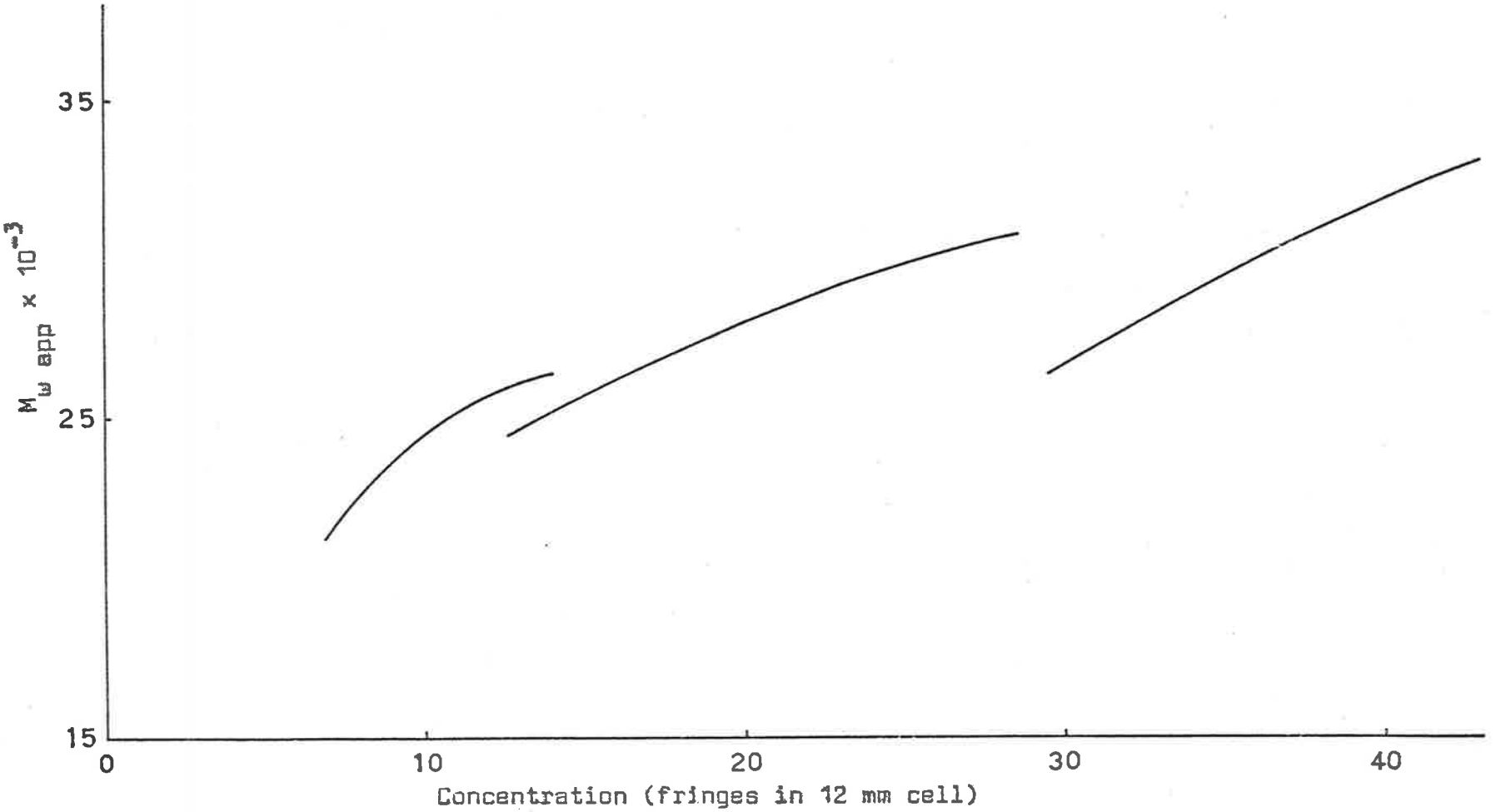

Fig. 3.3 : Apparent weight average molecular weight of α-chymotrypsin as a function of concentration in phosphate buffer at pH 6.2, I = 0.2, T = 20°C. The curves were obtained from three different sedimentation equilibrium experiments.

α-chymotrypsin[74], it is not necessary to know the diffusion coefficient as the molecular weight is related empirically to the sedimentation coefficient. Globular proteins are considered to be proteins for which the molar frictional coefficient f/f_o is less than or equal to 1.30 and since f/f_o depends on the solvation and asymmetry of a molecule it is a measure of the closeness of the molecular shape to a sphere. For a large number of globular proteins Atassi and Gandhi[75] showed that for $M > 40,000$, M and S^o were related by the equation

$$S^o = 1.62 + (4.170 \times 10^{-5})\ M \qquad 3(1)$$

and for $M < 30,000$ the relationship had the form

$$S^o = 0.68 + (7.416 \times 10^{-5})\ M \qquad 3(2)$$

They found also that proteins with molecular weights in the range 25,000 to 35,000 gave consistent results with both of these equations.

Halsall[76] later showed that the straight lines described by equations 3(1) and 3(2) were merely chords to a more general relationship between sedimentation coefficient and molecular weight. This is expressed[77,78] by

$$\frac{S[\eta]^{1/3}}{M^{2/3}} = 2.5 \times 10^6\ \frac{(1 - \bar{v}\rho)}{\eta_s N} \qquad 3(3)$$

where S is the sedimentation coefficient (in Svedbergs), $[\eta]$ is the intrinsic viscosity, η_s is the solvent viscosity, N is the Avagadro number, and the other symbols are as previously defined. Equation 3(3) can be rearranged with minor approximations to the form

$$S = kM^{2/3} \qquad 3(4)$$

or

$$\log S = \log k + \frac{2}{3} \log M \qquad 3(5)$$

Halsall plotted values of log S versus log M for a large number of globular proteins and fitted a straight line to the points by the method of least squares to give the equation

$$\log S = \bar{3}.383 \pm 0.044 + \frac{2}{3} \log M \qquad 3(6)$$

This general equation fitted globular proteins in the molecular weight range 17,000 to 49 x 10^6 whereas the equations of Atassi and Gandhi were not applicable below 9,000 or above 300,000. Halsall emphasized that the equation was necessarily approximate because the constant k implied assumptions about uniformity of hydration, density and shape.

When the molecular weight is calculated for α-chymotrypsin from equation 3(6) using $S^0_{20,w}$ = 2.6 S a value of 35,000 ± 5,000 is obtained. However, when the Atassi and Gandhi relations 3(1) and 3(2) are used molecular weights of 23,500 and 25,900 respectively are obtained. Since the molecular weight of

α-chymotrypsin is about 24,000[79] it is concluded that the empirical equations of Atassi and Gandhi are more accurate within the ranges specified than the more general equation of Halsall which for low molecular weights is subject to very large errors.

II PRELIMINARY SEDIMENTATION EQUILIBRIUM EXPERIMENTS

Three sedimentation equilibrium experiments were performed at different initial concentrations of α-chymotrypsin in phosphate buffer pH 6.2 and 0.2 ionic strength. The apparent weight average molecular weights ($M_{w\ app}$) calculated at different positions in the cell are shown as functions of concentration in Fig. 3.3 . The $M_{w\ app}$ values were evaluated by fitting a quadratic function to the lnj versus x^2 data by the method of least squares as described in Chapter 5. A typical Rayleigh interference photograph is shown in Fig. 3.2(b).

Two features of the curves illustrated in Fig. 3.3 require comment. Firstly the magnitude of $M_{w\ app}$ at the lowest concentration (6 fringes) is 21,000 implying a monomer molecular weight much lower than the accepted value of about 24,000[79]. Secondly, since the curves do not interlace, they are not segments of a unique molecular weight versus concentration curve expected for simple association of a pure macromolecular substance.

α-chymotrypsin is a protease and as such is prone to autolysis. It is apparent from the molecular weight data that there was material present with molecular weight less than that of the monomer and it is simplest to attribute this to products of autolysis. The presence of such material could also give rise to non-interlacing of the curves.

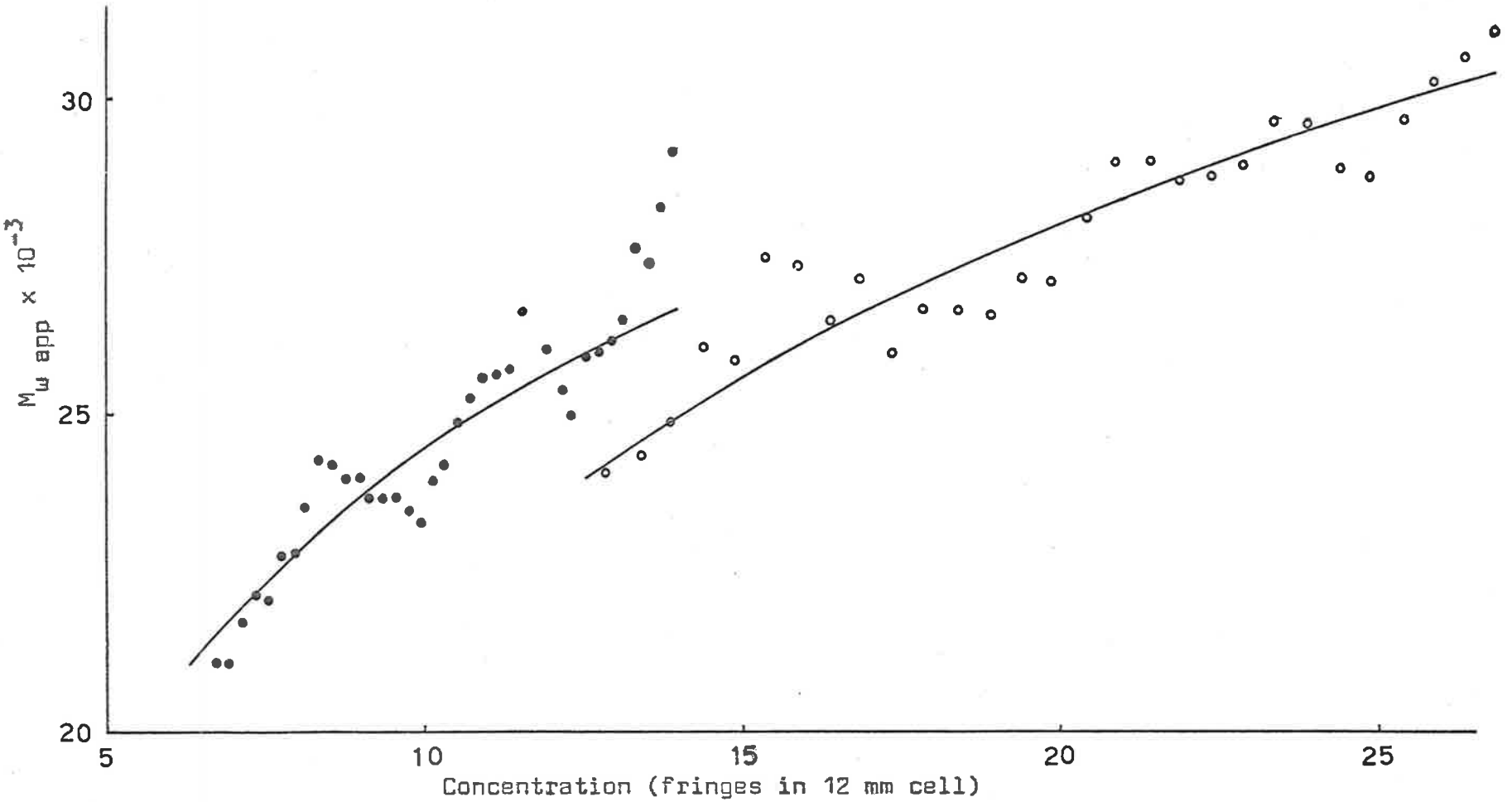

Fig. 3.4 : Apparent weight average molecular weight of α-chymotrypsin as a function of concentration in phosphate buffer at pH 6.2, I = 0.2, T = 20°C. The filled and open circles were obtained by differentiation of lnj versus x^2 data by the Mean Value Theorem. The curves were obtained by analytical differentiation of fitted curves.

Results similar to the non-interlacing of molecular weight curves described here, had previously been noted by workers using both the sedimentation equilibrium[19,20,80] and the Archibald approach to sedimentation equilibrium[13] techniques. Rao and Kegeles[13] found that molecular weight values for α-chymotrypsin, evaluated at the top and at the bottom of the cell during approach to sedimentation equilibrium experiments, showed time dependent behaviour. The values from the top of the cell decreased with increasing time while values from the bottom of the cell increased. Thus, as time increased, the molecular weights evaluated lay farther away from the smooth curve drawn through the values obtained soon after the start of the experiment. This behaviour was presumed to be due to the finite rate of re-equilibration between monomers and polymers. Obviously this reasoning does not apply to a system at sedimentation equilibrium. Squire and Li ascribed the non-interlacing to experimental error in measurement of schlieren patterns, as such errors were not random, a bias regarding the centre of the schlieren image was retained from point to point. Adams did not put forward an explanation of the discontinuities observed in his study of insulin but believed it was a real effect on the basis of the observations of the workers mentioned above. Jeffrey, who also worked with insulin, concluded that the effect was due to experimental error in the fringe measurements and the treatment of the data.

This conclusion was based on the fact that the observed non-interlacing in curves, obtained by least squares fitting of lnj versus x^2 data and subsequent termwise differentiation, fell within experimental error. Jeffrey also found that interlacing of the curves was obtained when a Fourier series fitting of the lnj versus x^2 data was used.

To test the influence of the curve fitting technique on the molecular weight values the Mean Value Theorem was applied to the raw data and the results are shown in Fig. 3.4 . The molecular weight as a function of concentration was evaluated using the equation

$$M_{w\ app} = \frac{2RT}{(1 - \bar{v}\rho)\,\omega^2} \cdot \frac{\Delta \ln j}{\Delta x^2} \qquad 3(7)$$

where

$$\Delta \ln j = (\ln j)_{i+4} - (\ln j)_i$$

$$\Delta x^2 = (x^2)_{i+4} - (x^2)_i$$

and $M_{w\ app}$ applies to the concentration given by

$$\text{antilog}\ \tfrac{1}{2}[(\ln j)_{i+4} + (\ln j)_i] \approx (j)_{i+2}$$

It was expected that this method of treating the data would

lead to scatter of values. However, in spite of the scatter it appears that the trend of the molecular weight values is described well by those obtained from the differential of the polynomial fitted to lnj versus x^2 data. It appeared that the method of treating the data was not the cause of the non-interlacing of the molecular weight versus concentration curves. The oscillating nature of the scatter was thought to be due to personal bias in locating the centres of interference fringes.

The molecular weight of lysozyme was determined to test the experimental methods and the optical system which could give rise to incorrect molecular weight values if out of alignment. Sigma brand three-times-crystallized, dialysed and lyophilized lysozyme was dissolved in pH 5.4 acetate-KCl buffer (0.15M KCl and 0.02M acetate) and dialysed against several changes of buffer. The concentration was determined by differential refractometry and two sedimentation equilibrium experiments were carried out at 20^{o}C and a speed of 10,000 rpm. The lnj versus x^2 plots obtained from measurement of the Rayleigh interference patterns at equilibrium were linear and the slopes determined by a linear least squares fit of the data gave an apparent molecular weight of $13,600 \pm 100$.

At pH 5.4 the net charge on lysozyme is about +6.5[81] and therefore the apparent weight average molecular weight determined at finite concentration is given by[82]

$$M_{w\ app} = \frac{M_P \left[1 - \frac{Z}{2}\frac{M_B}{M_P} \cdot \frac{(1 - \bar{v}_B\rho)}{(1 - \bar{v}_P\rho)}\right]\left[1 - \frac{Z}{2}\frac{M_B}{M_P}\frac{\theta_B}{\theta_P}\right]}{1 + \frac{Z^2}{2}\frac{M_B}{M_P}\frac{c_P}{c_B}} \qquad 3(8)$$

where the subscripts B and P refer to the supporting (1:1) electrolyte and protein respectively. The quantities θ_B and θ_P are the specific refractive increments and Z is the charge on the polyelectrolyte. Equation 3(8) applies at every point in the ultracentrifuge cell but for small correction terms it is probably valid to substitute the over-all concentrations and the molecular weight obtained by integration over the cell[81]. The supporting electrolyte was assumed to be entirely KCl and the value of M_P evaluated from equation 3(8) by substituting the following values:

$M_B = 74.56$

$\rho = 1.00617 + 0.00291\ c_P = 1.007$ ..... (Ref. 81)

$\bar{v}_P = 0.703$ ..... (Ref. 81)

$\theta_P = 0.1888$ ml/gm ..... (Ref. 83)

$\theta_B = 0.1475$ ml/gm ..... (Ref. 84)

$$\bar{v}_B = \frac{v^o + S_v\ c}{M_B} = \frac{26.81 + 2.327\ .15}{74.86} \qquad \text{..... (Ref. 85)}$$

$= 0.372$

$Z = +6.5$ .... (Refs. 81 and 83)

The calculated value of M_p = 14,350 ± 100 agreed with the value 14,540 ± 100 obtained by Sophianopoulos et. al.[81] thus discounting technical error and optical misalignment as causes of the low molecular weight values found for α-chymotrypsin.

The stock solutions of α-chymotrypsin were kept frozen and dilute solutions were prepared on the day of the sedimentation equilibrium experiments in order to minimise autolysis. However, it is concluded from the results shown in Figs. 3.3 and 3.4 that these precautions were not successful and that autolysis occurred resulting in the unexpectedly low values of molecular weight and possibly the non-interlacing of the molecular weight curves as well.

III ELECTROPHORESIS OF α-CHYMOTRYPSIN

Moving boundary electrophoresis experiments were carried out in Tris buffer pH 7.0 and 0.1 ionic strength at protein concentrations approximately 0.5 gm/dl. The schlieren boundary patterns obtained for Sigma and Worthington α-chymotrypsins are shown in Fig. 3.5 (a) and (b) and for PMS-α-chymotrypsin (Sigma) in Fig. 3.5 (c). Electrophoretic heterogeneity was evident in all cases, a major peak flanked on either side by a minor peak being observed.

According to the findings of Gilbert[15,16,71] and Winzor and Scheraga[86] the behaviour observed could result from a system with two forms (monomer and n-mer, $n > 2$) in rapid equilibrium. However, since similar behaviour was not observed in sedimentation velocity experiments it was concluded that the minor peaks were due either to protein impurities unrelated to α-chymotrypsin or to differently charged forms of α-chymotrypsin. The proportion of the impurities present, found by comparison of the areas under the peaks, was less for Worthington than for Sigma α-chymotrypsin indicating that the former should be used in preference to the latter for subsequent experiments. Inhibited α-chymotrypsin was prepared but the proportions of impurities present were not significantly less than in the uninhibited samples. In the inhibition process, both the α-chymotrypsin and inhibited protein were subjected to molecular sieve chromatography, the

(a)

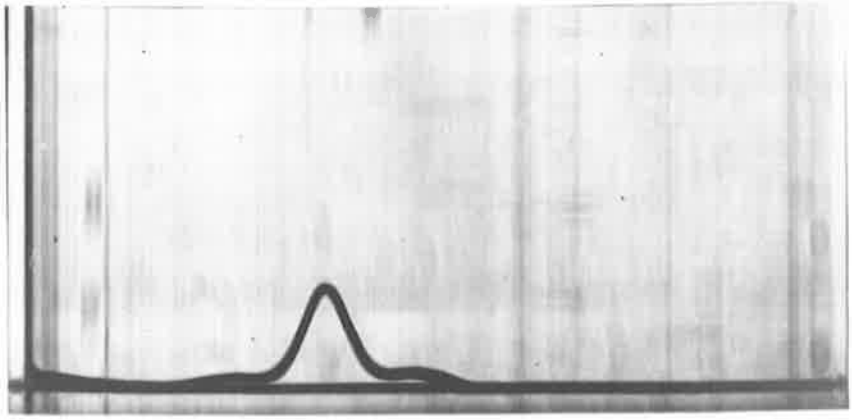

(b)

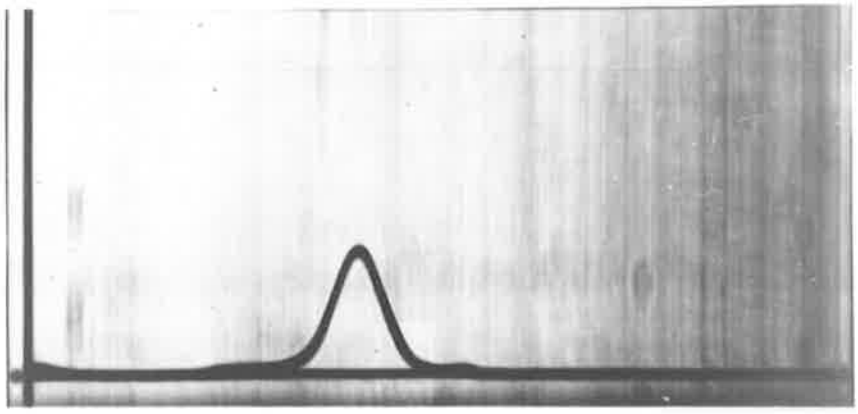

(c)

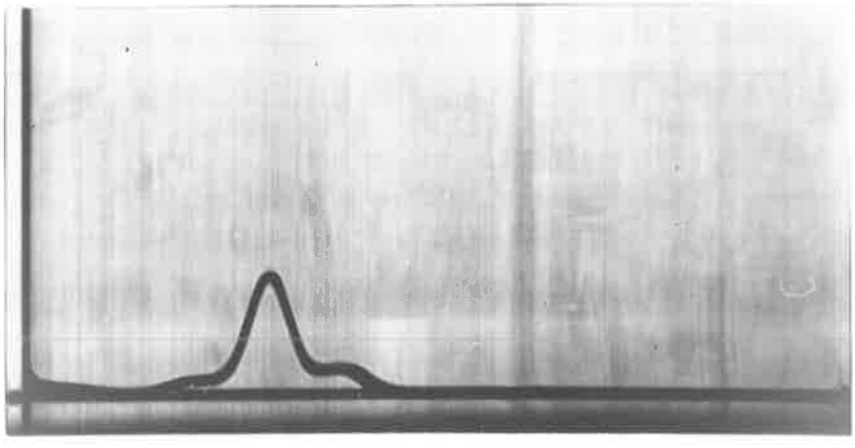

Fig. 3.5 : Electrophoresis schlieren patterns obtained with
(a) Sigma α-chymotrypsin
(b) Worthington α-chymotrypsin
(c) PMS-α-chymotrypsin.

maximum of the elution peak being retained in each case. Since this procedure did not remove the electrophoretic inhomogeneity it was concluded that the impurities were similar in molecular weight to α-chymotrypsin and probably differed from α-chymotrypsin in overall net charge.

Electrophoretic heterogeneity had previously been reported by Egan et. al.[87] who used countercurrent electrophoresis to study α-chymotrypsin over a range of pH (2.4 to 8.6) and ionic strength. The four-times-recrystallized α-chymotrypsin was prepared from eight-times-recrystallized chymotrypsinogen. The fractions separated electrophoretically were shown to have different esterase activities. From electrophoretic data and specific activity determinations Egan et. al. concluded that the polyphoretic nature of α-chymotrypsin was due to the presence of β-chymotrypsin and γ-chymotrypsin the bulk of the sample (91%) being α-chymotrypsin. Hofstee[88] found that the chymotrypsins were inhomogeneous in respect to binding to DNA where a fraction (≈10%) did not combine even in the presence of excess DNA. In the case of α-chymotrypsin the fraction which did not take part in binding increased proportionally with the decrease in enzymic activity during autolysis. Studies by Chervenka[89] and Martin and Frazier[90] of the urea denaturation of α-chymotrypsin indicated heterogeneity. The latter study also suggested that the presence of calcium ions (Ca^{2+}) stabilized α-chymotrypsin towards urea denaturation. It had previously been reported[91] that the presence of Ca^{2+} increased the stability of α-chymo-

trypsin towards heat denaturation and enhanced the proteolytic and esterolytic activities of α-chymotrypsin.

In the development of an "all-or-none" assay for chymotrypsin Erlanger and Edel[92] found that the presence of Ca^{2+} in the buffer was essential for accurate results. Assays performed in the absence of Ca^{2+} were consistently low. Erlanger, Cooper and Bendich[93] followed this finding with a study of the heterogeneity of α-chymotrypsin. The results obtained using the all-or-none assay and agar-gel electrophoresis supported the conclusion that the three-times-crystallized α-chymotrypsin used was not homogeneous but consisted of at least two components of unequal stability. Agar-gel electrophoresis patterns in the absence of Ca^{2+} showed the presence of two components but with Ca^{2+} present the system was electrophoretically homogeneous.

In the light of the electrophoretic heterogeneity observed with PMS-α-chymotrypsin and the evidence of Wu and Laskowski[91] on the Ca^{2+} inhibition of autolysis and Erlanger et. al.[92,93] on the absence of heterogeneity in the presence of Ca^{2+}, it was decided to perform sedimentation equilibrium experiments using α-chymotrypsin in the presence of Ca^{2+}.

IV SEDIMENTATION EQUILIBRIUM STUDY

Preliminary sedimentation equilibrium experiments were carried out using 1 mm solution columns to test the effects of Ca^{2+}, ionic strength and ethylenediaminetetraacetic acid (EDTA) on the molecular weight of α-chymotrypsin. The experiments were performed as described in Chapter 5 using protein solutions of 30 $\pm$ 1 fringes in Tris buffer pH 7.6 . The results are shown in Table 3.2 .

Table 3.2

Ionic Strength	$[Ca^{2+}]$	[EDTA]	Molecular Weight
0.05	-	-	56,600
0.05	0.01 M	-	35,600
0.05	-	0.01 M	51,500
0.20	-	-	27,200

It can be seen that the presence of a small quantity of Ca^{2+} causes a marked lowering of molecular weight as does a four-fold increase in ionic strength. The presence of EDTA, which was included to complex any divalent metal ions that might be present, had a much smaller effect in the opposite sense to that expected. The effect of Ca^{2+} in stabilizing α-chymotrypsin against self-association was perhaps not unexpected since the

presence of Ca^{2+} had been shown to stabilize the native α-chymotrypsin conformation in concentrated urea solutions[89,90].

Two sedimentation equilibrium experiments were performed on 3 mm columns of α-chymotrypsin at different concentrations in Tris buffer pH 7.6 and 0.05 ionic strength at 20°C. The molecular weight versus concentration curves obtained from the Rayleigh interference fringe photographs at equilibrium did not interlace. A high speed sedimentation equilibrium experiment gave a monomer molecular weight of 21,600 for α-chymotrypsin indicating that no appreciable autolysis had occurred. However, this does not rule out autolysis products or autolytically altered α-chymotrypsin as the cause of non-interlacing.

A series of sedimentation equilibrium runs using 1 mm columns was carried out at 20°C on α-chymotrypsin at several different concentrations in Tris buffer pH 7.6 and 0.05 ionic strength. The results of this series and a similar series at 5°C are shown in Fig. 3.6 . A single molecular weight value was obtained from each sedimentation equilibrium experiment in the manner described in Chapter 5. While these results must be regarded only as semi-quantitative because of the non-interlacing of molecular weight curves obtained with 3 mm columns, it is interesting to note the similarity between the values obtained at different temperatures. The correspondence of molecular weights at different temperatures indicates that

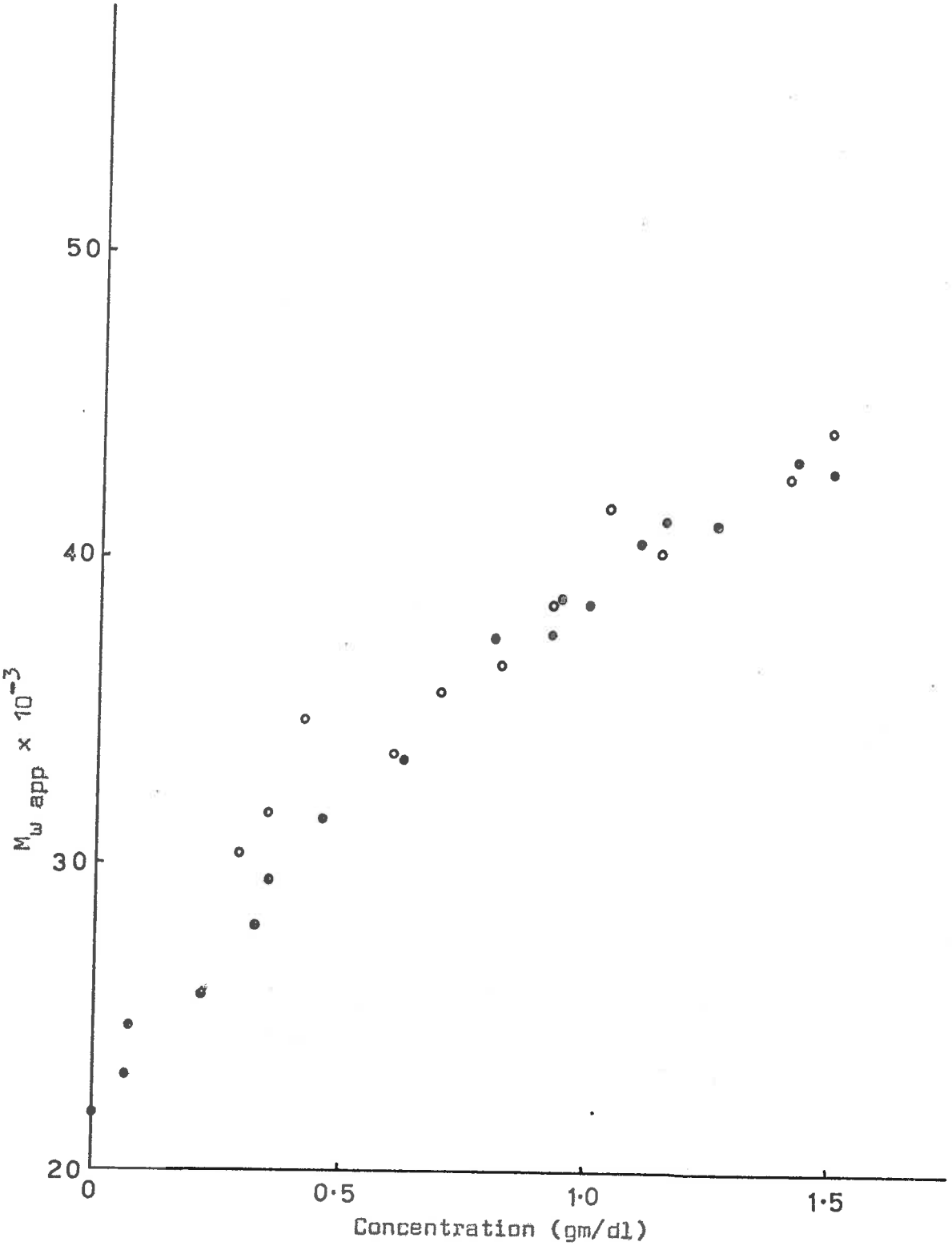

Fig. 3.6 : Apparent weight average molecular weight of α-chymotrypsin as a function of concentration in tris buffer pH 7.6, I = 0.05 including 0.01M Ca^{2+}. The data were obtained from sedimentation equilibrium experiments using 1 mm solution columns at 5°C (open circles) and 20°C (filled circles).

the enthalpy of the self-association reaction is either very small or zero. Both the Steiner[17,18] and the Adams[21-27] methods of analysis of the molecular weight versus concentration curves were applied to the data in Fig. 3.6 . The results of this analysis are discussed in Section VI (b) of this Chapter.

Anhydro-α-chymotrypsin was prepared from Worthington α-chymotrypsin by the method of Weiner et. al.[94]. The tosylated protein was first formed by reaction with p-toluenesulphonyl (tosyl) fluoride, the latter reacting with the serine residue at the active site of the α-chymotrypsin molecule, and anhydro-α-chymotrypsin formed by elimination of the tosyl group in alkaline solution. The overall effect is the

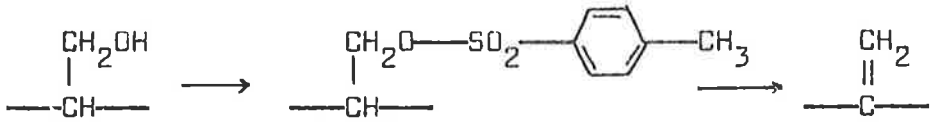

Serine hydroxyl group — Tosyl protein — anhydro protein

removal of a water molecule from serine at the active site. The inhibited protein was passed through a Sephadex column and the maximum of the protein elution peak retained. A stock solution for subsequent sedimentation equilibrium experiments was obtained by dialysis of the anhydro-α-chymotrypsin solution against Tris buffer pH 8.4 and 0.1 ionic strength. Anhydro-α-chymotrypsin was used to avoid, as far as possible, the effects of autolysis and the buffer at the isoelectric pH was

used to minimise charge effects.

Again, the molecular weight versus concentration curves, obtained from sedimentation equilibrium runs with 3 mm columns of protein solution at two different concentrations, did not interlace. A series of sedimentation equilibrium runs using 1 mm columns was performed and the results are shown in Fig. 3.7 . The monomer molecular weight of 19,000 indicated by these results was lower than expected and it appeared either that precautions taken to minimise autolysis were inadequate or that some degradation of the protein occurred during inhibition.

The activation of chymotrypsinogen is a complex reaction giving rise to other forms of chymotrypsin as well as α-chymotrypsin and it is not possible to purify the latter because of its autolytic action. This consideration coupled with the reports of heterogeneity and experimental results reported here strongly suggested that further attempts to quantitatively analyze the molecular weight versus concentration data would be fruitless and experiments on α-chymotrypsin were discontinued. This decision was later supported by the findings of Adams and Filmer[24] and of Teller et. al.[95] Adams and Filmer discontinued experiments with α-chymotrypsin when they found that even "chromatographically homogenous" material appeared heterogeneous on polyacrylamide gel electrophoresis. Teller et. al. found that calculated equilibrium constants varied widely, depending

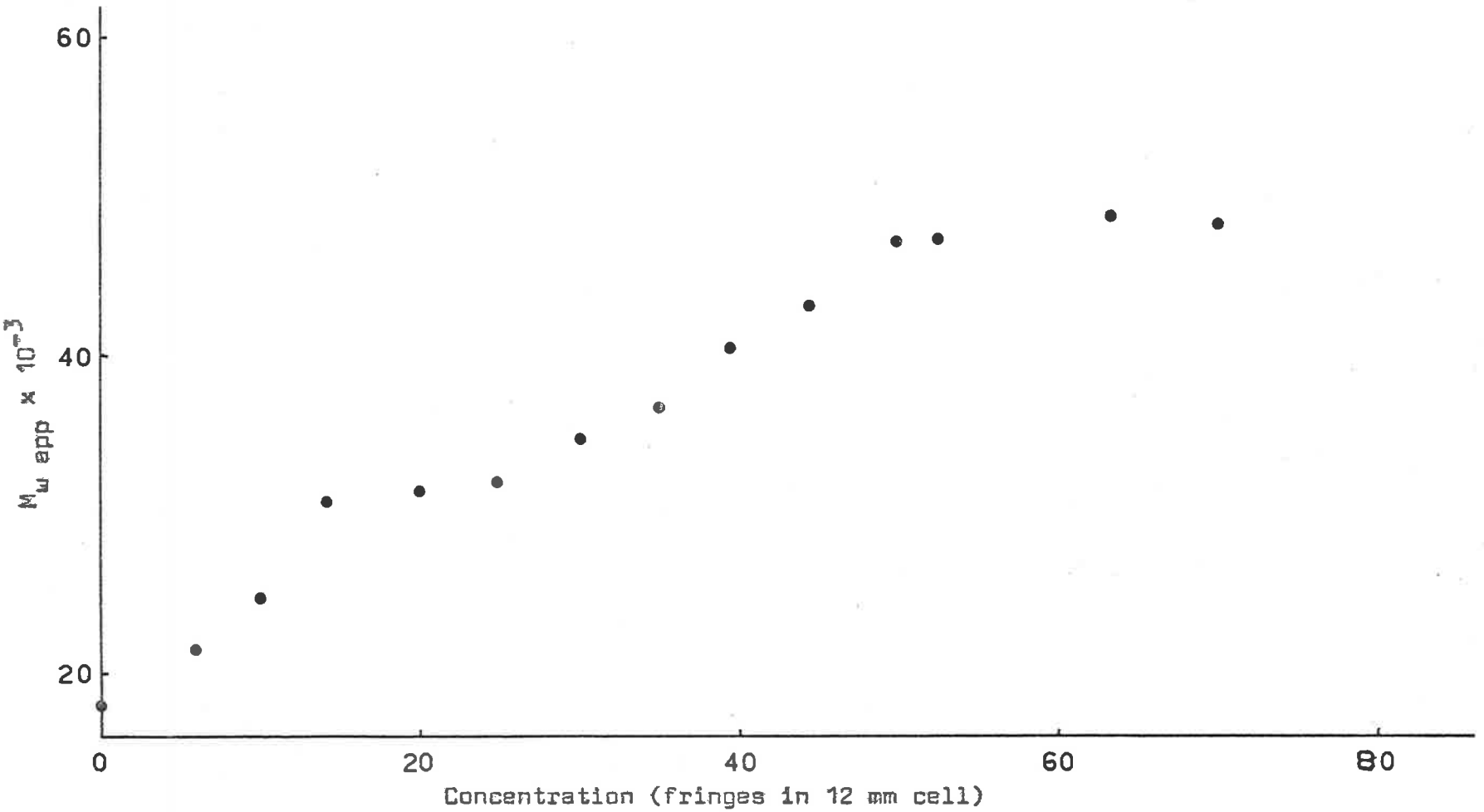

Fig. 3.7 : Apparent weight average molecular weight of anhydro-α-chymotrypsin as a function of concentration in tris buffer pH 8.4, I = 0.1 including 0.01M Ca^{2+}. The data were obtained from sedimentation equilibrium experiments using 1 mm solution columns at 20^{0}C.

on the source of the sample, and that significant amounts of unreacted or reactivated α-chymotrypsin were present in inhibited samples of the protein.

V ANALYSIS OF MOLECULAR WEIGHT DATA

The principles of the Steiner and Adams methods of analysis of molecular weight versus concentration data have been discussed in Chapter 2. The data displayed in Fig. 3.6 was analyzed according to these principles with the aid of a computer.

(1) Steiner Analysis

In the general case for a self-associating protein it is necessary to solve the equation

$$\varepsilon = 1 + 4k_2\gamma + 9k_2k_3\gamma^2 + 16k_2k_3k_4\gamma^3 + \cdots\cdots$$

where the only unknowns are the equilibrium constants ($k_2, k_3, k_4 \ldots$) and the order of the polynomial. The criterion used in the selection of the order of the polynomial was that all the coefficients should be positive or zero since negative equilibrium constants are meaningless, and the equilibrium constants were evaluated for the maximum order polynomial consistent with this criterion.

Two methods of fitting a least squares polynomial to the data were used. The first was a computer library subroutine LSQPOL based on an iteration algorithm and the second was based on matrix methods (See Chapter 4 Section III). Besides fitting a polynomial in γ to ε, a polynomial fit of γ to $\varepsilon - 1$ and to $\frac{\varepsilon - 1}{\gamma}$ was tried and the results are shown in Table 3.3 .

Table 3.3

Equilibrium constants for α-chymotrypsin

TRIMERISATION MODEL				
	Series 1[a]		Series 1 and Series 2	
Data Treatment	$k_2 \times 10^{-2}$[b]	$k_3 \times 10^{-3}$	$k_2 \times 10^{-2}$	$k_3 \times 10^{-3}$
ε versus $\bar{\nu}$ (LSQPOL)	5.57	6.14	5.80	5.96
ε versus $\bar{\nu}$ (MATRIX)	5.57	6.14	5.80	5.96
$\frac{(\varepsilon-1)}{\bar{\nu}}$ versus $\bar{\nu}$ (LSQPOL)	6.85	4.69	5.30	6.61
$\varepsilon-1$ versus $\bar{\nu}$ (MATRIX)	6.02	5.59	5.69	6.10

TETRAMERISATION MODEL						
	Series 1			Series 1 and Series 2		
Data Treatment	$k_2 \times 10^{-2}$	$k_3 \times 10^{-3}$	$k_4 \times 10^{-2}$	$k_2 \times 10^{-2}$	$k_3 \times 10^{-3}$	$k_4 \times 10^{-2}$
ε versus $\bar{\nu}$ (LSQPOL)		0[c]			0	
ε versus $\bar{\nu}$ (MATRIX)	7.40[d]	4.25	1.55	7.13	4.21	1.73
$\frac{(\varepsilon-1)}{\bar{\nu}}$ versus $\bar{\nu}$ (LSQPOL)	8.26	2.76	6.61			0
$\varepsilon-1$ versus $\bar{\nu}$ (MATRIX)	8.27[d]	3.52	2.45	6.25	5.16	0.97
GRAPHICAL	10	5	10			

(a) Series 1 experiments were performed at 20°C and Series 2 experiments at 5°C.

(b) Equilibrium constants reported as litre.mole^{-1}.

(c) Negative values of k have no physical meaning.

(d) Values obtained using smoothed data; negative k_4 value obtained using raw data.

The calculated curve for Series 1 using the trimerisation model ($k_2 = 5.57 \times 10^2$, $k_3 = 6.14 \times 10^3$) is shown in Fig. 3.8 while Fig. 3.9 shows the curve calculated, for Series 1 and 2 combined, from the equilibrium constants $k_2 = 5.80 \times 10^2$ and $k_3 = 5.96 \times 10^3$. The shapes of the two calculated curves are similar with the curve in Fig. 3.9 lying between 500 and 300 molecular weight units above that in Fig. 3.8 .

For the Series 1 data the curves calculated from all sets of equilibrium constants agree with that in Fig. 3.8 within $\pm$ 300 molecular weight units and appear to fit the experimental data equally well. Hence no choice of an association model or method of data treatment can be made from the fit of the calculated curves to the raw data. Only the fact that the graphical method supports association as far as tetramers makes it reasonable to conclude that this association scheme occurs. This conclusion is supported by analysis of the combined data although not by all methods of data treatment. However, it is felt that the results obtained by the rigorous matrix method would be more reliable than those obtained by the iterative LSQPOL method.

It is noteworthy that the curves calculated from the various sets of equilibrium constants for the combined data vary from the curve in Fig. 3.9 by only $\pm$ 150 molecular weight units. The improved agreement over the curves for Series 1 is due to the increased number of points emphasizing the necessity

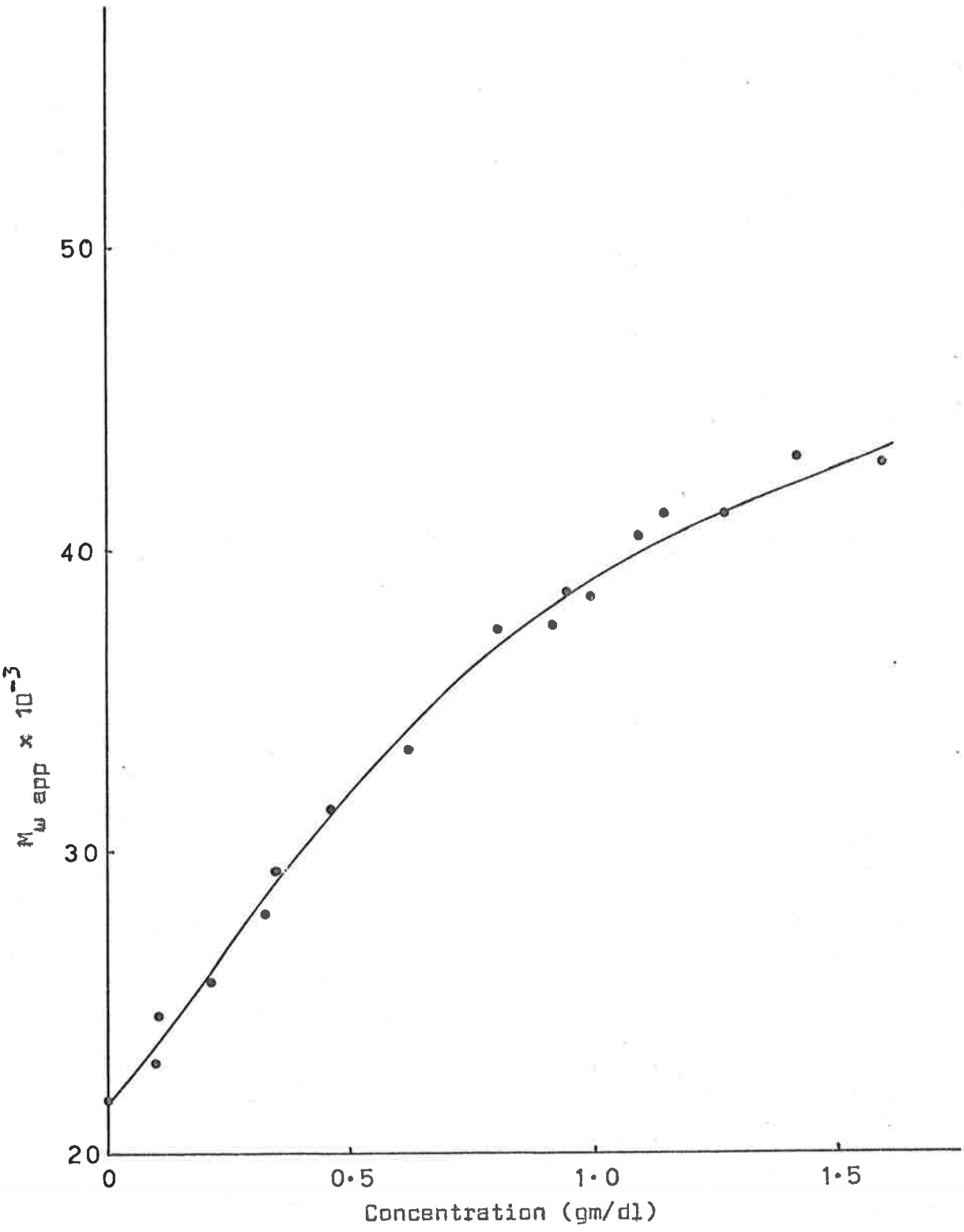

Fig. 3.8 : Results of Steiner analysis of experimental weight average molecular weight data obtained at 20°C (filled circles). The solid line was calculated for a monomer-dimer-trimer self-association for which $k_2 = 5.57 \times 10^2$ litre mole^{-1} and $k_3 = 6.14 \times 10^3$ litre mole^{-1}.

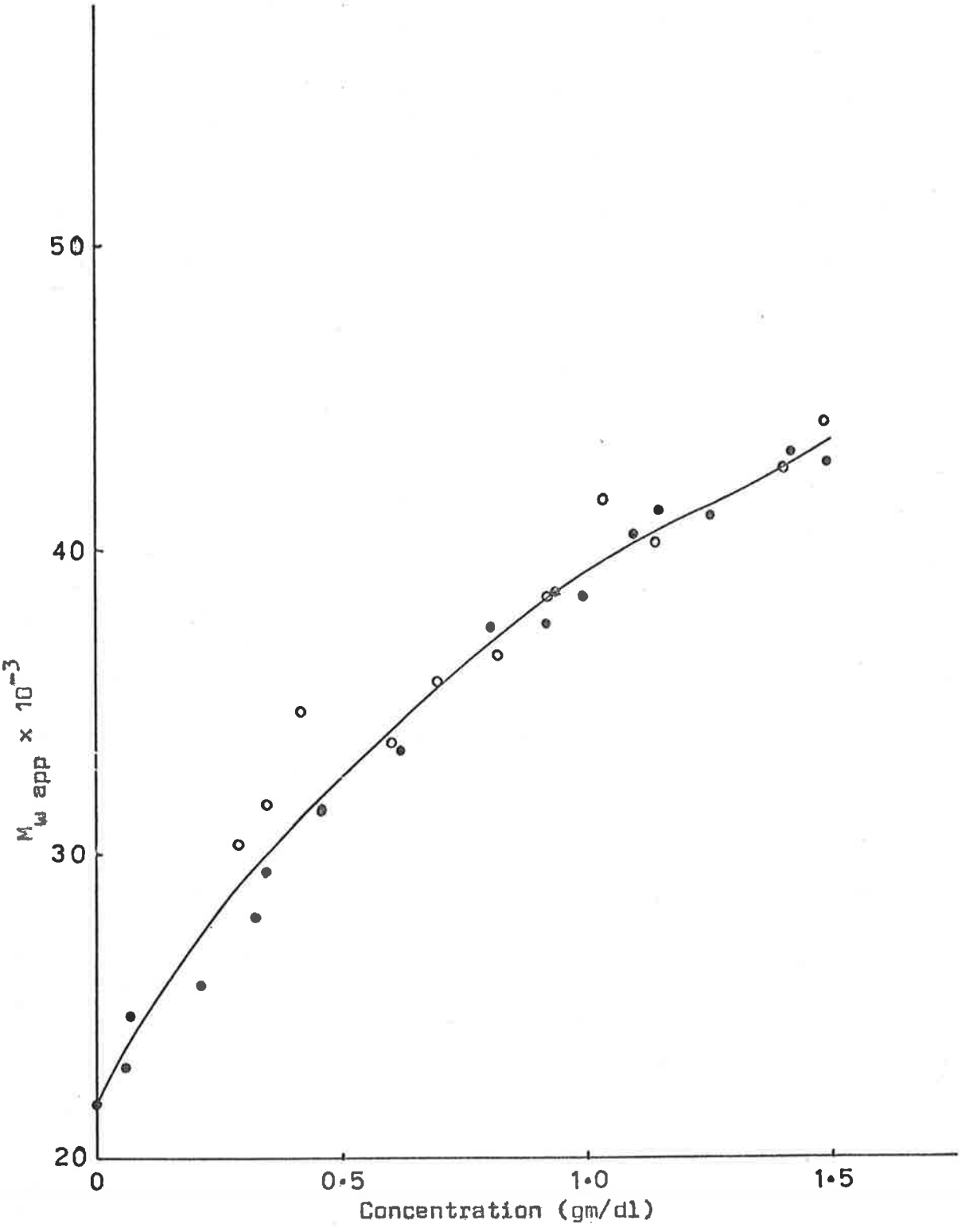

Fig. 3.9 : Results of Steiner analysis of experimental weight average molecular weight data obtained at $5^{0}C$ (open circles) and $20^{0}C$ (filled circles). The solid line was calculated for a monomer-dimer-trimer self-association for which $k_2 = 5.80 \times 10^{2}$ litre $mole^{-1}$ and $k_3 = 5.96 \times 10^{3}$ litre $mole^{-1}$.

for large numbers of molecular weight determinations over a wide range of concentration for reliable results. The scatter of the data combined with the small number of data points appear to be the main reasons for inconclusive results obtained. This is supported by the fact that smoothing of the data from Series 1 was necessary before two of the methods of data treatment gave positive values of k_4 (See Table 3.3) and by the results obtained with the combined data. While it is not expected that smoothing the data would alter the orders of magnitude of the equilibrium constants personal bias may affect the results and the procedure should be used only as a last resort.

(2) Adams Analysis

The method of analysis of molecular weight versus concentration curves proposed by Adams has been fully discussed in Chapter II. The recommended procedure was to solve equation 2(21).for BM_1, the only unknown, by successive approximation. Since this method would only give an accurate value of BM_1 at a single concentration a different method was used to solve for BM_1.

The penultimate equation in Adams'[27] derivation of 2(21) is

$$\frac{3cM_1}{M_{n\ app}} - c = 2c_1 + \frac{K_2 c_1^2}{2} + \frac{3BM_1 c^2}{2}$$

which, on substitution for $c_1 = \alpha \exp(-BM_1)$ (see equation 2(18)), becomes

$$\frac{3cM_1}{M_{n\ app}} - c = 2\alpha \exp(-BM_1) + \frac{K_2}{2}(\alpha \exp(-BM_1))^2 + \frac{3BM_1c^2}{2}$$

This equation was solved for K_2 at each data point from Series 1 for a range of values of BM_1. The value of BM_1 used was that which resulted in the average K_2 value with the smallest standard error. This average value of K_2 was also used with BM_1 to calculate values of K_3 which were averaged. This type of approach to the evaluation of BM_1 is supported by Magar[96] on statistical grounds.

The values obtained were:-

$$BM_1 = -0.01$$
$$K_2 = 1.16 \pm 0.06 \times 10^3 \text{ litre.mole}^{-1}$$
$$K_3 = 3.92 \pm 0.14 \times 10^3 \text{ litre.mole}^{-1}$$

The molecular weight-concentration curve computed using these values is shown in Fig. 3.10. It can be seen that the curve fits the data well. Since the value of BM_1 obtained was close to zero it would be expected that the K_2 and K_3 values obtained would be similar to those obtained by the Steiner method which assumes $BM_1 = 0.0$. A comparison of

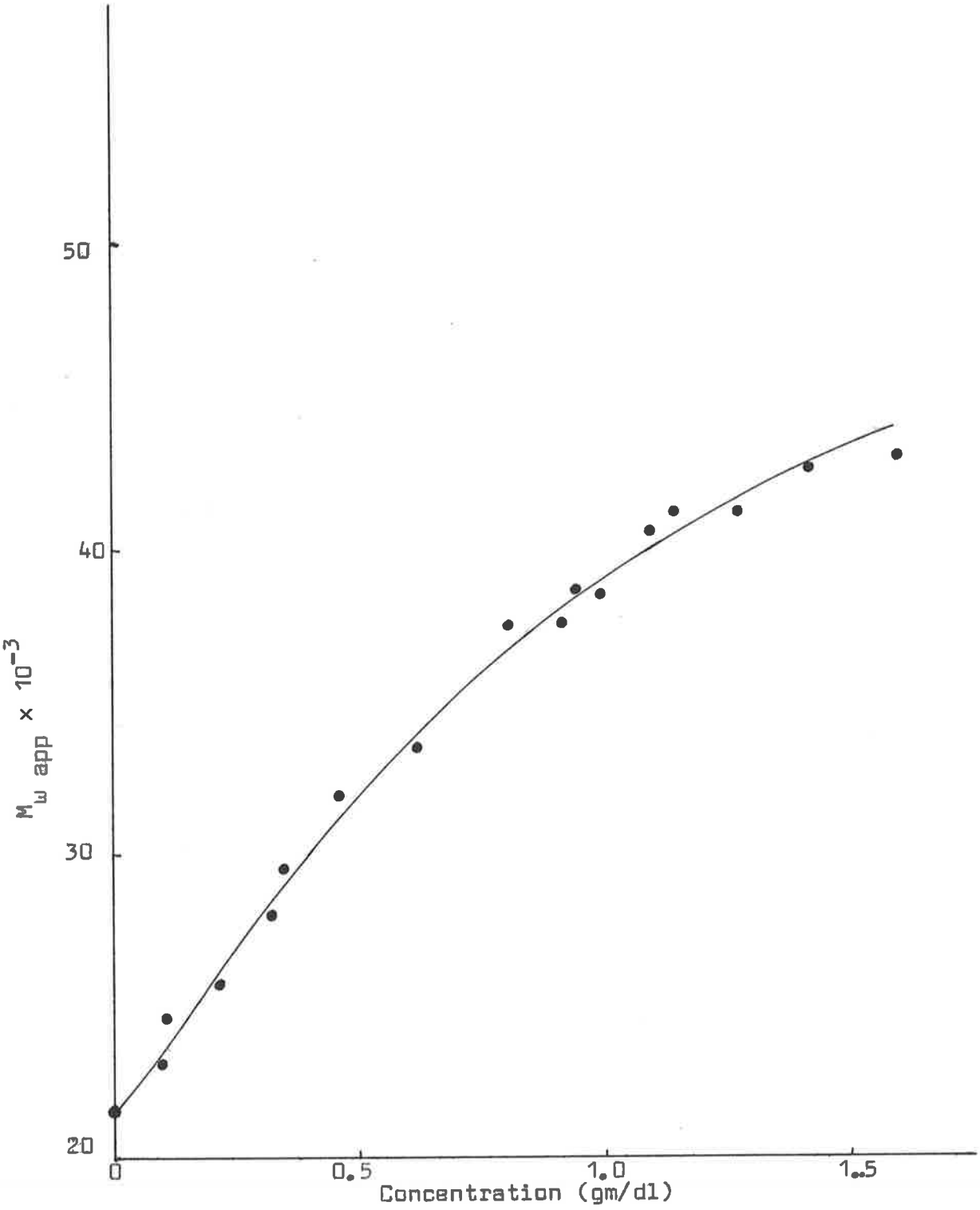

Fig. 3.10 : Results of Adams analysis of experimental weight average molecular weight data obtained at 20°C (filled circles). The solid line was calculated for a monomer-dimer-trimer self-association for which $BM_1 = -0.01$, $K_2 = 1.16 \times 10^3$ litre mole^{-1} and $K_3 = 3.92 \times 10^3$ litre mole^{-1}.

the above values with those shown in Table 3.3 shows that there is good agreement between the K_3 values but the K_2 value calculated by the Adams method is approximately twice that calculated by the Steiner method.

It was noted in the previous section that the values of equilibrium constants, calculated using different curve fitting methods, were more self-consistent when large numbers of data points were used. This observation prompted a critical study of the number of data points necessary for obtaining accurate values of BM_1 and K by the Adams method.

Molecular weight curves were computed for trimerisation of α-chymotrypsin using values of equilibrium constants of the same order as those found experimentally and values of BM_1 between -0.01 and -0.06. The molecular weight values at selected concentrations were then modified by random errors of $\pm$400, $\pm$500 and $\pm$600 molecular weight units. Under these conditions it was found that an accurate value of BM_1 could be obtained only if not less than 40 data points were used. As expected the more points used the more reliable were the values of equilibrium constants obtained. It was also found that data points, for which the calculated weight fraction of monomer (f) was less than 0.1, should be omitted from calculations as the introduced errors usually caused inaccurate (even negative) values of K_2. Table 3.4 illustrates the effect of increasing

the number of data points on the reliability of the calculated quantities.

Table 3.4

Effect of the number of data points on calculated equilibrium constants

	Actual Value	Calculated Value 17 points	Calculated Value 60 points
BM_1	-0.03	-0.05	-0.03
K_2 dl/gm	0.54	0.66	0.51
K_3 dl/gm	1.44	1.25	1.45

The main conclusion drawn from the computer simulation study was that the reliability of calculated quantities is suspect if only small numbers of data points are analysed by the Adams method. This also applies to the Steiner treatment. It should be pointed out, however, that, if interlacing molecular weight curve segments had been obtained from equilibrium experiments at different initial concentrations, sufficient data points could have been obtained from as few as four experiments since twenty or more measurements can be made on each 3 mm column experiment. Thus the crux of the problem is not merely an insufficient number of experiments but the non-interlacing of the molecular weight curve segments obtained from the experiments.

Chapter 4

EXPERIMENTS WITH INSULIN

I SEDIMENTATION EQUILIBRIUM EXPERIMENTS WITH ZINC-FREE INSULIN

Insulin was chosen for study because, as a consequence of its obvious biological importance, it has been widely studied and is one of the best characterised proteins available. Furthermore, a number of workers have decribed its self-association properties. Whilst Adams[20] and Jeffrey[19,49] have studied insulin at acid pH, there has been very little research on the self-association of insulin at alkaline pH. Both Adams and Jeffrey experienced difficulty with non-interlacing of molecular weight curves. However, the degree of non-interlacing was small (within experimental error) and Jeffrey showed that the non-interlacing could be eliminated by using a different method of curve fitting. Zinc is not bound to insulin at pH 2[58] and so the insulin was zinc-free in Jeffrey's experiments. It has been shown[48] that the presence of zinc has a marked effect on the degree of association of insulin and the simplest system for study at alkaline pH seemed to be the zinc-free protein. Kakiuchi[60] in his study of α-amylase association has demonstrated the complexity and non-interlacing inherent in a system where zinc ions (Zn^{2+}) played a stoichiometric part in the association and as a result of this it was expected that similar non-overlap with insulin would be avoided by elimination

of zinc. Thus zinc-free insulin was obtained for the present study by exhaustive dialysis at pH 2 followed by chromatography on G 25 Sephadex.

A series of sedimentation equilibrium experiments was carried out using 3 mm columns of Zn-free insulin solution at different initial concentrations in pH 8.0 barbiturate buffer at 0.05 ionic strength. The results of the experiments, performed at 20^{o}C, are shown in Fig. 4.1 . The two main features of these results are the non-interlacing and the minimum molecular weight of approximately 12,000.

The minimum molecular weight of 12,000, determined from a high speed sedimentation equilibrium experiment, was unexpected, since the molecular weight of the basic insulin unit, as determined by amino acid sequence analysis, is approximately 6,000. Marcker[52] obtained the latter value for insulin at alkaline pH, using vapour phase osmometry, as did Jeffrey at acid pH, using sedimentation equilibrium. However, Marcker obtained a value of 12,000 for the monomer molecular weight of insulin in acid solution and his molecular weight curves were radically different from those of Jeffrey. The results obtained by Marcker appeared less reliable than those obtained by Jeffrey, on the grounds that the sedimentation equilibrium technique is inherently more accurate than vapour pressure osmometry. Nevertheless, a very high dimerisation constant would have to exist, under the conditions of the

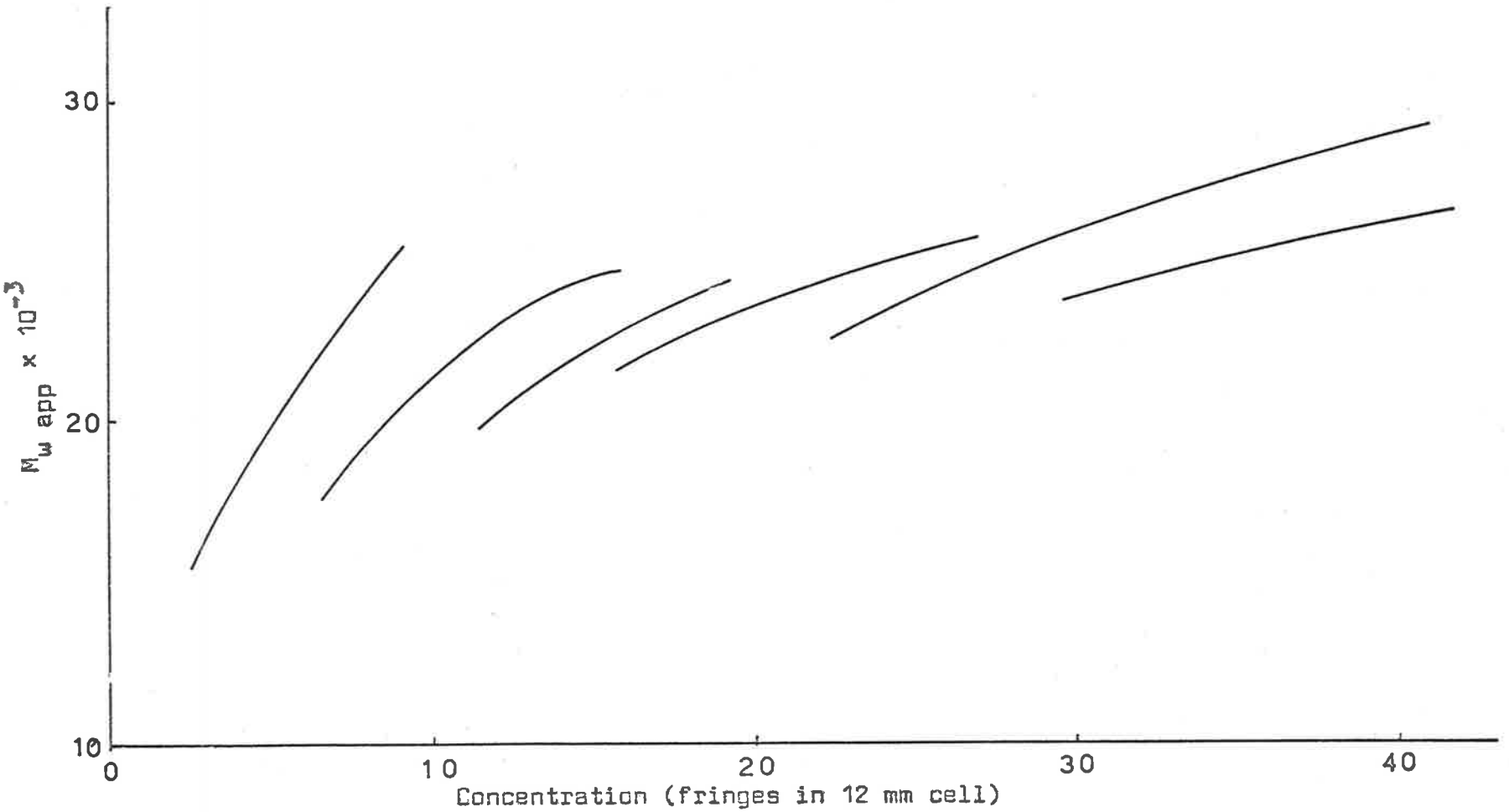

Fig. 4.1 : Apparent weight average molecular weight of zinc-free insulin as a function of concentration in barbiturate buffer pH 8.0, I = 0.05. The data were obtained from sedimentation equilibrium experiments using 3 mm solution columns at 20°C.

experiments reported here, for the 6,000 molecular weight units to remain undetected by the high speed sedimentation equilibrium technique which permits measurements to be made to optical concentrations as low as 0.5 fringe (0.013 gm/dl).

The degree of non-interlacing of the molecular weight curves from different experiments was a disturbing feature of results shown in Fig. 4.1 since the usual methods of analysis are based on the assumption of a unique 1:1 relationship between molecular weight and concentration. Molecular weight differences of 1,000 to 4,000 exist between the various curves and while it is just possible that the lower value could arise from experimental error the higher values could not. With the increasing use of the sedimentation equilibrium technique and the development of theoretical methods of molecular weight curve analysis more reports of non-interlacing and possible causes have appeared in the literature. Since this problem seriously limits the applicability of analytical methods based on a unique molecular weight versus concentration curve some of the possible causes of non-interlacing are discussed in Section 4-II.

II THE PROBLEM OF NON-INTERLACING MOLECULAR WEIGHT CURVES

(1) Early Work

The first workers to recognise the problems of non-interlacing of molecular weight versus concentration curves from sedimentation equilibrium experiments at different initial concentrations, were Squire and Li[80], who used schlieren optics in their work on adrenocorticotropic hormone (ACTH). They felt that the results were due to bias in location of the centre of the schlieren image on the photographic plate. While this explanation is reasonable, it is expected that bias of this type would be much less evident in experiments where Rayleigh interference optics are employed. An effect similar to non-interlacing was observed by Rao and Kegeles, who used the approach-to-equilibrium technique to study α-chymotrypsin. With increasing time, molecular weights determined at the meniscus fell below the smooth line drawn through the molecular weights determined soon after the start of the experiments. Since the system was not at equilibrium the observations could be simply explained by non-instantaneous re-equilibration of the species originally at equilibrium, but perturbed by the ultracentrifugal field. The work of Adams[20] and of Jeffrey[19,49], discussed in the previous section and in Chapter 3, again drew attention to non-interlacing since they employed the potentially more accurate Rayleigh interference optical system. It seemed

likely from Jeffrey's analysis that the non-interlacing was an artifact of the curve fitting procedure applied to the lnj versus x^2 data.

(2) Effect of Pressure

Until recently[97,98] theories of sedimentation equilibrium of reacting systems had not taken into account the effect of pressure on the equilibrium constants for the reactions. It was generally assumed that the partial specific volume of the associated protein species was the same as that for the monomer and hence that the equilibrium constants for the association were independent of pressure. This assumption was based on the fact that the experiments were carried out at low angular velocity and hence with a low pressure gradient. In the experiments reported here (Fig. 4.1), the total pressure increase from the meniscus to the bottom of the solution column in each experiment ranged from 2 to 5 atmospheres. Josephs and Harrington in their studies of myosin, have shown that this assumption does not always apply, since the equilibrium constant of the myosin monomer-polymer system showed a marked dependence on hydrostatic pressure. A similar dependence of equilibrium constants on pressure in the insulin system could give rise to the non-interlacing molecular weight curves obtained. From Fig. 4.1 it can be seen that a smooth curve could be drawn through the molecular weights evaluated at the meniscus in each

experiment. Since this seemed to support the hypothesis that the self-association of insulin was pressure dependent, the data was tested for a pressure effect.

The first test was an empirical one based on the assumption of a linear dependence of partial specific volume on the pressure. This was carried out very simply by modifying the computer program to replace the factor $(1 - \bar{v}\rho)$ by the expression $(1 - \bar{v}_p \rho)$ where

$$\bar{v}_p = \bar{v} (1 - F6 \times \tfrac{1}{2} \omega^2 \Delta x^2)$$

The factor $\frac{1}{2} \omega^2 \Delta x^2$ is equal to the hydrostatic pressure and F6 is a constant, the magnitude of which was determined approximately as the value required to lower the molecular weight from an overlying curve to equal the molecular weight at the meniscus of the underlying curve. The best value of F6 appeared to be 1.75×10^{-8} which altered the curves in Fig. 4.1 to those in Fig. 4.2 . The latter curves interlace within experimental error and on this basis experimental evidence of a pressure effect was sought.

A sedimentation equilibrium experiment was carried out on a 3 mm column of insulin at a concentration of approximately 30 fringes. A similar experiment was carried out on an aliquot of the same solution but including 0.25 ml liquid paraffin in each cell compartment. This overlay of oil with a density of 0.85 gm/ml had the effect of increasing the pressure at the top of

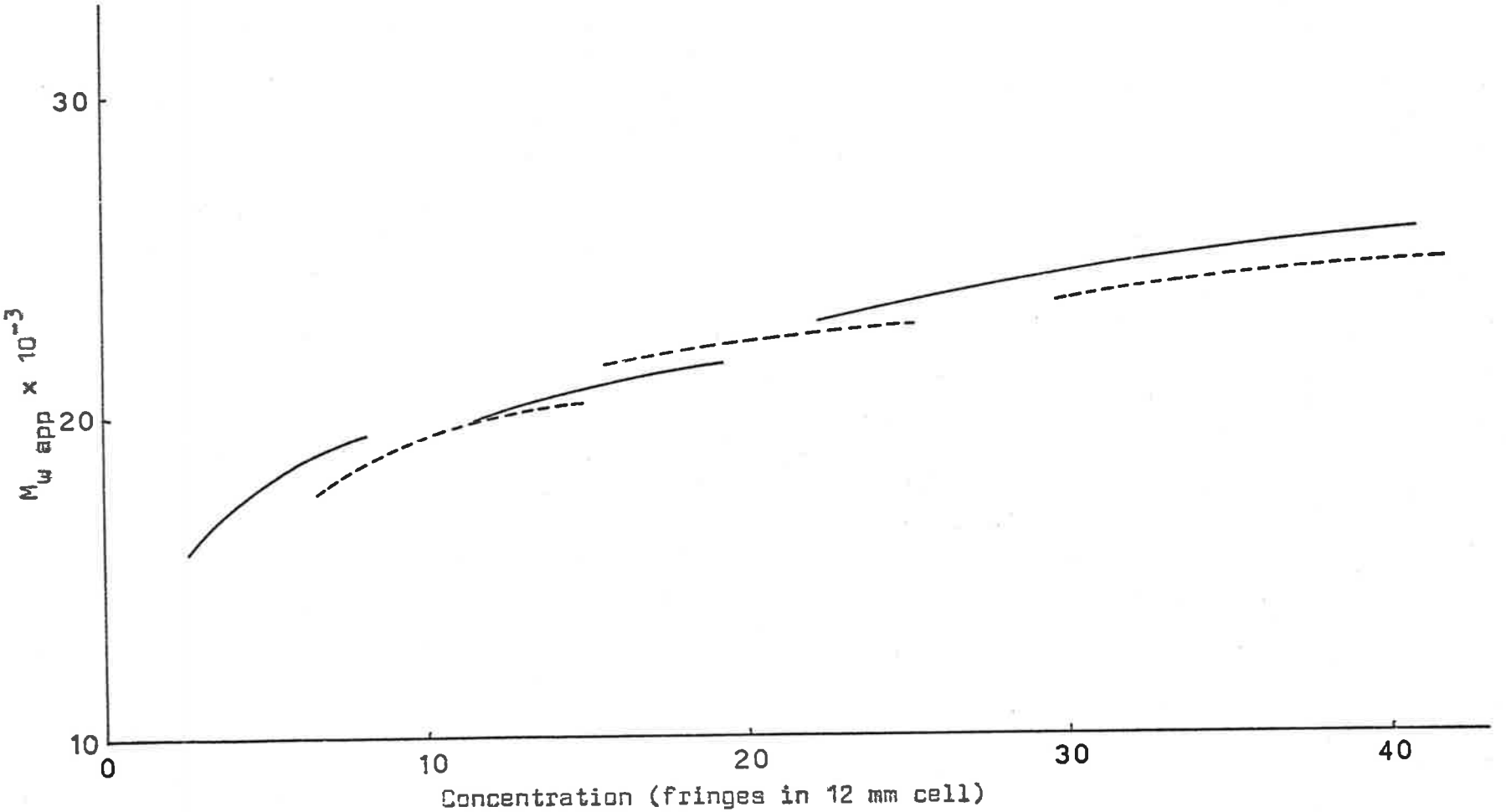

Fig. 4.2 : Modified apparent weight average molecular weight versus concentration curves for zinc-free insulin in barbiturate buffer pH 8.0, I = 0.05, T = 20°C. The curves are the result of modification of the data shown in Fig. 4.1 by a hypothetical pressure effect on the partial molar volume of the zinc-free insulin (see text).

the solution column to approximately 5 atmospheres. Since this increase of pressure at the meniscus was approximately equal to the maximum increase in pressure down the solution column of the sedimentation equilibrium experiments shown in Fig. 4.1, markedly different molecular weight curves were expected if the non-interlacing was due to a pressure effect. Comparison of the molecular weight curves shown in Fig. 4.3, however, rules out pressure dependent equilibria because the curves are coincident within experimental error.

Sedimentation velocity runs were carried out at 44,770 rpm and 63,650 rpm using aliquots of the same solution as used in the previous equilibrium experiments in order to test for an effect at higher pressures. The presence of pressure dependent equilibria would result in curvature of lnx versus time data[100] used to calculate sedimentation coefficients and different values of sedimentation coefficients determined at different angular velocity. Sedimentation coefficients of 2.48 S and 2.49 S were determined from the experiments at 44,770 rpm and 63,650 rpm respectively, and no curvature of the lnx versus time data was apparent in either case. The maximum pressure to which measurement was made was 55 atmospheres at 44,770 rpm and 120 atmospheres at 63,650 rpm. These results indicate that there is no significant pressure effect on the self-association of insulin up to 120 atmospheres.

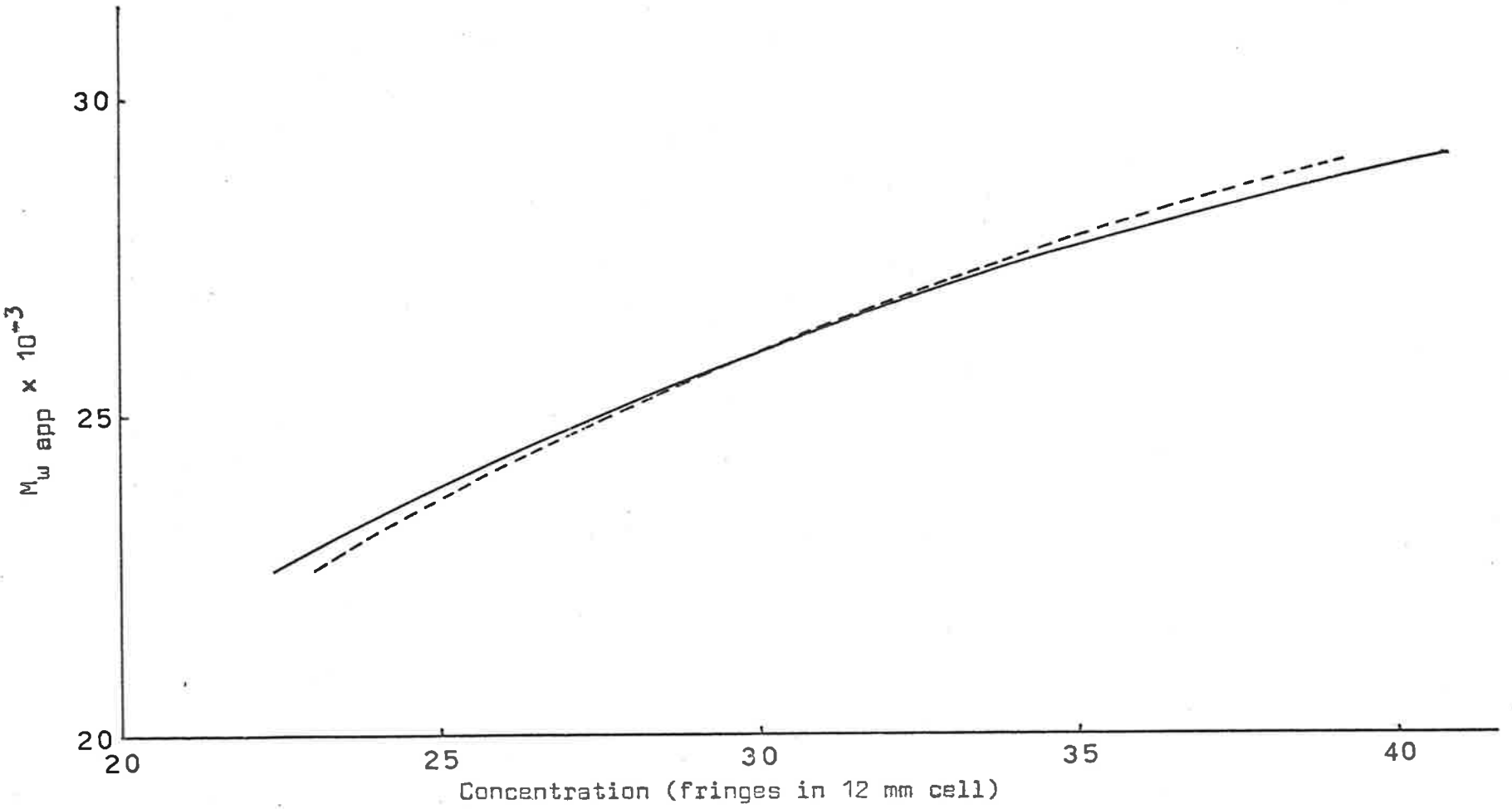

Fig. 4.3 : Apparent weight average molecular weight of zinc-free insulin as a function of concentration in barbiturate buffer pH 8.0, I = 0.05, T = 20°C. The results were obtained from experiments carried out at 9950 rpm using 3 mm columns from the same stock solution of 30 fringes concentration. In one case (see broken line) an overlay of oil was included.

(3) Mechanical and Optical Effects

Adams and Filmer[24], in a paper verifying the analytical methods developed earlier by Adams[20-23] for reacting systems at sedimentation equilibrium, reported non-interlacing in experiments with lysozyme. From the reported curves it appeared that the maximum difference between molecular weights from different runs was approximately 1,500 at a concentration of 25 fringes (See Fig. 7 of Adams and Filmer[24]). They considered that the most likely cause was mechanical feedback from the drive or instantaneous speed fluctuations both of which could probably be overcome with a new drive using electronic speed control. It would be worthwhile checking this hypothesis by carrying out duplicate experiments in a machine with electronic speed control. Since significantly different molecular weight curves were obtained at 15°C and 25°C, Adams and Filmer considered that thermal gradients in the rotor could give rise to non-interlacing. While this is not likely to be the cause of non-interlacing with α-chymotrypsin which gave temperature independent molecular weight curves (see Chapter 3), it cannot be ruled out in the case of insulin since all experiments were carried out at 20°C.

Errors in optical constants could give rise to errors in molecular weight values but these errors would mainly effect the magnitude such that the whole molecular weight curve would be shifted to higher or lower values. An error in the value of

the fringe width would give rise to incorrect concentration (fringe) values but, since a small error in fringe width can be readily detected during the measuring of the fringe photographs, this type of error can be ruled out.

Distortion of the cell windows caused by the cell assembly procedure or by the centrifugal field was recognized as a possible source of error and was tested for by taking an interference photograph as soon as the operating speed had been reached and before redistribution of solute was noticeable. In the cases when horizontal fringes were not obtained in this interference photograph the cell was, after completion of the equilibrium run, emptied and cleaned without being dismantled and a "blank" run performed using buffer in each cell compartment. This procedure was only necessary for high speed sedimentation equilibrium experiments. The agreement between the value of the molecular weight of lysozyme found by other workers and that reported in Chapter 3 of this thesis indicated that any errors due to incorrect optical constants, optical misalignment or distortion were unlikely to cause the non-interlacing observed.

(4) Concentration Effect

Molecular weights calculated from experimental sedimentation equilibrium data are very sensitive to error in the initial concentration (j_o). An error in j_o of a few percent can cause curvature of a normally linear plot of

lnj versus x^2 giving rise to an incorrect value of molecular weight and indicating association in a system where there is none. In an associating system where the plot of lnj versus x^2 is curved an error in j could cause a change in the curvature and an error in calculated molecular weights.

The initial concentration of the protein stock solution of about 40 fringes can be determined to within 0.05 fringes by the differential refractometer and since protein solutions of lower initial concentration were prepared by weight dilution the initial concentrations were known very accurately. However, once the protein solution was placed in the cell compartment adsorption of the protein on the cell walls could have occurred since the ratio of surface area to volume in the cell is large. Adams and Filmer[24] pointed out that caution should be used when using data below 0.3 gm/dl (12 fringes for insulin). Application of the method of La Bar[101] could possibly overcome the problem of adsorption at low concentrations but owing to technical difficulties this method could not be tested. Increase of the initial concentration of protein by evaporation of solvent was minimised by preparing the protein solution from the stock solution and loading the cell within a period of twenty minutes.

Figure 4.4 illustrates the effect on the molecular weight curve assuming a 10% loss of protein by adsorption. The curve was obtained by inserting in the computer program a

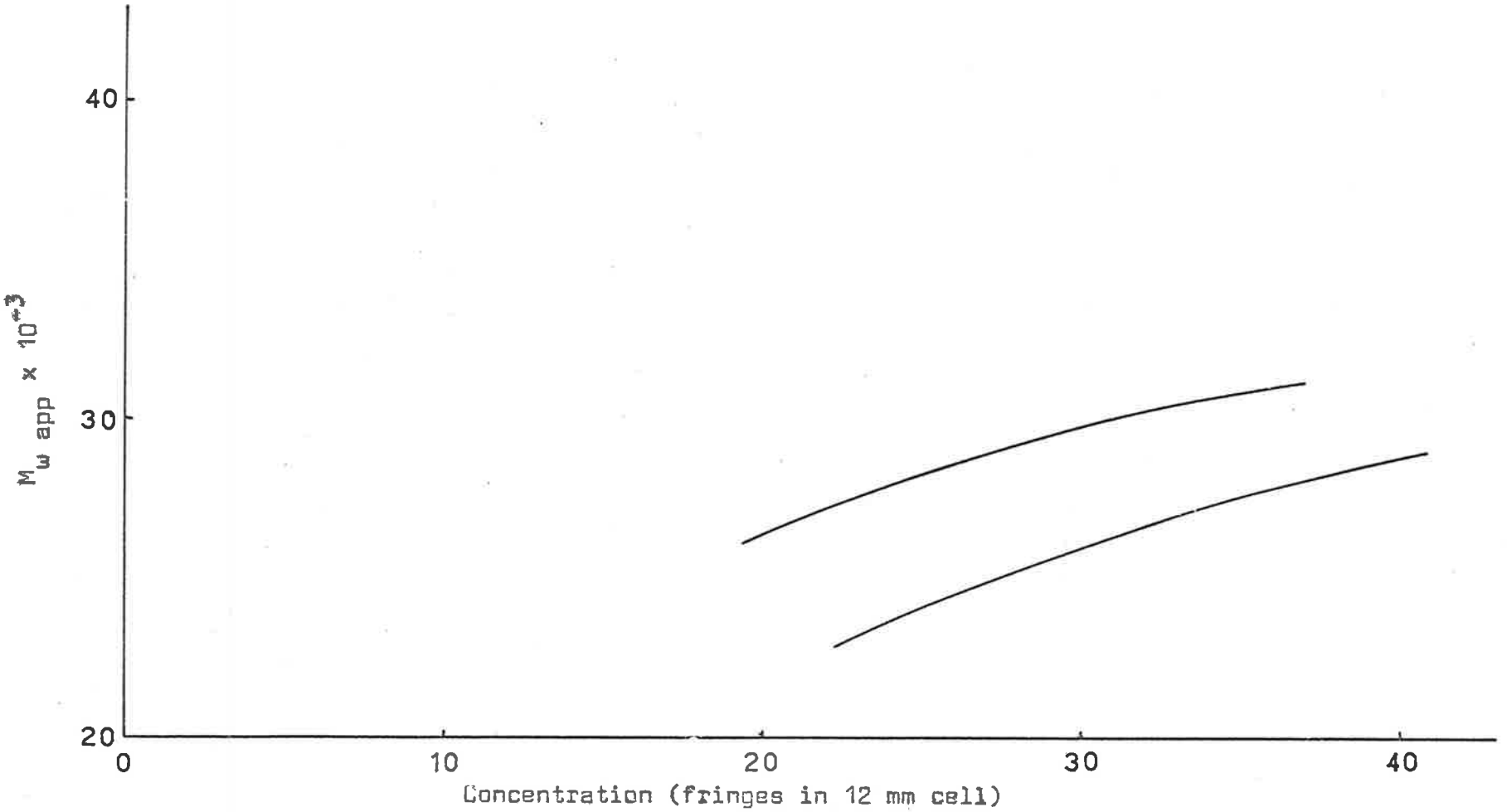

Fig. 4.4 : Illustration of the effect on calculated apparent weight average molecular weights of a lowering of solute concentration by adsorption on cell walls. The upper curve was calculated from the data in the lower curve assuming a 10% lowering of concentration.

value of j_D equal to 90% of that determined experimentally. It can be seen that, although the molecular weight values are radically different, the slope of the molecular weight versus concentration curve is not greatly changed even with this large change in concentration. Thus, since the slopes of the molecular weight curves from other experiments were also changed only slightly, it was considered that the non-interlacing could not be explained in terms of adsorption.

Two experiments were carried out at the same initial concentration to test the reproducibility of the experimental procedure. The solutions were prepared from the stock solution by separate weight dilutions prior to the sedimentation equilibrium runs which were performed on different days. The excellent agreement between the lnj versus x^2 data is evident in Fig. 4.5 .

(5) Chemical Causes of Non-interlacing

Kakiuchi[60], in his study of Bacillus Subtilis α-amylase, showed that this protein underwent reversible dimerisation through a zinc ion.

$$2 \text{ Monomers} + Zn^{2+} \rightleftharpoons \text{Dimer}$$

Since the dimerisation was dependent on the concentration of Zn^{2+} the plots of molecular weight versus concentration of protein from different sedimentation equilibrium experiments did

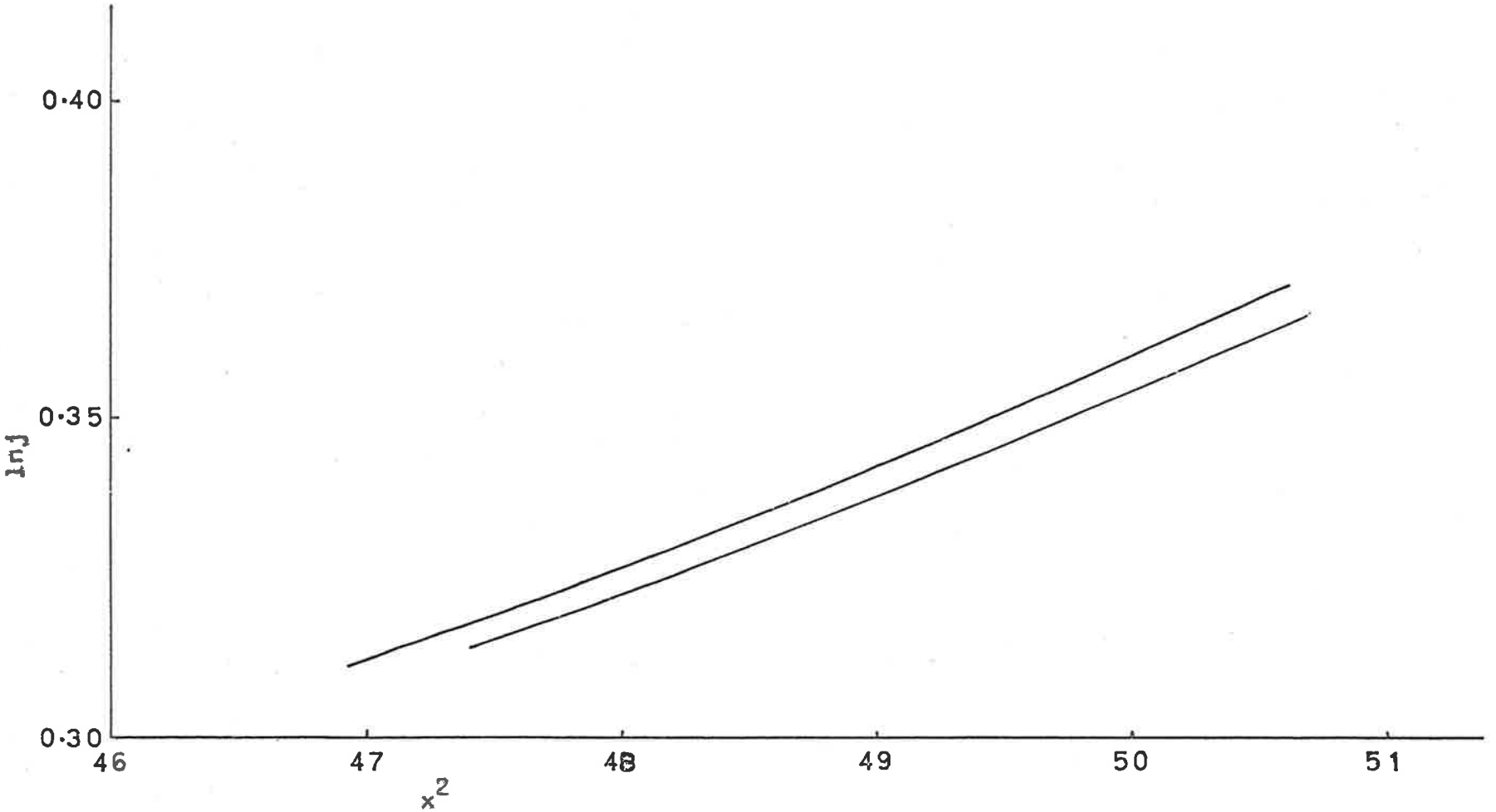

Fig. 4.5 : The natural logarithm of the concentration (fringes in 12 mm cell) as a function of x^2. The two curves resulted from different experiments at the same speed and temperature on 3 mm columns of 30 fringe insulin solution obtained from separate weight dilutions of stock.

not fall on a single curve. However, because of the simplicity of the reaction it was possible to analyse the sedimentation equilibrium data for the equilibrium constant by extension of the equations developed by Svedberg and Pederson[102]. This type of analysis would be impossible without knowledge of the stoichiometry of the association and the total concentrations of both protein and metal ion.

It is well known that the crystallization of insulin is dependent on the presence of zinc ions[103] and that association is promoted by zinc ions[48]. It is reasonable to assume that Zn^{2+} takes part in the association in a manner similar to that shown for Bacillus Subtilis α-amylase. The stoichiometry of the association reaction for insulin is not known but from the magnitude of the molecular weights (greater than 100,000) indicated from sedimentation velocity studies in the presence of Zn^{2+} it is obvious that the reaction is complex and includes species much higher than the dimer.

Since it is theoretically possible to analyse an association involving a metal ion, sedimentation equilibrium runs on insulin in barbiturate buffer pH 8.0 and 0.1 ionic strength containing 5×10^{-5} M Zn^{2+} were performed at 20^{0}C. The results of these runs are shown in Fig. 4.6 . The very poor reproducibility of the molecular weight curves at low initial concentration of protein was noted and this line of experimentation was discontinued. The data shown in Fig. 4.6

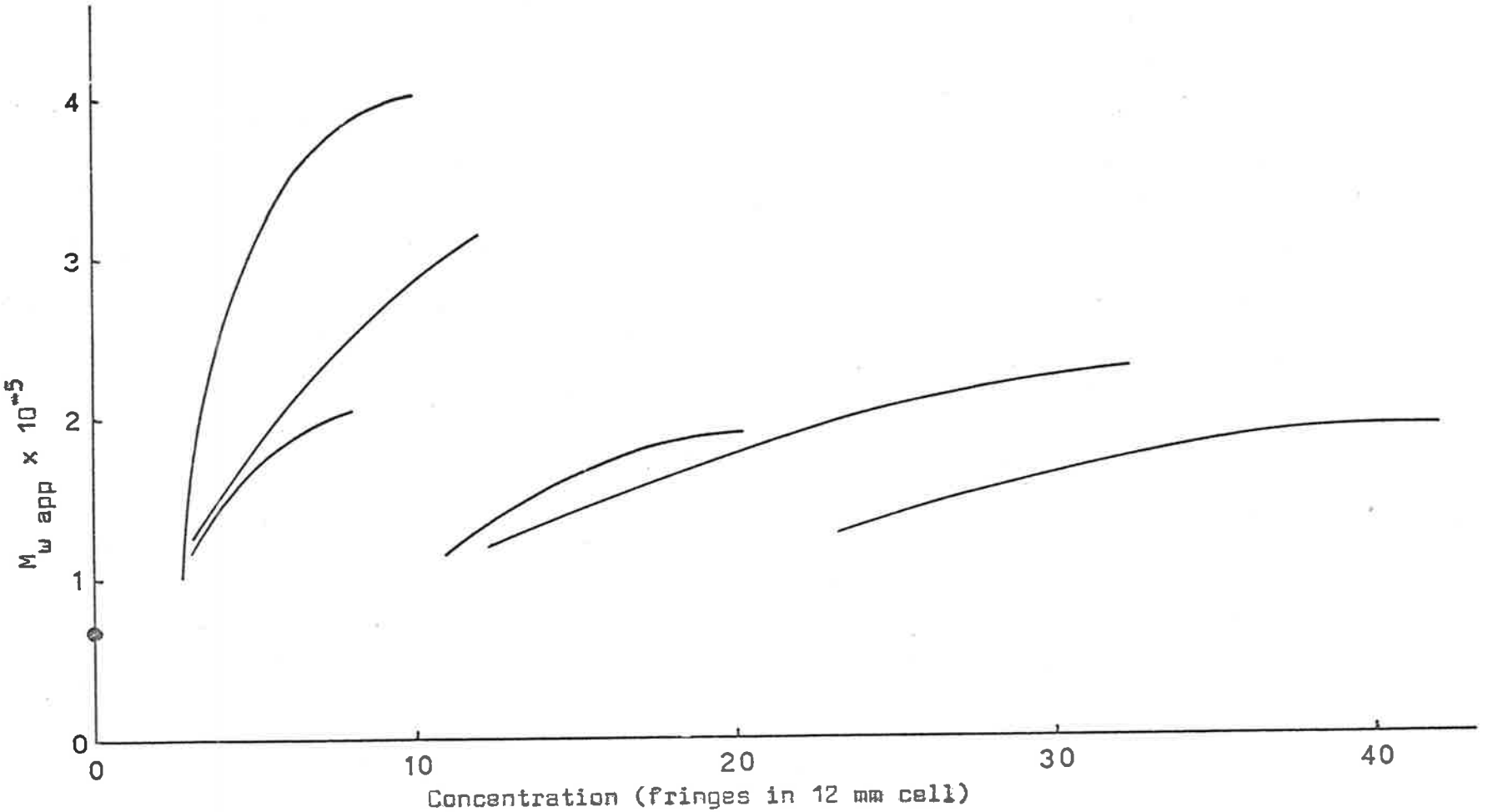

Fig. 4.6 : Apparent weight average molecular weight as a function of concentration of insulin in barbiturate buffer pH 8.0, I = 0.1 including 5×10^{-5} M Zn^{2+}. The data were obtained from sedimentation equilibrium experiments on 3 mm solution columns at $20^{\circ}C$.

are interesting in that they illustrate the marked effect of Zn^{2+} on the molecular weight. The minimum molecular weight of 68,000 obtained from high speed sedimentation equilibrium experiments at two widely different speeds (20,410 rpm and 44,770 rpm) was unexpectedly high and indicated that the main effect of Zn^{2+} was on associations up to the hexamer (of 12,000 molecular weight unit).

Roark and Yphantis[68] pointed out that non-interlacing would occur in a system where a proportion of a monomer homogeneous with respect to molecular weight had been altered in such a way that the association constants were markedly different, e.g.

$$2A \rightleftharpoons D \qquad\qquad 2A' \rightleftharpoons D'$$

$$A+D \rightleftharpoons T \qquad\qquad A'+D' \rightleftharpoons T'$$

where

$$K_2 \gg K_2'$$

$$K_3 \gg K_3'$$

This possibility gained some support from the observation of Cunningham et. al.[58] that zinc-free insulin is electrophoretically heterogeneous, giving rise to two peaks, one of which disappears when zinc is bound. Keeping in mind the

extreme effect of Zn^{2+} and other heavy metal ions on the degree of association of insulin it appeared that the above situation could arise if there was incomplete elimination of Zn^{2+} from solution or if heavy metal ions were leached from glassware (e.g. sapphire cell windows) or the cell centrepiece. Association constants for equilibria including Zn^{2+} would be expected to be much greater than those for the equivalent association excluding Zn^{2+} because of the much larger molecular weights observed in the presence of Zn^{2+} (See Fig. 4.6 and reference 48). Beef heart lactate dehydrogenase had previously been shown[104] to leach metal ions from glassware or cell centrepieces resulting, in some cases, in precipitation. This problem was completely overcome by coating all glassware and cell centrepieces with 1:25 dilution of Beckman Desicote in chloroform. Accordingly a series of sedimentation equilibrium runs was carried out incorporating the use of Desicote as a coating on all glassware and the cell centrepiece. Barbiturate buffer pH 8.0 and 0.1 ionic strength including 10^{-4}M EDTA was used and the experiments performed at 20^{0}C. The results of these experiments are shown in Fig. 4.7 . Since the non-interlacing exhibited is worse than in the previous zinc-free insulin series (Fig. 4.1) it is unlikely that any Zn^{2+} or similar ion is the cause of non-interlacing. However, this does not rule out the possibility of a "two-pathway" association, of the type referred to by Roark and Yphantis[68], without the

participation of Zn^{2+}. A theoretical treatment of this type of system has been proposed by Steiner[105] but the method involves the use of number average molecular weight and solubility information which could not be obtained.

In studies on β-lactoglobulins A and B it was found that data from different experiments did not interlace due to a reaction between the protein and the layering oil. By omitting the layering oil good interlacing was obtained. However, in the course of the study of α-chymotrypsin and insulin, no similar reaction was apparent since no precipitate was observed at the solution-oil interface, nor was there any significant difference between interference patterns photographed at 20 hours and 24 hours, so that a time dependent reaction seemed unlikely.

One of the effects of the presence of monomer or higher species which cannot take part in association-dissociation reactions is to produce non-interlacing of molecular weight curves obtained from sedimentation equilibrium experiments at different initial concentrations. These incompetent species could be produced as a result of one or more of the processes used to extract and purify the protein. Haschemeyer and Bowers[124] have put forward a theory for the analysis of a system containing incompetent species but with the limitation that at least one species is fully competent. This theory was applied to the zinc-free insulin data and the results are reported in Section 4-III.

III ANALYSIS OF ZINC-FREE INSULIN DATA

(1) Theory

The following analysis is based on that of Haschemeyer and Bowers[124]. At sedimentation equilibrium the distribution of an ideal solute, i, of molecular weight M_i, is given by

$$\frac{d\ln c_i}{d(x^2)} = \frac{M_i(1 - \bar{v}\rho)\omega^2}{2RT} = H_i \qquad 4(1)$$

where c_i is the concentration at the radial position x and the other symbols are as defined previously. Where several solutes coexist the total concentration at each radial position c(x), is the sum of the individual solute concentrations $c_i(x)$, obtained by integration of equation 4(1) between the meniscus position x_m, and x. Thus

$$c(x) = \sum_i c_{im} e^{H_i(x^2 - x_m^2)} \qquad 4(2)$$

where c_{im} is the concentration of solute i at the meniscus. This equation may be rewritten as

$$c(x) = \sum_i c_{im} e^{iH(x^2 - x_m^2)} \qquad 4(3)$$

for self-associating systems if it is assumed that $\bar{v}$ is unchanged by the association. For ideal self-associating

systems the relation between the total concentration and that of each component may be written in terms of the monomer concentration c_1 and the equilibrium constant for the i-th association. Thus

$$c = \sum_i K_i c_1^i \qquad 4(4)$$

where K_1 is unity. The distribution for a purely self-associating system is obtained by substitution of equation 4(4) in equation 4(3)

$$c(x) = \sum_i K_i c_{1m}^i \, e^{iH(x^2 - x_m^2)} \qquad 4(5)$$

If the system contains a proportion of incompetent molecules (i.e. molecules unable to take part in the association) then the concentration of the i-th species must be considered as the sum of the concentrations of competent (cc) and incompetent (cI) molecules. Then c_{im} becomes

$$c_{im} = cI_{im} + cc_{im} = cI_{im} + cc_{1m}^i K_i \qquad 4(6)$$

and equation 4(5) becomes

$$c(x) = \sum_i (cI_{im} + cc_{1m}^i K_i) \, e^{iH(x^2 - x_m^2)} \qquad 4(7)$$

For each sedimentation equilibrium experiment c(x) is measured as a function of x, and, as the monomer molecular weight is known, the only unknowns are the values of c_{im}. These unknowns can be evaluated for associating systems, whether or not incompetent species are present, by rewriting equation 4(3) in the following way

$$\underset{\sim}{b} = P\underset{\sim}{c} \qquad 4(8)$$

where P is an l x n matrix of $e^{iH(x^2 - x_m^2)}$, $\underset{\sim}{b}$ is the l x 1 vector of c(x), and $\underset{\sim}{c}$ is the n x 1 unknown vector of c_{im}. The number (l) of simultaneous equations in c_{im} obtained from a sedimentation equilibrium experiment is invariably greater than the number (n) required for a unique solution (the solution is said to be over-determined), and because the equations are obtained from experimental results there is no solution which will satisfy all equations exactly i.e. it is impossible to solve

$$\underset{\sim}{0} = P\underset{\sim}{c} - \underset{\sim}{b}$$

Hence for each proposed "solution" there is a non-zero remainder given by

$$\underset{\sim}{r} = P\underset{\sim}{c} - \underset{\sim}{b} \qquad 4(9)$$

The "solution" chosen is the one which minimises the sum of

the squares of the remainder i.e. $\underset{\sim}{r}^T\underset{\sim}{r}$ (where $\underset{\sim}{r}^T$ is the transpose of $\underset{\sim}{r}$) is minimised. It can be shown[125] that this occurs when

$$M\underset{\sim}{c} = P^T\underset{\sim}{b} \qquad 4(10)$$

where $M = P^TP$ is an n x n matrix. A solution for $\underset{\sim}{c}$ can then be obtained by standard matrix inversion methods. Since the combination of i values represents the set of species present (e.g. i = 1,2,4 represents a monomer-dimer-tetramer system) there are many possible combinations of i values. However, combinations resulting in any $c_{im} < 0$ are discarded since negative concentrations are meaningless.

Conservation of mass requires that $\int_{x_m}^{x_b} c(x)\, dx^2$ is unchanged by redistribution due to sedimentation. Since, before sedimentation, $c(x) = c_o$ the statement of conservation of mass becomes

$$c_o(x_b^2 - x_m^2) = \int_{x_m}^{x_b} c(x)\, dx^2 \qquad 4(11)$$

and c_o can be evaluated by integration of the experimental c(x) curve. In considering the conservation of mass it is necessary to differentiate between associating and non-associating species[126]. Thus for non-associating systems equation 4(11) may be written separately for each component

to give, after rearrangement

$$c_{io} = \frac{1}{x_b^2 - x_m^2} \int_{x_m}^{x_b} c_i(x)dx^2 = c_{im}\left[\frac{e^{H_i(x_b^2 - x_m^2)}}{(x_b^2 - x_m^2)H_i}\right] - 1 \qquad 4(12)$$

while for self-associating systems the appropriate expression is

$$c_o = \sum_i c_{io}$$

$$= \sum_i c_{im}\left[\frac{e^{iH(x_b^2 - x_m^2)}}{(x_b^2 - x_m^2)iH}\right] - 1$$

$$= \sum_i c_{1m}{}^i K_i E_i \qquad 4(13)$$

When incompetent molecules are present the molecular weight curves from different experiments (performed at different speeds and/or initial concentrations) do not interlace in the regions where the concentration ranges overlap. However, the molecular weight distributions may be analysed for the special case where at least one species is fully competent. Since both the fraction of the incompetent species in the solutions and the equilibrium constants are the same for all experiments, it is possible to develop an

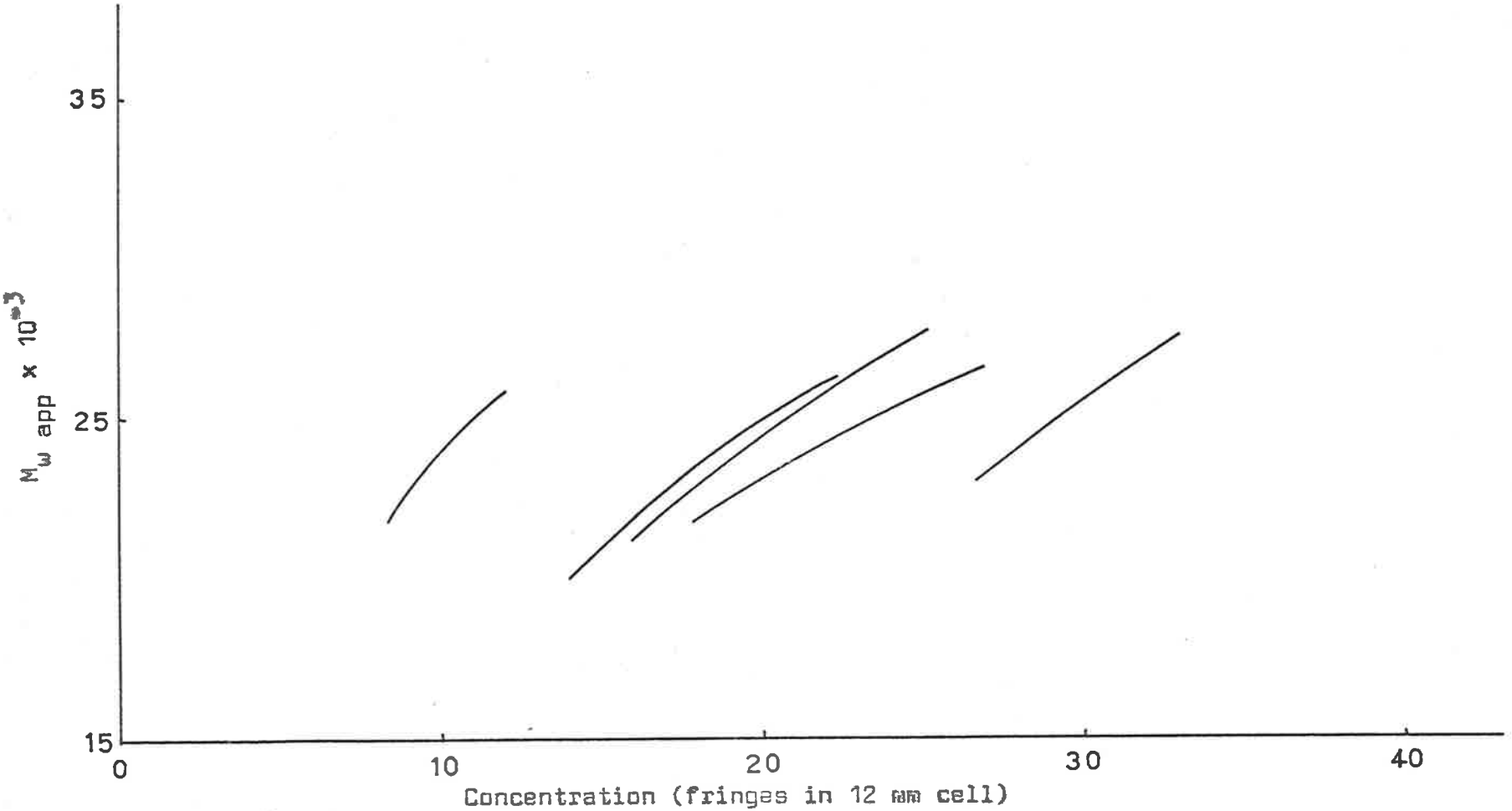

Fig. 4.7 : Apparent weight average molecular weight as a function of concentration of zinc-free insulin in barbiturate buffer pH 8.0, I = 0.1 including 10^{-4} M EDTA. The data were obtained from sedimentation equilibrium experiments on 3 mm solution columns at 20°C.

equation for the concentration of incompetent monomer in terms of the fully competent species i. Thus for a pair of experiments

$$cI_{1m} = \frac{c_{1m}' \left(\frac{c_{im}}{c_{im}'}\right)^{1/i} - c_{1m}}{f \left(\frac{c_{im}}{c_{im}'}\right)^{1/i} \frac{E_1}{E_1'} - 1} \qquad 4(14)$$

where ' quantities refer to the second experiment, $f = \frac{c_o'}{c_o}$ and i refers to the fully competent species. It is then possible to calculate the various equilibrium constants from

$$K_i = \frac{f\, c_{im} \frac{E_i}{E_i'} - c_{im}'}{f\, cc_{im}{}^{i} \frac{E_i}{E_i'} - cc_{im}{}'^{i}} \qquad 4(15)$$

In the analysis of the zinc-free insulin data it was necessary to assume that the monomer was fully competent and therefore an equation similar to 4(14) was required for solution of cI_{im} where $i > 1$. It can be shown that the appropriate equation is

$$cI_{im} = \frac{c_{im}' \left(\frac{c_{1m}}{c_{1m}'}\right)^{i} - c_{im}}{f \left(\frac{c_{1m}}{c_{1m}'}\right)^{i} \frac{E_i}{E_i'} - 1} \qquad 4(16)$$

For the associating proportion of species i , $cc_{im} = c_{1m}{}^{i}K_i$ and therefore

$$\frac{cc_{im}}{cc'_{im}} = \left(\frac{c_{1m}}{c'_{1m}}\right)^{i} \qquad 4(17)$$

Substitution of $c_{im} = cI_{im} + cc_{im}$, $\frac{c'_o}{c_o} = f$ and equation 4(17) into 4(16) followed by rearrangement gives

$$\frac{cI_{io}}{c_o} = \frac{cI_{io}'}{c'_o}$$

which is a statement of the assumption that, in the initial solution, the fraction of incompetent i-mer is identical for all experiments.

(2) Application of Theory

The sedimentation equilibrium data from experiments with zinc-free insulin in barbiturate buffer pH 8.0 and 0.1 ionic strength were analyzed according to the theory of Haschemeyer and Bowers. Each experiment gave a set of molecular weight versus concentration data which formed a set of over-determined linear equations of the type shown in equation 4(3). These equations were solved for c_{im} using a computer program (See program EXPO Appendix C). Although equation 4(3) was derived for a purely self-associating

system, it was valid to use this equation since later equations for systems containing incompetent material were derived from it (See derivation of equation 4(7)).

The values of iH were calculated assuming a monomer molecular weight of 12,000 and the self-association models tested were as shown in Table 4.1 where X denotes the species assumed present.

Table 4.1

Self-association models tested

Monomer	Dimer	Trimer	Tetramer	Pentamer	Hexamer	Shown in EXPO as
X	X	X	X	X	X	Combination 2,4,6, 8,10,12
X	X	X			X	Combination 2,4,6, 12
X	X	X				Combination 2,4,6
X		X			X	Combination 2,6,12
X		X				Combination 2,6

Of the models tested, the only ones which gave physically possible values of c_{im} for all sedimentation equilibrium experiments were the monomer-trimer-hexamer and monomer-trimer models. The c_{im} values, obtained for these models by analysis of the molecular weight data from each sedimentation equilibrium experiment, are shown in Table 4.2 .

Table 4.2

EXPERIMENT	UC87	UC83	UC85	UC92	UC86
CONCENTRATION (fringes)					
c_o	9.98	14.85	19.98	30.00	35.23
Monomer-trimer-hexamer					
c_{1m}	4.98	7.83	9.64	12.89	16.40
c_{3m}	1.56	3.43	5.88	8.13	12.61
c_{6m}	0.05	0.13	0.18	0.76	0.76
Monomer-trimer					
c_{1m}	4.67	7.40	9.11	10.27	14.65
c_{3m}	1.87	3.96	6.57	11.33	15.08

The analysis thus far was directed towards finding the species present in solution and no assumption about the presence of incompetent species had been made.

For completeness the analysis included various self-association models in which the monomer molecular weight was assumed to be 6,000. However, in all such cases the solutions included values of c_{im} which were physically impossible (i.e. $c_{im} < 0$ or $c_{im} > c_o$) thus indirectly supporting the experimental determination of a 12,000 molecular weight unit as the monomer under the conditions employed.

(a) Model 1 : Monomer-trimer-hexamer

Since experiments UC87 and UC83 had overlapping concentration ranges they were paired and analyzed. The

c_{1m} and c_{3m} values from Table 4.2 were used in equation 4(14) to evaluate the meniscus concentration of incompetent monomer for UC87 (cI_{1m87}) assuming that the trimer was the fully competent species. In this calculation the quantities denoted by ' referred to the UC83 values. The calculation was repeated using the UC87 values as the ' quantities in order to evaluate cI_{1m83}. Experiments UC83 and UC85 were also paired and the above procedure used to evaluate cI_{1m83} and cI_{1m85}. The results of these calculations are shown in Table 4.3 . Since the values of cI_{1m83}, evaluated from different pairs of experiments, are not equal it was concluded that the assumption of fully competent trimer was incorrect.

Evaluation of cI_{1m} values for the two pairs of experiments was repeated assuming fully competent hexamer. The results, shown in Table 4.3, indicate that the assumption of fully competent hexamer was incorrect.

Table 4.3

Calculated meniscus concentrations of incompetent monomer assuming fully competent trimer or hexamer.

	Competent Trimer	Competent Hexamer
cI_{1m87}	3.94	4.22
cI_{1m83}	0.64	2.25
cI_{1m83}	6.48	6.94
cI_{1m85}	1.04	3.96

Equation 4(16) was then developed so that cI_{3m} and cI_{6m} values could be evaluated assuming fully competent monomer. The results obtained from the same two pairs of experiments are shown in Table 4.4 .

Table 4.4

Calculated meniscus concentrations of incompetent trimer and hexamer assuming fully competent monomer.

	Trimer (i=3)	Hexamer (i=6)
cI_{im87}	1.70	0.05
cI_{im83}	3.46	0.10
cI_{im83}	3.47	0.13
cI_{im85}	5.90	0.17

From Table 4.4 it is apparent that the values of cI_{3m83} (3.46 and 3.47) evaluated from the two different pairs of experiments are in excellent agreement and that the corresponding cI_{6m83} values (0.10 and 0.13) agree quite well. Since this agreement supported the assumption that the system contained fully competent monomer the next step in the analysis was the evaluation of the meniscus concentration of competent trimer (cc_{3m}) and hexamer (cc_{6m}) using equation 4(6). These quantities, evaluated from the cI_{im} values in Table 4.4

and c_{im} values in Table 4.2 are shown in Table 4.5 .

Table 4.5

Calculated meniscus concentrations of competent trimer and hexamer assuming fully competent monomer.

	Trimer (i=3)	Hexamer (i=6)
cc_{im87}	-0.14	0.00
cc_{im83} (a)	-0.03	0.01
cc_{im85}	-0.02	0.01

(a) Average values of cI_{im83} used.

Although negative concentrations are physically impossible it is apparent from Table 4.5 that, except for cc_{3m87}, all cc_{im} values are close to zero. If the cc_{3m87} value is ignored these results imply that both the trimer and the hexamer are completely incompetent. However, this contradicts the assumption of fully competent monomer since the fully competent monomer must be in equilibrium with some competent trimer or hexamer. Thus the monomer-trimer-hexamer system with fully competent monomer cannot explain the data.

Alternatively the complete incompetence of trimer and hexamer could be interpreted as meaning that the monomer is also completely incompetent giving rise to a model in which

monomer, trimer and hexamer are present but do not undergo association or dissociation. For such a model the fraction of each species in the initial solution, $\frac{cI_{io}}{c_o}$, should be the same in each experiment. Table 4.6 shows these values calculated for experiments UC83, UC85 and UC87.

Table 4.6

	UC87	UC83	UC85
$\frac{cI_{10}}{c_o}$	0.639	0.611	0.465
$\frac{cI_{30}}{c_o}$	0.340	0.367	0.369
$\frac{cI_{60}}{c_o}$	0.027	0.023	0.017

The $\frac{cI_{io}}{c_o}$ values from UC87 and UC83 agree quite well but the values from UC85 are quite different except for $\frac{cI_{30}}{c_o}$. Since there was agreement between UC87 and UC83 the values of $\frac{cI_{io}}{c_o}$ from these experiments were averaged and used to calculate the molecular weight curves shown in Fig. 4.8. As might be expected the agreement between calculated and experimental curves is best for the low concentration experiments UC87 and UC83. However, the calculated curves do

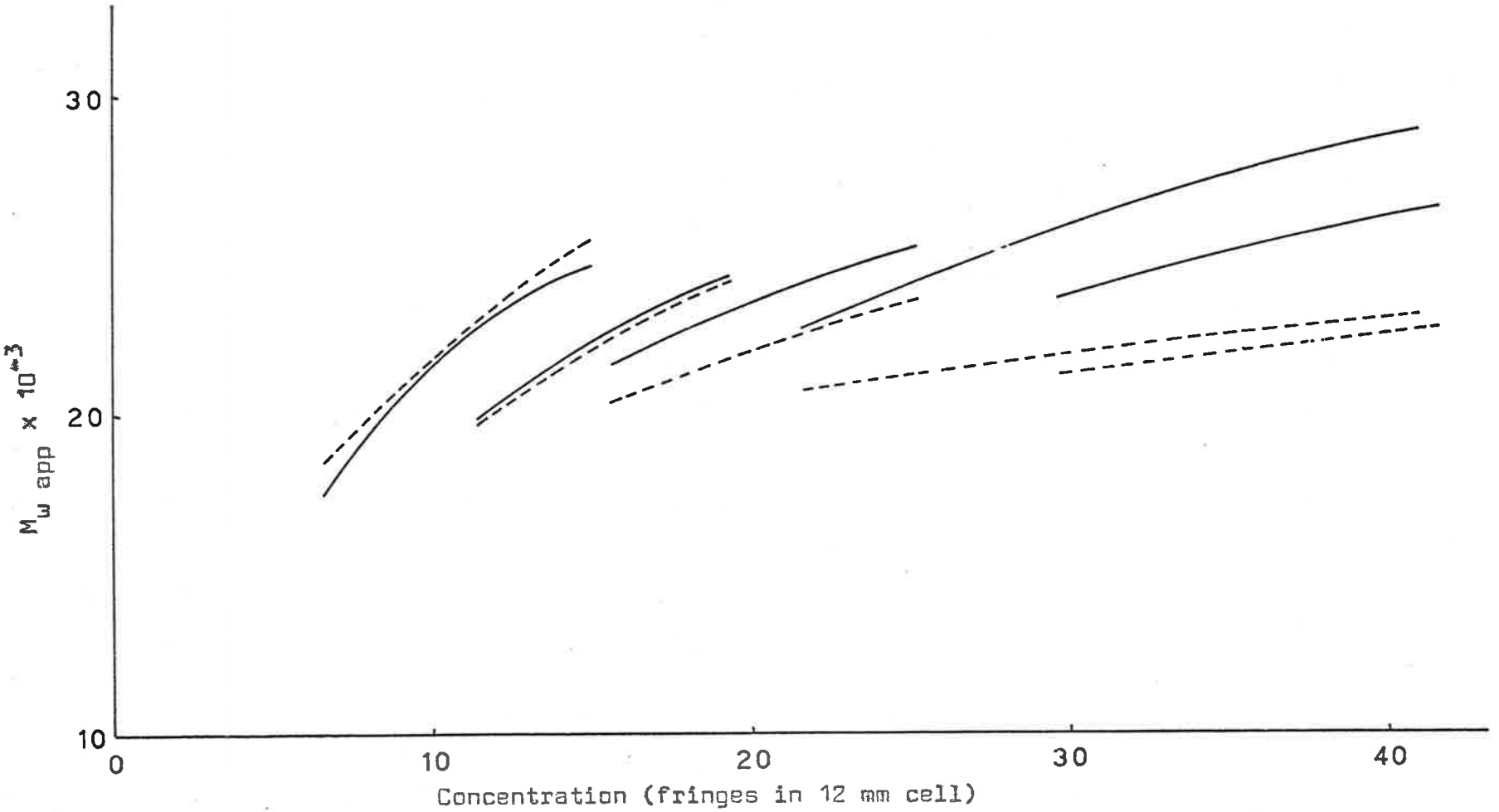

Fig. 4.8 : Application of Haschemeyer and Bowers theory to the experimental data represented by the solid lines. The broken lines were calculated for a solution containing non-associating (incompetent) monomer, trimer and hexamer species such that

$$\frac{cI_{10}}{c_0} = 0.625, \quad \frac{cI_{30}}{c_0} = 0.353 \quad \text{and} \quad \frac{cI_{60}}{c_0} = 0.025 .$$

not agree with the experimental curves from experiments at higher initial concentrations and it must be concluded that the non-associating three-species model is incorrect.

(b) Model 2 : Monomer-trimer

The procedure used for this model was the same as that used for Model 1. The experiments were paired as before and cI_{1m} values calculated using equation 4(14). However, all calculated cI_{1m} values were physically impossible and the assumption that the trimer was completely competent was discarded. Next, the monomer was assumed completely competent and equation 4(16) was used to calculate values for the meniscus concentration of incompetent trimer cI_{3m}. These are shown in Table 4.7 .

Table 4.7

Calculated meniscus concentrations of incompetent trimer and fraction of incompetent trimer, assuming fully competent monomer.

	cI_{3m}	$\frac{cI_{30}}{c_o}$
UC87	0.63	0.137
UC83	1.26	0.135
UC83	1.03	0.110
UC85	2.04	0.128

The cI_{3m83} values, calculated from different pairs of experiments, showed reasonable agreement but not as good as the agreement obtained for Model 1. For the monomer-trimer model with fully competent monomer to be correct the fraction of incompetent trimer in the initial solution ($\frac{cI_{30}}{c_0}$) should be the same in all experiments. These values, shown in Table 4.7, agreed well enough to warrant the calculation of the equilibrium constant, K_3, by application of equation 4(15). The average value of $K_3 = 7(\pm 1)\times 10^{-3}$ was the same as that calculated using the much simpler equation

$$cc_{im} = c_{1m}{}^{i} K_i$$

Molecular weight curves computed using the average values of $\frac{cI_{30}}{c_0}$ and K_3 are shown in Fig. 4.9 . From the lack of agreement between the calculated and experimental curves it is evident that this model fails to explain the experimental data.

Since neither of the models tested fits the data adequately it must be concluded that the system cannot be analyzed by the Haschemeyer and Bowers theory. This means only that it cannot be assumed that one species is completely competent. Therefore the possibility remains that a monomer-trimer-hexamer or a monomer-trimer association may be present in which a fraction of all species is incompetent.

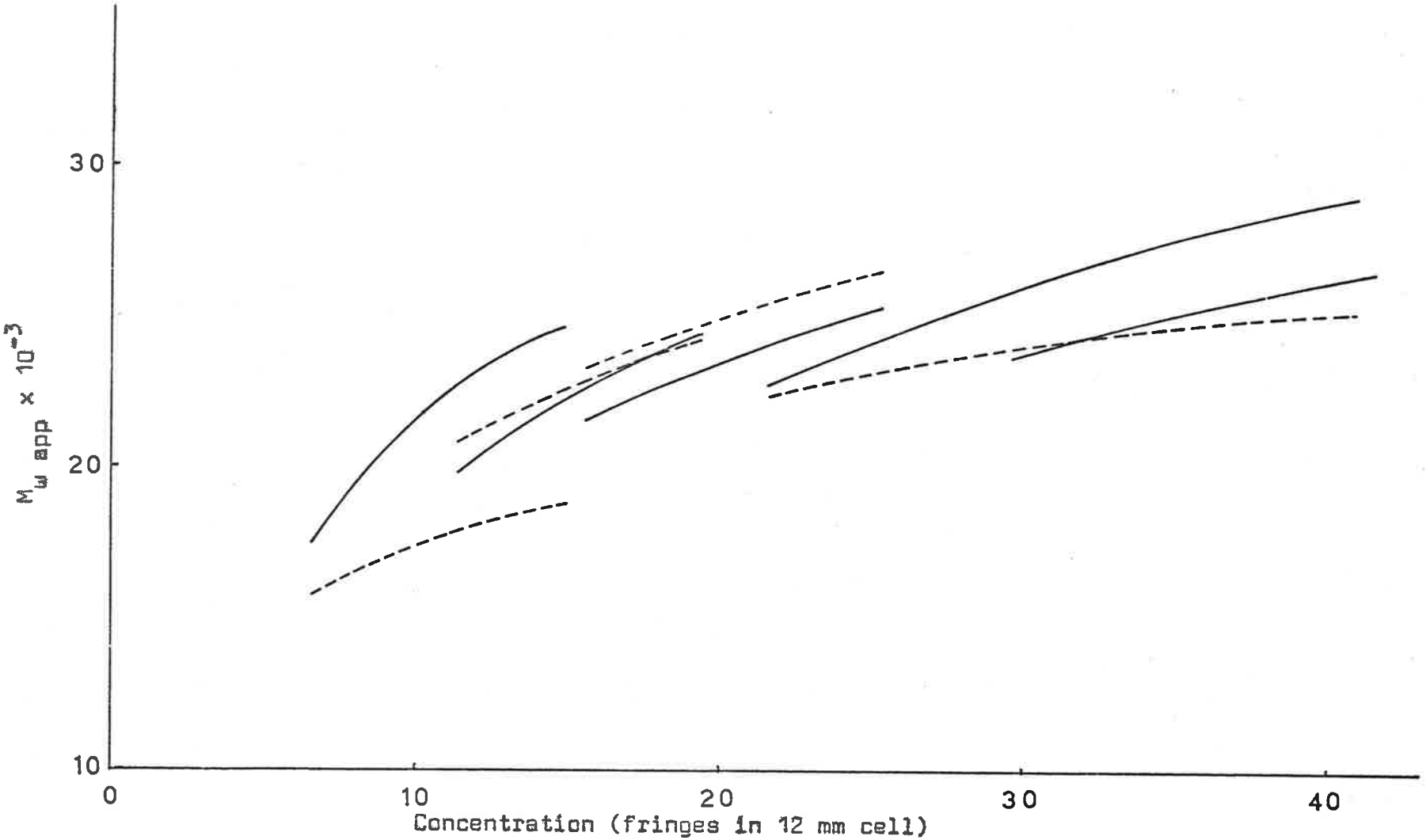

Fig. 4.9 : Application of Haschemeyer and Bowers theory to the experimental data represented by the solid lines. The broken lines were calculated for a solution containing fully competent monomer in self-association equilibrium with trimer such that $\frac{cI_{30}}{c_0} = 0.128$ and $K_3 = 7 \times 10^{-3}$ fringe^{-2}.

IV GENERAL DISCUSSION

The initial aim of the research reported here was to test the various theories available for analysis of the concentration dependent molecular weight curves of self-associating protein systems. It was frequently found that non-interlacing molecular weight curves were obtained from sedimentation equilibrium experiments at different initial protein concentrations. The phenomenon of non-interlacing had previously been reported and, although many possible causes had been advanced, no satisfactory explanation has been put forward. Since interlacing of molecular weight curve segments is necessary for the application of a number of analytical methods developed for simple self-association, the cause of the non-interlacing was sought. To this end many sedimentation experiments were carried out to test a number of possible causes. A photographic plate measuring device was developed to obtain data free from subjective bias (See Appendix A). Computer programs were developed to analyze the data and, in the case of the Adams analysis (Chapter 3, section V (2)), the method was tested on simulated molecular weight data.

It is believed that adequate tests and control experiments were carried out to check the accuracy of the ultracentrifuge and the techniques used and therefore that the non-interlacing was a real effect due to complex

self-association. The results obtained with the α-chymotrypsin system (discussed in Chapter 3) pointed to autolysis as a possible cause and a complicating factor which could not be completely eliminated by inhibition of the protein. For the insulin system there is the possibility of a 2-pathway association (which could not be tested) and/or the presence of impurities. It is possible that impurities such as "big insulin", referred to by Roth et. al.[127], or pro-insulin[128] might affect the association since it is unlikely that impurities of this size would be removed by dialysis or G-25 sephadex chromatography. The insulin used for the work reported in this thesis was obtained from the same supplier as that used by Jeffrey[19,49] and each molecular weight species had been found to behave in a fully competent manner. Hence the difficulties reported were not expected despite the different pH of solution and known sensitivity of insulin towards metal ions at pH greater than 7. Particular attention was paid to the possibility of pressure dependence of the insulin self-association. However, the results of both equilibrium and velocity experiments showed clearly that there is no significant effect of pressure on the insulin system.

It must be emphasized that satisfactory interlacing of molecular weight curves has been observed for some self-associating systems. The self-associations of purine[129],

cytodine[130] and adenosine-5'-phosphate[131] have been investigated and in each case good interlacing was found. This may have been due to the fact that these are low molecular weight, non-protein substances which are relatively easily purified. However, the self-association of the proteins β-lactoglobulin A[26] and β-lactoglobulin B[66] have been successfully studied by the sedimentation equilibrium method since good interlacing of molecular weight curve segments was obtained. In the latter case the variation in molecular weight from one segment to the next appeared to be 500 or less whereas for the former, agreement between segments was good at higher concentrations but at approximately 15 fringes concentration the variation in $\frac{M_1}{M_{w\ app}}$ indicated a difference in molecular weight of 4,500. An interesting facet of the investigation of the β-lactoglobulins was the initial failure of the segments to interlace due to interaction of the protein with layering oils, and the subsequent interlacing of segments when the oil was omitted. It is unlikely that a similar effect could be responsible for the non-interlacing reported in this thesis since no precipitation of protein was observed and the calculated molecular weight distributions did not change significantly with time after reaching equilibrium.

In a study of the self-association of chymotrypsinogen A, Nichol[132] encountered non-interlacing molecular weight

curve segments, but was able to dismiss interaction of the protein with layering oil or aluminium salts as possible causes. However, he was not able to eliminate either pressure effects or heterogeneity as a cause of the non-interlacing. Nichol also found that self-association of chymotrypsinogen A increased with decreasing ionic strength but was not affected by temperature in agreement with the findings reported here for α-chymotrypsin and indicating that the mode of association is similar for both proteins. In a subsequent study of chymotrypsinogen A by Hancock and Williams[133] the interlacing was satisfactory at low concentrations (molecular weight deviations of 500 or less) but not as good at higher concentrations where the maximum deviation was about 1,000. Hancock and Williams held the opinion that the better conformity to the simple theoretical requirement of a smooth molecular weight versus concentration curve was due to improved precision of the experimental results.

It appears therefore that, apart from careful experimental technique, the most important single factor to be considered in a study of protein self-association is the homogeneity of the protein. It is suggested that any study of self-association should be preceded by a study of the homogeneity of the protein not only from the point of view of molecular weight of the monomer but also from the point of view of the charge. While this may not be sufficient to

separate competent and incompetent monomers, it should be sufficient to eliminate radically different forms of the same protein and simplify the system. If the main aim is to test analytical methods, it is also necessary to take care in choosing a system which is not likely to be complicated by side reactions such as autolysis. However, in general, it is the protein itself which is of interest and therefore there will be many protein systems to which analytical methods may only be applied in a semi-quantitative manner.

Chapter 5

EXPERIMENTAL

I GENERAL

Bovine pancreatic α-chymotrypsin was obtained from the Sigma Chemical Company (lot number 113 B - 0130) and from the Worthington Biochemical Corporation (three-times-crystallized CDI 6127-8). Anhydro-α-chymotrypsin was prepared from Worthington α-chymotrypsin by the method of Weiner et. al.[94] and the degree of inhibition determined by an adaptation of the method of Snoke and Neurath[106].

The assay was based on the α-chymotrypsin catalyzed hydrolysis of the specific substrate N-acetyl-L-tyrosine ethyl ester.

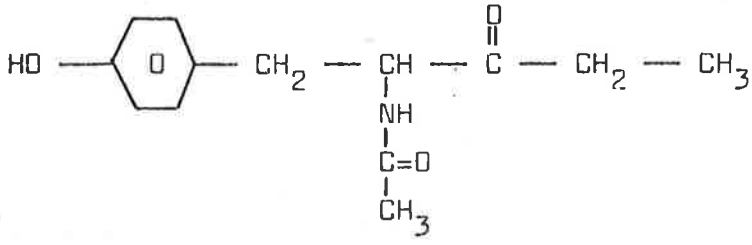

N-acetyl-L-tyrosine ethyl ester

On hydrolysis the ester ($R-\overset{O}{\overset{\|}{C}}-X$) released acid ($R-\overset{O}{\overset{\|}{C}}-OH$) at an initial rate determined by the concentration and activity of the enzyme (H-E) in accordance with the reaction scheme

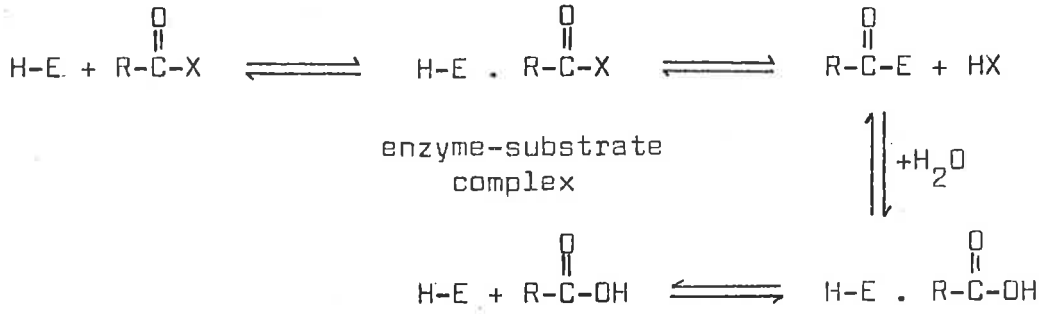

The assay was carried out in 0.05 ionic strength phosphate buffer pH 7.8 containing 30 percent by volume of methanol. The reaction mixture consisted of (a) 4 ml phosphate buffer

(b) 5 ml 0.015 M N-acetyl-L-tyrosine ethyl ester in phosphate buffer

(c) 1 ml enzyme solution in phosphate buffer.

Solutions (a) and (b) were placed in the reaction vessel of a Radiometer automatic titration unit set to act as a pH-stat. The syringe was filled with 0.204 M sodium hydroxide and the reaction started by addition of solution (c). The volume of sodium hydroxide required to neutralize the liberated acid was recorded as a function of time on the attached titrigraph. Comparison of the slopes of the linear graphs, for equal concentrations of α-chymotrypsin and anhydro-α-chymotrypsin, showed the activity of the latter to be 0.71% of the former.

Bovine zinc insulin from the Australian Commonwealth Serum Laboratories (pool 33 unmodified B 584-06) was used in all insulin experiments.

Sucrose and all buffer salts used were analytical grade reagents, and all solutions were prepared with glass distilled water. The pH was measured with a Radiometer PHM4 pH meter, standardised with 0.05 M potassium hydrogen phthalate. The compositions of the various buffers used in the sedimentation experiments are shown in tables 5.1 and 5.2 . All buffers were made up to one litre.

Table 5.1

Buffers used in experiments with α-chymotrypsin

pH	Ionic Strength	Tris[a](gm)	KNO_3(gm)	$Ca(NO_3)_2$(gm)	EDTA[b](gm)	HNO_3[c](ml)
7.6	0.05	3.1495	-	1.6410	-	10.91
8.4	0.05	17.0802	-	1.6410	-	27.28
7.6	0.05	7.8012	-	-	-	27.28
7.6	0.20	31.1320	-	-	-	109.12
7.6	0.05	3.1495	3.0333	-	-	10.91
7.6	0.05	3.1495	2.4266	-	0.3723	10.91

(a) Tris(hydroxymethyl)amino methane

(b) Diaminoethane tetraacetic acid disodium salt

(c) 1.833 N

Table 5.2

Buffers used in experiments with insulin

pH	Ionic Strength	Barbitone(gm)	Sodium Barbitone(gm)	NaCl(gm)	$Zn(NO_3)_2 \cdot 6H_2O$(gm)	EDTA(gm)
8.0	0.1	1.8466	2.5773	5.1144	-	-
8.0	0.06	1.8466	1.2886	5.1012	0.0148	-
8.0[a]	0.1	1.8466	2.5773	5.1012	-	0.0029

(a) adjusted to pH 8.0 by addition of KOH

Protein stock solutions were routinely prepared by dissolution of about 0.5 gm protein in 10 ml of buffer. The solution was placed in Visking 18/32 dialysis tubing and dialysed at $4^{o}C$ against 500 ml of buffer on a rocking dialyser. The diffusate was replaced with 500 ml of fresh buffer, at 24 hour intervals, four times. The dialysate and the final diffusate were stored in a refrigerator until required. Stock solutions of α-chymotrypsin were frozen to minimise autolysis.

Solutions of protein used in sedimentation equilibrium experiments were prepared by dilution of portions of stock solution with diffusate. The dilutions were performed accurately by weight and the concentrations in interference fringes found from

$$j_{(\text{diluted solution})} = j_{(\text{stock solution})} \cdot \left(\frac{\text{weight of stock solution}}{\text{weight of diluted solution}}\right)$$

It was assumed that the refractive index increment of the protein solutions was a linear function of concentration on a weight/volume scale as is found experimentally for most proteins[62]. The concentrations obtained by weight dilution should therefore be corrected by a factor $\frac{\text{density of diluted solution}}{\text{density of stock solution}}$ but this ratio is so close to unity that it was omitted.

The concentration of the stock solution was determined using a differential refractometer similar to that described by Cecil and Ogston.[107] The inner compartment contained about 1 ml of solution and the outer compartment contained about 1½ ml of solvent in our instrument.

The differential refractometer was calibrated with solutions of sucrose which had previously been dried for 5 days in a vacuum oven at 110°C. The solutions were made up by weight with glass distilled water and all weights converted to weights in vacuo by the formula

$$W_v = W_a(1 + d(1/d_2 - 1/d_1)) \qquad 5(1)$$

where W_v is the weight in vacuo, W_a is the weight in air, d is the density of moist air, d_2 is the density of the material being weighed and d_1 is the density of the balance weights. Wet and dry bulb thermometer readings and the barometric pressure were used in conjunction with tables[108] to obtain the density of moist air. The refractive increments of the sucrose

solutions at a wavelength of 5461 A^{o} were obtained from the data of Gosting and Morris[109] using tabulated density values of sucrose solutions[110]. A mercury vapour lamp was used with a Kodak Wratten 77A filter to supply monochromatic light of wavelength 5461 A^{o}.

The inner and outer compartments of the refractometer cell were filled with distilled water and the deviation of the light beam measured. The inner compartment was then cleaned and dried, filled with one of the sucrose solutions and the deviation measured. Six readings of the deviation were obtained for each solution and averaged. The net deviation was obtained by subtracting the deviation obtained with water in the central compartment from the average value obtained with the sucrose solution in the central compartment. The ratio of the refractive index increment (Δn) to the net deviation (D) measured above was found to be constant to about $\pm$ ½% over the concentration range 0.2% to 3%. The value of the constant $\frac{\Delta n}{D}$ depends on the dimensions of the instrument and was recalculated whenever optical or mechanical adjustments were made to the refractometer. Knowledge of the constant $\frac{\Delta n}{D}$ allowed the refractive index increment of any solution to be obtained from measurement of the deviation it produced in the refractometer.

The refractive index increment of a protein solution was found from the deviation produced with the protein

dialysate in the central compartment of the refractometer and the buffer diffusate in the outer compartment, by application of the relation.

$$\Delta n_{protein} = D_{protein} \cdot \left(\frac{\Delta n}{D}\right)_{sucrose}$$

The concentration of the solution in terms of interference fringes in a 12 mm light path ultracentrifuge cell was then obtained from the expression

$$j = \frac{\Delta n \cdot l}{\lambda}$$

where Δn is the measured refractive index increment, l is the optical path length and λ is the wavelength of the monochromatic light used (5461 A^{o}). Conversion to concentration on weight/volume scale was carried out for α-chymotrypsin using the value $\frac{dn}{dc} = 0.193$ ml/gm[44] and for insulin using the value $j = 37.00 \pm 0.05$ fringes[19] for 1% solution in a 12 mm cell.

II ELECTROPHORESIS

Electrophoresis experiments were carried out in a Beckman Spinco model H electrophoresis-diffusion instrument at 1^{0}C and at a protein concentration of about ½%. Schlieren photographs of the boundaries in the ascending and descending limbs of the instrument were recorded on Kodak Royal Pan sheet film.

III MOLECULAR SIEVE CHROMATOGRAPHY

Chromatography of protein solutions was carried out on a 40 cm x 2.5 cm column of G-25 fine Sephadex. The column was packed in the usual way[111] and tested for uniformity of packing by passing a solution of Blue Dextran 2000 through the column. An Isco[112] model UA recording ultraviolet analyzer operating at a wavelength of 254 mμ was used, in connection with an attached fraction collector, to locate the elution peak of the protein solution. The counter mechanism of the fraction collector was generally set to change tubes after 46 drops which corresponded to about 2 ml of solution.

All elutant buffers were made up with freshly boiled glass distilled water and if not used immediately were degassed before use. The column temperature was regulated at about $4^{\circ}C$ when running α-chymotrypsin solutions in order to minimise autolysis.

IV ULTRACENTRIFUGE EXPERIMENTS

A Beckman Spinco model E ultracentrifuge fitted with a phaseplate as the schlieren diaphragm was used for sedimentation velocity and sedimentation equilibrium experiments. The "Rotor Temperature Indicator and Control" unit on the ultracentrifuge, used in conjunction with the refrigeration system, permitted control of the temperature within $\pm$ 0.1^{o}C during experiments. Each rotor thermistor unit was calibrated with a bomb calorimeter thermometer which had previously been standardized in a thermostat controlled to $\pm$ 0.002^{o}C.

Measurements of the speed were made using a stopwatch and odometer readings. For sedimentation velocity experiments speed measurements were initiated soon after reaching the operational speed and continued until all photographs had been taken. In the case of the much longer sedimentation equilibrium experiments the timing was commenced not less than 30 minutes before taking the Rayleigh interference photographs and continued until the photographs had been satisfactorily developed.

Monochromatic light of 5461 A^{o} wavelength was obtained from a mercury arc lamp using a Kodak Wratten 77A filter. All schlieren and interference photographs were recorded on Kodak scientific plates, type IIG, and developed for 90 seconds in full strength Kodak D8 developer. The plates were

fixed in acid fixer, and washed in a flow of deionized water for 10 minutes before drying.

Correct alignment and focussing of all components in the optical system is essential if accurately measureable Rayleigh interference fringes are to be obtained. The optical system was checked completely before commencing the work described in this thesis. It was again checked prior to experiment UC 51 at the time of fitting an upper chamber lens and limiting aperture mount which could be removed (for lens cleaning) and reproducibly replaced. The latter assembly obviated the need to realign the upper limiting aperture whenever the upper chamber lens was removed. As some of the alignment and focussing methods are modifications of standard methods a complete description of the procedure used is given in Appendix A.

(1) Sedimentation Velocity Experiments

Sedimentation velocity experiments with α-chymotrypsin were carried out at a speed of 59,780 rpm at about 20^{o}C in phosphate buffer pH 6.2 and ionic strength 0.2. The concentrations ranged from 0.1 gm/dl to 0.9 gm/dl and were prepared from two different stock solutions by weight dilution. The concentrations of the stock solutions were determined by differential refractometer measurements. A single sector 12 mm light path cell was used and was filled almost to capacity.

A schlieren photograph was taken immediately after reaching the set speed to establish the meniscus position as a check for possible leakage later in the experiment. After the sedimentation boundary had resolved from the meniscus 10 to 15 schlieren photographs were taken automatically at set time intervals. The position of the maximum ordinate (peak) of the refractive index gradient curve was measured using a Pye two-dimensional comparator.

The photographic plate was aligned on the stage of the comparator so that the meniscus image was parallel to the vertical crosshair of the microscope. Five readings, at different vertical (Y) positions, of the horizontal (X) position of each reference edge were made. The mean value of the two sets of readings gave the positions of the centripetal and centrifugal reference edges which respectively corresponded to positions 5.7 cm and 7.3 cm from the axis of rotation. The average of the two reference positions was taken as corresponding to the point 6.5 cm from the axis of rotation and all subsequent measurements of schlieren peak positions were referred to this position. Five readings of the horizontal position of the schlieren peak were made and the mean calculated. The distance, on the photographic plate, of the schlieren peak from the reference point was converted to true distance by allowing for magnification produced by the optical system.

The distance (x) from the axis of rotation to the peak at various times was calculated[113] and the sedimentation coefficient evaluated from the slope of the straight line fitted, by the method of least squares, to the log x versus time data. This follows from the definition of the sedimentation coefficient as the sedimentation velocity of solute molecules in a unit centrifugal field

$$S = \frac{dx/dt}{\omega^2 x} = \frac{1}{\omega^2} \cdot \frac{d\ln x}{dt} \qquad 5(2a)$$

where ω is the angular velocity and dx/dt is the sedimentation velocity. The sedimentation coefficient was then converted to the standard basis corresponding to a reference solvent having the viscosity and density of water at $20^{\circ}C$ by the following expression

$$S_{20,w} = S \cdot \frac{\eta}{\eta_{20,w}} \cdot \frac{(1 - \bar{v}\rho)_{20,w}}{(1 - \bar{v}\rho)} \qquad 5(2b)$$

where η is the viscosity of the solution at the temperature of the experiment, $\eta_{20,w}$ is the viscosity of water at $20^{\circ}C$, $\bar{v}$ is the partial specific volume (assumed constant irrespective of solvent) and ρ is the density of the solvent.

The sedimentation coefficient is the weight-average sedimentation coefficient of the species present in the plateau

region[70] and is more correctly found from the rate of movement of the point corresponding to the second moment of the concentration gradient curve[14]. The error incurred by using the maximum ordinate of the concentration (refractive index) gradient curve is negligible if the curve is symmetrical[14].

Sedimentation velocity experiments with zinc-free insulin in barbiturate buffer pH 8.0, 0.1 ionic strength were carried out at 20°C and at speeds of 50,740 rpm and 63,650 rpm. The concentration of insulin was about 0.8 gm/dl.

(2) Sedimentation Equilibrium Experiments

Sedimentation equilibrium experiments were generally carried out in 12 mm light path, double sector interference cells. The centrepiece was of aluminium-filled epoxy resin in all except one series of experiments with insulin when a carbon-filled epoxy resin centrepiece was used. Quartz cell windows were used for experiments at speeds less than 30,000 rpm and sapphire windows were used at higher speeds. The cells were completely dismantled and thoroughly cleaned and dried before each experiment. In the series of insulin experiments where Beckman Desicote was used to prevent leaching of metal ions, all glassware, including the cell windows and the cell centre-pieces, was thoroughly coated with a 1:25 solution of Beckman Desicote in chloroform[104]. A few experiments at low initial concentration of protein were performed in a 30 mm light path,

double sector cell with an aluminium-filled expoxy resin centrepiece. Following the suggestion of Richards and Schachman[114], the refractive index of the solvent (diffusate) was increased for all experiments to approximately that of the solution (dialysate) by addition of 1,3-butanediol. This procedure enhances the quality of the interference fringe pattern by using low order fringes. 1,3-butanediol can be used for this purpose as it is miscible with water and, since its density (1.005 gm/ml) is so close to that of dilute buffer solutions, no redistribution of it during centrifugation is detectable.

Cells were filled by means of a micrometer syringe so that the height of the solvent column was greater than that of the solution column by less than 0.5 mm. The assembled cell was tightened and filled according to Table 5.3; the oil used was Beckman Fluorochemical FC 43 and was introduced into the solution sector before the solution.

Table 5.3

Cell Length	12 mm	12 mm	30 mm
Volume of Oil (ml)	0.025	0.025	0.060
Volume of Solution (ml)	0.100	0.033	0.250
Volume of Solvent (ml)	0.130	0.063	0.330
Approx. Height of Column (mm)	2.8	0.8	2.7

The speed selected for the experiment was calculated to give a ratio of between two and four to one for concentration of protein at the bottom of the cell to concentration at the meniscus. The following equation was solved for ω assuming $\frac{c_b}{c_a} = 3$ and approximate values for M, $(1 - \bar{v}\rho)$, b and a

$$\ln \frac{c_b}{c_a} = \frac{M(1 - \bar{v}\rho)}{RT} \omega^2 \cdot \frac{b^2 - a^2}{2} \qquad 5(3)$$

where c_b is the concentration at the cell bottom, c_a is the concentration at the meniscus, M is the molecular weight, $\bar{v}$ is the partial specific volume, ρ is the density, ω is the angular velocity, R is the gas constant, T is the absolute temperature, b is the distance in centimetres of the cell bottom from the axis of rotation and a is the distance of the meniscus from the axis of rotation. The speeds used ranged from 6,000 rpm to 16,000 rpm.

For experiments with 1 mm columns the equations of Van Holde and Baldwin[64] Method III were used to calculate the speed. It is possible to assign a concentration value equal to the initial concentration (within 2%) to the point x', defined by $(x')^2 = \frac{(a^2 + b^2)}{2}$, provided that H 0.1 where

$$H = \frac{M(1 - \bar{v}\rho)}{2RT} \omega^2 \cdot \frac{b^2 - a^2}{2} \qquad 5(4)$$

Equation 5(4) was solved for the angular velocity, ω , with H = 0.1 and approximate values of the other variables, and the nearest machine speed below that calculated, was used.

The duration of the experiment was calculated, using the equations of Van Holde and Baldwin[64], as the time required for the system to approach to within 0.1% of equilibrium. For most experiments the calculated times for 3 mm columns were approximately 20 hours but for convenience most runs were allowed to go for 24 hours. An initial check on the calculations for a predicted 20 hour experiment showed constancy, within experimental error, of the total fringe count across the cell in photographs taken at 20 hours and at 24 hours. Since the column height appears in the equation as the square, the times required for the experiments on 1 mm columns were reduced to $^1/_9$ of those required for 3 mm columns and generally required not more than 3 hours. High speed experiments of the type described by Yphantis[115] were performed using 3 mm columns. Yphantis recommended that the value of the quantity $\frac{\omega^2 M(1 - \bar{v}\rho)}{RT}$ should be about 5. It is important that speeds no lower than those calculated according to Yphantis be used, since too low a speed results in a significant concentration of solute at the meniscus and leads to error in results. The calculated value of the speed was used only as a guide and the shape of the fringe pattern was checked at intervals for a sufficient length of horizontal fringes near

the meniscus and measureable fringes lower in the cell.

As soon as the rotor reached the set speed a photograph of the interference fringe pattern was taken to check straightness of the fringes before any appreciable redistribution. Deviations from straightness might be due to distortion of the windows either by the cell tightening process or by the centrifugal field. When significant deviation from straightness was observed the experiment was followed by a blank run. The cell was emptied and carefully cleaned and dried without dismantling. The cell was filled with water to the same levels as in the main experiment, run to the set speed and the photographs obtained used to correct the equilibrium fringe pattern. A blank run was performed routinely with each high speed experiment. A schlieren photograph at 90° diaphragm angle was also taken after reaching the set speed in order to facilitate the location of the meniscus and the bottom of the column. Erlander and Babcock[116] have shown that the true position of the meniscus is at a position $^{1}/_{3}$ of the width of the meniscus image away from the apparent end of the solution column and similarly for the true position at the solution-oil interface.

V MEASUREMENT OF INTERFERENCE FRINGE PATTERNS

The Rayleigh interference fringe patterns were measured on a two-dimensional microcomparator[117] capable of measuring to 2 microns. The fringe patterns on the photographic plates mounted on the stage were observed at 60-fold magnification on a viewing screen on which cross-lines were etched. Alignment of the photographic plate on the stage of the comparator was accomplished by centring the horizontal cross-line on the central fringes of the patterns generated at each end of the plate by the reference slits in the counterbalance. As in the case of schlieren photographs the arithmetic means of several readings each of the two reference edge positions were averaged to give the reference point corresponding to 6.5 cm from the axis of rotation. All horizontal distances (X) on the photographic plate were referred to this point. The true positions of the meniscus and the bottom of the solution column were determined by prior measurement of a schlieren photograph as described in the previous section.

Measurement of Rayleigh interference fringe patterns may be carried out either by measurement of the vertical positions of the centres of fringes at various X positions (usually equal increments) from the meniscus to the bottom of the column, or by the measurement of the radial positions of

the fringes at equal fringe increments. The latter method is preferred when the data is to be processed on hand calculating machines since this simplifies the trapezoidal integration referred to in the next section. However, since the data for all experiments, other than those with 1 mm columns, were processed by computer[118], the former method was routinely used. In all cases the fringes involved were the interference minima which appeared as the light portions of the pattern.

Analysis of experiments with 1 mm columns was carried out according to Method III of Van Holde and Baldwin[64] which required the slope of the fringes, $\frac{dj}{dx}$, at the point (x') where the concentration was the same as in the original solution. This point defined by $(x')^2 = \frac{(b^2 + a^2)}{2}$ was determined from a schlieren photograph and corresponding position on the photograph (X') calculated from equation 5(6). At X' and at four other points, 0.1 mm and 0.2 mm away on either side of X', the vertical (Y) positions of the three adjacent fringes were each measured twice by locating the cross-lines at the centres of the fringes (See Fig. 5.1(a)). The mean of each set of six Y values was taken as the vertical position of the central fringe. Since the concentration, in fringes, at x' was j_o the j values at the other x positions were calculated from

$$j_i = j_o + \frac{Y_i - Y_o}{w} \qquad 5(5)$$

5.1 : (a) A diagrammatic representation of a Rayleigh interference fringe pattern from a 1 mm solution column at sedimentation equilibrium. The arrow indicates the position

$$x' = \left(\frac{a^2 + b^2}{2}\right)^{1/2}$$

and the dots indicate positions where X and Y readings were made.

(b) A diagrammatic representation of a Rayleigh interference fringe pattern from a 3 mm solution column at sedimentation equilibrium. The dots indicate the positions where X and Y readings were made and the arrow indicates the position where it was necessary to drop down to lower fringes in the measuring procedure.

(c) A diagrammatic representation of a Rayleigh interference fringe pattern , obtained in a high speed sedimentation equilibrium experiment, illustrating the horizontal nature of the fringes near the top of the solution column.

N.B. In all diagrams the centrifugal direction increases from left to right.

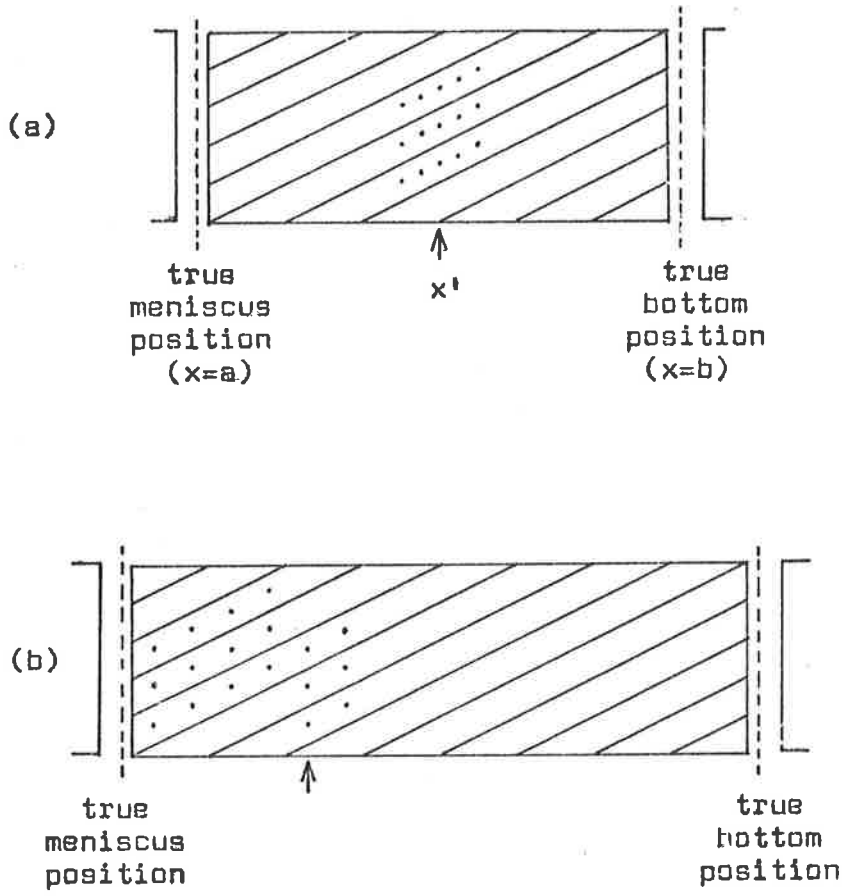
(a)
true
meniscus
position
(x=a)
x'
true
bottom
position
(x=b)
(b)
true
meniscus
position
true
bottom
position
(c)

Fig. 5.1

where w is the fringe width and the Y values are the mean values for the central fringe. The fringe width, 0.282 mm, was an average value of the width of straight reference fringes measured in several photographs and was used in all calculations. The X positions on the photographic plate were converted to true distances (x) from the axis of rotation by

$$x_i = 6.5 + (X_i - X_{6.5}) \cdot F2 \qquad 5(6)$$

where F2 is the magnification due to the optical system. The magnification factor was determined by the normal Spinco procedure using a ruled glass disc in the rotor. The slope of the straight line fitted, by the method of least squares, to the values of j versus x was used to obtain the apparent weight average molecular weight ($M_{w\ app}$) at concentration j_o from

$$M_{w\ app} = \frac{RT}{(1 - \bar{v}\rho)\omega^2} \cdot \frac{1}{x' j_o} \cdot \left(\frac{dj}{dx}\right)_{x=x'} \qquad 5(7)$$

For experiments with 3 mm columns the procedure of measuring the Y values at the centres of three adjacent fringes was again used. However, the method of locating the fringe centres was different. Instead of locating the cross-lines by eye at the fringe centre a measuring device, incorporating a light dependent resistor (LDR) in a wheatstone bridge

circuit, was used. The construction and operation of the measuring device is fully described in Appendix B. The LDR was mounted on the viewing screen of the microcomparator and the circuit was designed to operate a neon light at an adjustable light intensity incident on the LDR. The instrument was designed to make use of the symmetry of the interference fringes about the minima. For a particular fringe the instrument was adjusted so that the neon light operated at a position between the interference minimum and adjacent maxima. This meant that the neon light operated on either side of the interference minimum at positions assumed to be equidistant from the centre of the fringe on the basis of fringe symmetry. Thus at each X position six Y values were obtained and the arithmetic mean taken as the vertical position of the central fringe. Graphical extrapolation of four points at each end of the column was used to determine the vertical positions at the true meniscus and bottom positions which had been determined from a schlieren photograph as described previously. Since it was not possible to follow the three fringes for the whole length of the column it was necessary to drop down one or more fringes as shown in Fig. 5.1 (b). When this was done it was necessary to add the fringe width or multiple of it to the subsequent Y values to equate them with the vertical positions of the original fringes. The same procedure was used for measuring photographs of high speed

experiment fringe patterns except that no extrapolation to the cell bottom was needed (See Fig. 5.1 (c)).

As shown in Chapter 2 the basic equation for evaluation of the apparent weight average molecular weight $M_{w\ app}$ is

$$M^{(x)}_{w\ app} = \frac{2RT}{(1 - \bar{v}\rho)\ \omega^2} \cdot \left(\frac{d\ln j}{d(x^2)}\right)^{(x)} \qquad 5(8)$$

where the symbols are as previously defined and the superscript x denotes that the value of the quantity at distance x from the axis of rotation applies. In order to evaluate $\frac{d\ln j}{d(x^2)}$ at a given x a relation between lnj and x^2 is needed. For an ideal homogeneous solute there exists a linear relationship between lnj and x^2 and the slope of the straight line gives the molecular weight. In the case of non-ideal associating systems the plot of lnj versus x^2 is curved depending both on the extent of deviation from ideal behaviour and on the degree of polymerisation. A plot of lnj versus x^2 which is concave upwards indicates polydispersity whereas a plot which is concave downwards indicates non-ideality[63]. It is also necessary to know the actual value of the concentration at the meniscus before a relationship between lnj and x^2 can be found. Once the concentration distribution is determined by measurement of the fringe pattern the concentration at the meniscus in terms of interference fringes, j_m, can be evaluated from[114]

$$j_m = j_o - \frac{x_b^2(j_b - j_m) - \int_{x_m}^{x_b} x^2\, dj}{x_b^2 - x_m^2} \qquad 5(9)$$

where j_o is the initial concentration in fringes, $(j_b - j_m)$ is the number of fringes from the meniscus to the solution bottom at equilibrium and x_m and x_b are the distances of the solution meniscus and bottom from the axis of rotation. The actual value of the concentration at any x distance is obtained by adding the true value of the meniscus concentration to the concentration evaluated from the fringe pattern where the meniscus concentration is taken as zero.

For low speed sedimentation equilibrium experiments the raw data, comparator X positions each with six associated Y values, were processed in the computer according to the program SEDEQ listed in Appendix C. Included in this data were the extrapolated values of Y for the true meniscus and bottom positions. In order to evaluate $M_{w\ app}$ values of (i) the comparator X position (F 1) corresponding to the 6.5 cm (F 3) reference position, (ii) the optical magnification factor (F 2), (iii) the fringe width (F 4), (iv) the factor $\frac{2RT}{(1 - \bar{v}\rho)\,\omega^2}$ (F 5) and the initial concentration in fringes (j_o) were read in. The six Y values were averaged and converted to j values, taking the meniscus concentration as zero, by the expression

$$j_i = \frac{Y_{i\ av} - Y_{m\ av}}{F4}$$

and corresponding X values converted to x values by equation 5 (6) and squared to give x^2 values. The integral

$$\int_{x_m}^{x_b} x^2\, dj$$

of equation 5 (9) was evaluated by trapezoidal integration and the meniscus concentration calculated. True values of concentration j at the different x positions were calculated as described in the previous paragraph. In order to derive an expression for $\frac{dlnj}{dx}$ it was assumed that the relationship between lnj and x^2 could be described by a series expansion

$$lnj = a + b\bar{x} + c\bar{x}^2 + \ldots\ldots \qquad 5(10)$$

where $\bar{x} = x^2$. A computer library program LSQPOL was used to fit polynomials, up to degree 4, to the data by the method of least squares. Differentiation of the fitted polynomial gave the required value of $\frac{dlnj}{d(x^2)}$ i.e.

$$\frac{dlnj}{d\bar{x}} = b + 2c\bar{x} + \ldots. \qquad 5(11)$$

or

$$\frac{dlnj}{d(x^2)} = b + 2c(x^2) + \ldots. \qquad 5(12)$$

Values of $\frac{d\ln j}{d(x^2)}$ were calculated from equation 5(12) and used in equation 5(8) to evaluate $M_{w\ app}$ at each x position thus giving a set of $M_{w\ app}$ values at different concentrations for each fitted polynomial.

A modified version of program SEDEQ was used to analyze data from high speed sedimentation equilibrium experiments since it was not necessary to know the initial concentration. Both a straight line and a quadratic were fitted to the lnj versus x^2 data. Values of j less than 0.4 fringes were omitted due to the inherent inaccuracy of the lower j values.

Appendix A.

ALIGNMENT OF THE RAYLEIGH INTERFERENCE OPTICAL SYSTEM

A diagrammatic representation of the Rayleigh interference optical system used in the analytical ultracentrifuge is shown in Fig. A.1 . The monochromatic beam of light is split into two by two narrow parallel slits in the lower window holder of a double sector ultracentrifuge cell. One sector of the cell contains solvent and the other solution so that the concentration gradient in the solution sector (manifest as a refractive index gradient) causes an interference pattern, resulting from interference between the two beams, to be warped in a manner determined by the change in concentration with distance from the axis of rotation. The upper limiting aperture containing two parallel slits acts as a light chopper so that interference only occurs when both cell sectors are directly beneath the slits. The upper limiting aperture is positioned so that the slits are symmetrical about a radius from the axis of rotation. This has the advantage over the alternative method of positioning of one slit along the radius, that conjugate levels are compared. A disadvantage of the symmetrical positioning is that the slits are inclined at an angle α to the direction of sedimentation. However, since this angle is approximately 2^{o}, the correction factor $\frac{1}{\cos^{2}\alpha}$

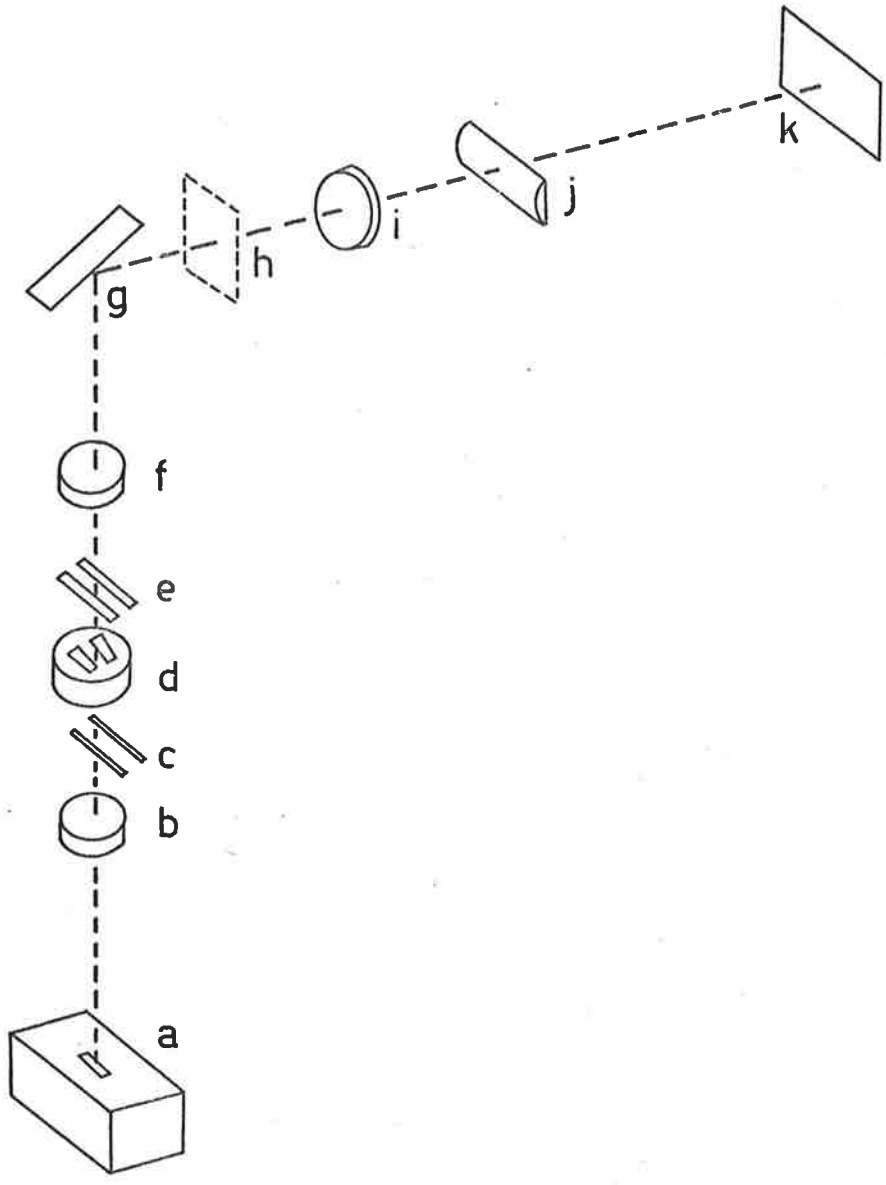

Fig. A.1 A sketch of the Rayleigh optical system employed in the ultracentrifuge: a, light source; b, lower collimating lens; c, Rayleigh mask; d, double sector cell; e, limiting aperture; f, condensing lens; g, mirror; h, focal plane of upper lens; i, camera lens; j, cylinder lens; k, photographic plate. The sketch is not to scale.

is less than experimental error in locating the fringe centres.

The following alignment and focussing procedures were used.

1. Height of the Light Source

The light source was positioned vertically in the focal plane of the lower collimating lens by the double image method. A ¼ inch wide strip of tape was placed across the centre of the lower lens, above which was placed a plane mirror. The light source was adjusted vertically until a single reflected image was obtained. A single reflected image can only be obtained when the light source is in the focal plane of the lens, a double reflected image being obtained when the light source is at other vertical positions.

2. Position of the Light Source on the Optic Axis of the Lenses

Since the Rayleigh interference optics are particularly sensitive to distortions which are greatest near the edges of lenses it is important that the upper limiting aperture should be symmetrical about a diameter of the upper lens as well as about a radius from the centre of rotation.

In order to locate the centre of the upper lens a brass cylinder was made so that the lens holder just fitted over it and the centre of the face of the cylinder was marked. The stop controlling the lateral position of the aperture mask was set so that one slit of the off-set mask was located

centrally about the centre of the brass cylinder inserted in place of the upper lens. Additionally the off-set mask was converted to a centre point mask by placing tape over the slits and leaving open only a section about 1 mm square corresponding to the centre of the cylinder. The upper lens was then replaced in the lens holder with tape wound around it so that it fitted tightly. This procedure assumes that the centre of the lens holder coincides with the centre of the lens. Another mask was made to locate the centre of the lower lens. An aluminium disc was pinned to the lower lens holder so that it could be replaced reproducibly. The lens holder was placed in a lathe and a $^{1}/_{16}$ inch hole drilled through the aluminium disc with a centre drill. The lens was replaced and again tape was used to seat the lens tightly in the holder.

The full-surfaced mirror was removed and a ground glass disc placed on top of the optical tube leading from the chamber. Two diametrical marks, at right angles to each other, were drawn on the ground glass disc which was located with its centre at the centre of the vertical optical tube and with one diameter pointing along the horizontal optical tube. The light source was moved in the plane of the lower lens until the light beam passed through both lens centre-mask holes and could be observed impinging on the ground glass plate. It was noted that the point of impact of the light beam on the ground glass plate corresponded to the centre of the optical tube.

3. Position of the Light Source on the Cell Axis

For the light beam to enter the cell parallel to the plane of the meniscus the beam must be parallel to the axis of rotation. It was assumed by virtue of the cell construction that this condition is satisfied when the light beam is perpendicular to the cell windows. A counter-balance and a cell with an aluminised lower cell window (to act as a mirror) were loaded into an ANJ rotor leaving the other two cell holes vacant and the rotor set spinning at low speed. The interference light source mask was replaced by a point source mask. The point source mask was marked $^{1}/_{8}$ inch either side (front and back with respect to the ultracentrifuge) of the hole and the light source moved so that the reflected image was located first at one scribe mark and then at the other. Marks were pencilled on the ground glass disc, along the diameter perpendicular to the direction of the horizontal optical tube, at the positions where the transmitted light beam impinged when the light source was in the positions described above. The light source was moved so that the transmitted beam impinged on the ground glass plate at a position midway between the pencil marks. The position of the light source was identical to that found in 2. thus confirming that the axis of the lenses coincided with the cell axis.

4. Position of the Full-Surfaced Mirror

The full-surfaced mirror was positioned on the optical track so that the image of the point source fell on the centre of the photographic plate when one of the chamber lens centre-masks was in position. The camera and cylinder lenses were positioned so that the image was not displaced.

5. Position of the Schlieren Diaphragm

The interference light source mask was placed in position and the chamber closed and evacuated. Two reference pencil lines were marked at the ends of the diaphragm image on a ground glass plate in the camera position. The schlieren diaphragm was positioned on the optical track so that rotation of the diaphragm from 90^{0} to 0^{0} produced no tilt of the image with respect to the pencilled reference lines.

6. Position of Camera Lens

A ground glass plate was placed over the lower collimating lens. The rotor containing the ruled disc was rotated in the partially closed chamber until the vertical scale lines appeared sharpest at the viewing screen. The chamber was closed and evacuated and the camera lens position adjusted to give best visual definition of the vertical scale lines.

7. Position of the Cylinder Lens

The vacuum chamber was opened and a ground glass plate placed in front of the full-surfaced mirror. The cylinder lens was positioned to give best focus of the diaphragm.

8. Location of the Upper Aperture Mask

The full-surfaced mirror was removed and replaced by the ground glass disc. The off-set mask, with only the off-centre slit taped over, was placed in position. With the interference light source mask in position, the upper aperture mask holder was rotated so that the image of the slit was parallel to the ground glass disc diameter which was perpendicular to the direction of the horizontal optical track. The full-surfaced mirror was replaced and a rotor with a hair fixed radially across a cell hole was placed in the chamber. The rotor was moved to locate the hair image centrally in the image of the mask slit. The initial adjustment of the mask holder was so sensitive that no final adjustment was necessary since the hair image could be located symmetrically in the centre of the slit image.

9. Rotational Position of the Cylinder Lens

The orientation of the cylinder lens axis perpendicular to the conjugate levels was accomplished by a modification of the optical procedure used by Richards and Schachman[114], which

used the rotating cell as the prime reference. The modified cell consisted of double sector interference cell window holders and a single sector centrepiece, and was filled with 0.5% Bovine Serum Albumin solution. Use of this cell ensured that both light beams passed through a solution of identical concentration gradient. The solution was centrifuged at 59,780 rpm until the boundary was a third of the way down the cell when the speed was reduced to 24,630 rpm in order to obtain good fringes. The tilt of the cylinder lens was adjusted until straight interference fringes were obtained; the final position was judged from photographs. A very small error in orientation causes the interference fringes near the bottom of the cell to be curved.

10. Rotational Position of the Light Source

The vacuum chamber was opened until the interference patterns from the double aperture barely overlapped and the light source slit rotated to give the sharpest fringes.

11. Final Focus of Camera and Cylinder Lenses

A ground glass plate was placed over the lower collimating lens and the rotor containing the ruled disc adjusted as in section 6. The chamber was closed and evacuated. Five photographs were taken moving the camera lens at 1/32 inch intervals about the optimum visual position. A similar set

of photographs were taken moving the cylinder lens. The final positions were judged from the photographs; the camera lens is at the focal position when the vertical scale lines are most distinct and the cylinder lens is in focus when the image of the schlieren diaphragm is most distinct.

Appendix B.

A PHOTOMETRIC ATTACHMENT FOR FACILITATING COMPARATOR MEASUREMENT OF INTERFERENCE FRINGE PHOTOGRAPHS

To obtain information from schlieren and interference photographs for the application of detailed theoretical treatments, much careful measurement is required. This can be both time-consuming and a source of eye-strain for the person making the measurements. It is relatively simple to measure the position of maximum gradient of a schlieren pattern in order to calculate the sedimentation coefficient but much more measurement is required to obtain the square root of the second moment which describes the true boundary position in the case of a skewed boundary[14]. Similarly the measurement of interference fringe patterns, described in Chapter 5 (VI), for sedimentation equilibrium experiments is difficult.

It is therefore advantageous to have a rapid and simple method for measuring the photographic records. Indeed for absorption optics the introduction of the automatic scanner[119] has eliminated the need for photographic records. Methods have been previously reported[120-122] for measurement of schlieren and interference patterns but these involve complex and expensive instrumentation. A detailed description follows of a simple and inexpensive photometric system which was

developed specifically for comparator measurement of interference fringe patterns but which could also be used for rapid, detailed measurement of schlieren photographs.

A light dependent resistor (LDR) is mounted in a holder at the centre of the viewing screen of a two dimensional microcomparator[117]. The circuit, basically a wheatstone bridge circuit (Fig. B.1), causes a neon light to ignite when illumination falling on the LDR is below an adjustable preset value.

The transformer T1 supplies 25 volts AC. After rectification filtering and stabilizing by D1 the voltage is fed to the amplifier which consists of transistors TR1 and TR2 in a differential connection. When the circuit is at balance TR3 is held cut off by D2 and TR4 held cut off due to insufficient voltage through R1. Since TR4 is not carrying current the meter M1 does not indicate and there is insufficient gate voltage across R2 to turn on the silicon controlled rectifier (SCR) and ignite the neon light.

A decrease in the intensity of light falling on the LDR causes its resistance to increase, unbalancing the differential amplifier bridge which results in a greater voltage being fed into TR3. If this new voltage exceeds the D2 voltage by about 0.2v, TR3 will conduct rapidly and turn on TR4, and as TR4 is now conducting there is enough drive voltage present across R2 to turn on the SCR and ignite the neon lamp.

Fig. 8.1 : Photometric plate measurer circuit:

T1	power transformer
LDR	Clairex CL603
SCR	BTY79/400
N	60 V neon light
M1	F.S.D. 50 μA
TR1, TR2, TR3	BC 108
TR4	AC 128
C1	1000 μF, 50 V
C2	1000 μF, 25 V
D1	OAZ 234
D2	OAZ 204
D3, D4, D5, D6, D7	10D2
R1, R7, R9	10 KΩ
R2, R14	330 Ω
R3	470 Ω
R4	12 MΩ
R5	2 MΩ
R6	470 Ω , 1 W
R8	3.3 KΩ
R10	15 KΩ
R11	4.7 KΩ
R12	2.2 KΩ
R13	1.5 KΩ
R15	150 KΩ
R16	4.7 KΩ, 10 W
R17	22 KΩ

All resistors 0.5 W except where stated.

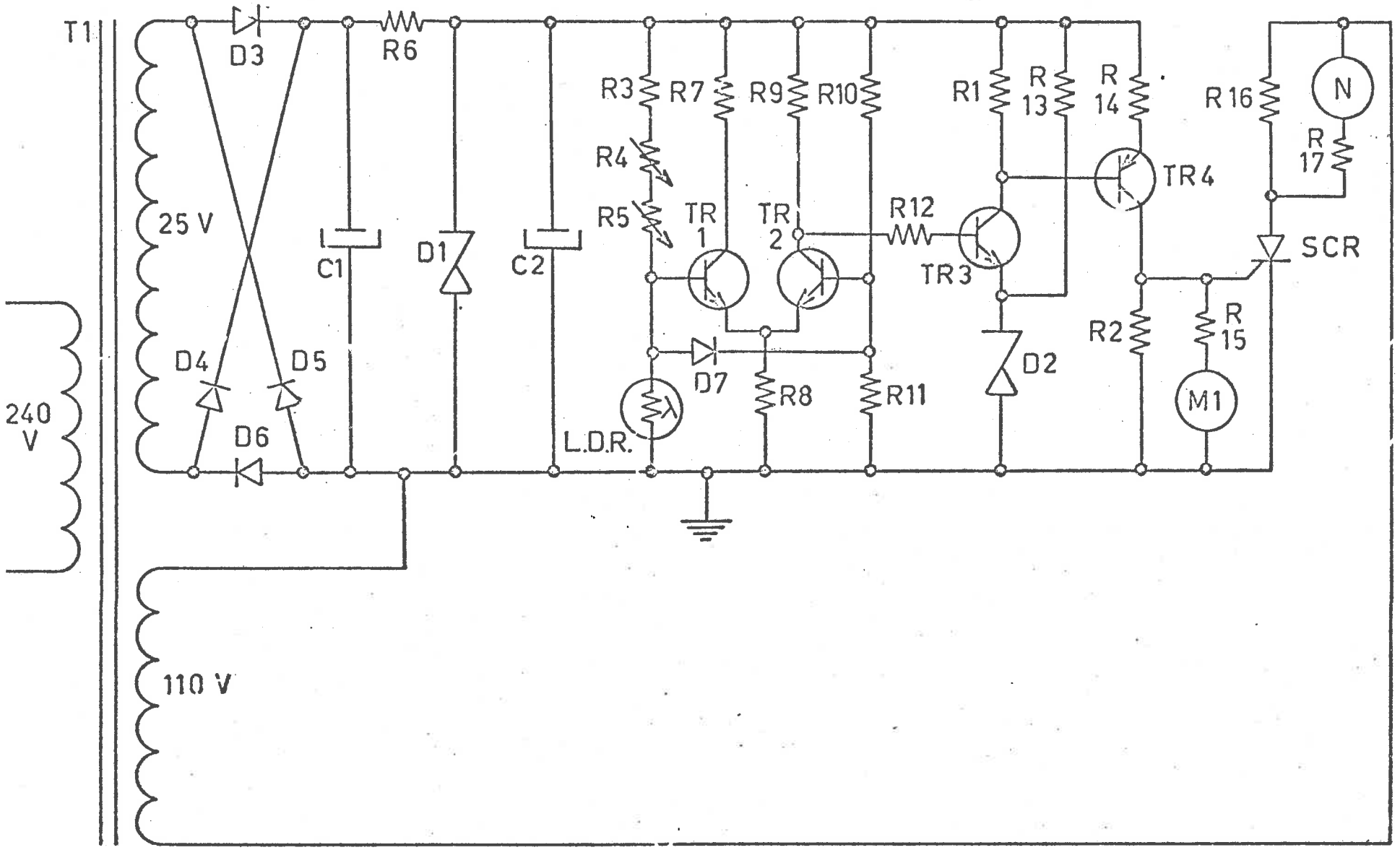

Fig. 8.1 : Photometric plate measurer circuit

Also M1 will indicate drive voltage to the SCR gate.

Two variable resistors R4 (coarse) and R5 (fine) enable the differential amplifier to be balanced over a wide range of light levels.

A constant intensity light source is necessary to obtain meaningful results and accordingly a transistor-stabilized constant voltage power supply was built to power the 6V, 24W projection lamp of the microcomparator.

The LDR (Clairex CL603; Clairex Corporation, New York) is mounted as shown in Figure 8.2 in an opaque polyvinyl-chloride tube and held against the viewing screen by a clear perspex (polymethylmethacrylate) disc. The perspex handle enables any desired orientation of the 1 mm x 4 mm light sensitive strip to be obtained. The ground glass viewing screen is made transparent at the position of the LDR by attaching a small circular microscope cover-slip to the screen with vaseline. This increases the intensity of light falling on the LDR by reducing scattering.

It is necessary to exclude all light from the screen while making measurements, but provided this is done the room may be illuminated without noticeable effect on the measurements.

The following method has been routinely employed to measure Rayleigh interference fringe patterns where it is necessary to locate the interference minima or light portions of the pattern at various horizontal x positions. The method

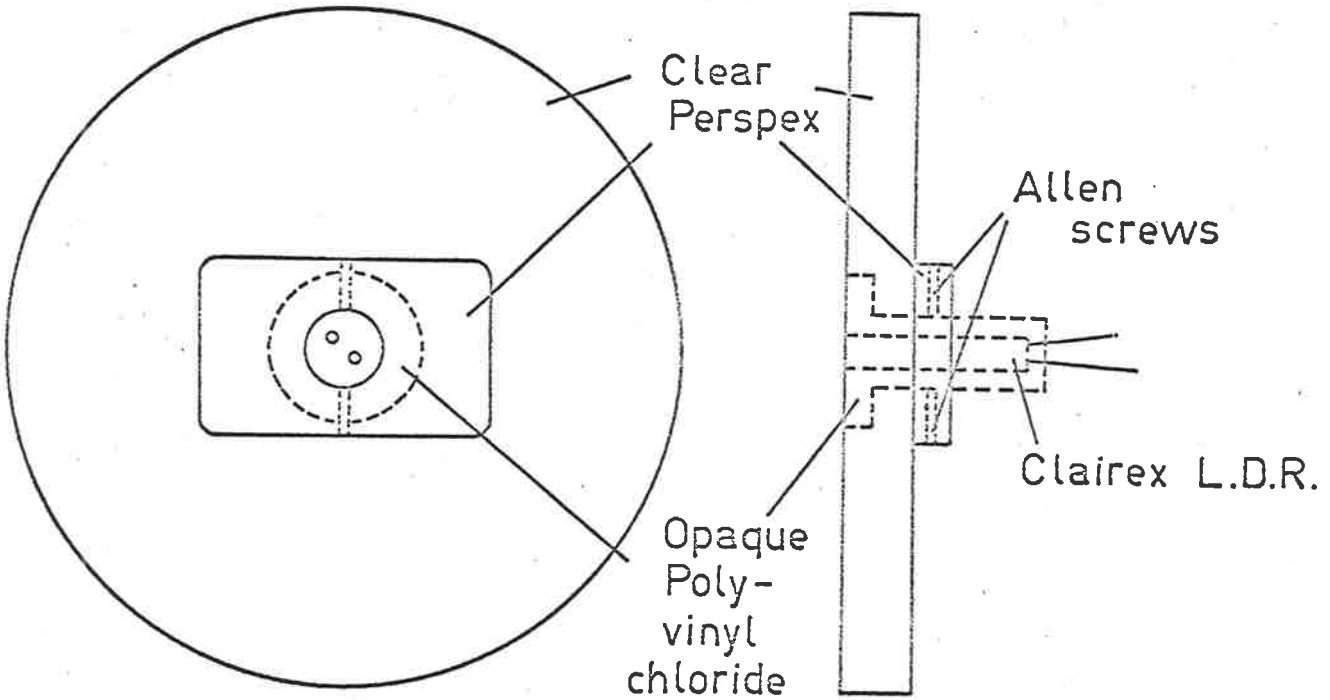

Fig. B.2 : Mounting for LDR.

makes use of the symmetry of interference fringes about the minima (and maxima).

R4 and R5 are adjusted so that the neon light does not ignite while the LDR is near the centre of the light fringe but ignites before it reaches the centres of the black fringes on either side in the y direction. The centre of the light fringe is then taken as the average of the two y values at which the neon light just ignites. For constant R4, R5 and light intensity these values are reproducible to two microns.

The ultimate accuracy depends on the quality of the photograph. Both 60-fold and 25-fold magnifications have been used and it is found that best reproducibility is obtained when the light sensitive strip is aligned parallel to the fringes.

The reference positions - inner edges of the reference fringes produced by the counterbalance - are located in the following way. The LDR is adjusted in the y direction until level with the central reference fringe. The x position of the reference edge image is then found by assuming a linear transition from light to dark at the inner edge of the dark fringe. The setting of R5 at which the neon light ignites at x positions about 30 microns either side of the boundary are noted. R5 is set half way between the two settings noted above and the reference position is taken as that at which the neon light just ignites. Meniscus positions are located on

schlieren photographs in a manner similar to that for locating the centre of the fringe except that in this case the x position is found rather than the y position.

The measuring system described has several advantages. It eliminates eye-strain when many photographs have to be measured and measurements can be made more reapidly than by eye. The measurements are less subjective and reproducibility is better than for measurement by eye. The mean deviation observed for repetitive readings of a particular fringe position, judged by eye, in an interference pattern was found to be 3.6 microns (for 9 positions each measured 20 times) corresponding to 0.013 fringes. This is somewhat worse than 0.009 fringes reported by Ansevin[122]. However, for the same number of measurements of the same fringe positions using the fringe measuring device described here, the mean deviation was found to be 1.6 microns corresponding to 0.006 fringes. This is comparable to the mean deviation of 0.005 fringes reported by Dew[123] with a different type of photometric measuring system, and much more precise than the computer densitometer measuring system of Moore et. al.[120]

The main disadvantages of the plate measuring system are the need for a constant intensity light source and high quality photographs. Even with the transistor-stabilized power supply long-term variations in light intensity can be detected. Whether this is due to variation in power supply or temperature

variation of the tungsten filament is not certain. Care must be taken to keep the surface of the photographic plate clean as dust particles are readily detected.

The system described could also be used to make rapid and accurate measurements of schlieren photographs as in the case of a skewed boundary where the square root of the second moment is required.

Appendix C.

COMPUTER PROGRAMS

I PROGRAM SEDEQ

The computer program SEDEQ was designed to facilitate the determination of apparent weight average molecular weight ($M_{w\ app}$) versus concentration curves. The necessary data is obtained by measurement of Rayleigh interference photographs (See Chapter 5, section V) taken at sedimentation equilibrium. The first data card contains values for the following:-

(i) the number of data points, M

(ii) the comparator X position corresponding to the 6.5 cm reference position, F1

(iii) the optical magnification factor, F2

(iv) F3 = 6.5 cm

(v) the fringe width, F4 = 0.0282 cm

(vi) $F5 = \dfrac{2RT}{(1 - \bar{v}\rho)\omega^2}$

(vii) the initial fringe concentration, cc .

The subsequent M data cards each hold a comparator X value (CX(J)) and 6 comparator Y values (CY1,CY2....CY6). A trapezoidal integration method is used to calculate the meniscus concentration CJ(1), according to equation 5(9). Least squares polynomials of order 1 to 4 are fitted to the

lnj (Y(J)) versus x^2 (XSQ(J)) data by calling the computer library program LSQPOL. Each polynomial is analytically differentiated to obtain $\frac{d\ \ln j}{d\ x^2}$ values which are used in accordance with equation 5(8) to obtain an $M_{w\ app}$ value at each concentration.

```
      PROGRAM SEDEQ(INPUT,OUTPUT)
      DIMENSION XSQ(100),Y(100),CX(100),AVCY(100),FRED(100),DXSQ(100),DF
     CRED(100),AREA(100),CJ(100),W(100)
      COMMON A,C(21),D(200),TITLE(8)
   99 READ 19,(TITLE(J),J=1,8)
   19 FORMAT(8A10)
      IF (TITLE(1).EQ.10H           )STOP
      READ 20,M,F1,F2,F3,F4,F5,CC
   20 FORMAT(I3,F7.3,F7.4,F4.1,F6.3,E11.4,F6.2)
      PRINT 22
   22 FORMAT(/////12X1HJ7X3HXSQ12X4HAVCY11X4HFRED11X4HDXSQ11X5HDFRED11X4
     CHAREA/)
      AREA(0)=0.0
      DO 23 J=1,M
      READ 21,CX(J),CY1,CY2,CY3,CY4,CY5,CY6
   21 FORMAT(7F7.3)
      XSQ(J)=((CX(J)-F1)*F2+F3)**2
      AVCY(J)=(CY1+CY2+CY3+CY4+CY5+CY6)/6.0
   23 FRED(J)=(AVCY(1)-AVCY(J))/F4
      DO 25 J=1,M
      DXSQ(J)=(XSQ(J+1)+XSQ(J))/2.0
      DFRED(J)=FRED(J+1)-FRED(J)
      AREA(J)=AREA(J-1)+DXSQ(J)*DFRED(J)
   25 PRINT 24,J,XSQ(J),AVCY(J),FRED(J),DXSQ(J),DFRED(J),AREA(J)
   24 FORMAT(10XI3,E15.5,5E15.4)
      A=XSQ(M)*FRED(M)-AREA(M-1)
      B=XSQ(M)-XSQ(1)
      CJ(1)=CC-A/B
      Y(1)=ALOG(CJ(1))
      DO 36 J=2,M
      CJ(J)=CJ(J-1)+DFRED(J-1)
      Y(J)=ALOG(CJ(J))
   36 W(J)=1.0
      DO 30 NORDER=1,4
      CALL LSQPOL(M,XSQ,Y,W,0,31,4,1,NORDER,0)
      PRINT 26
   26 FORMAT(/////12X1HJ7X3HXSQ14X1HY12X5HYCALC14X6HMOL WT12X4HCONC/)
      DO 29 I=1,M
      SZ=0.0
      NUT=NORDER+1
      DO 28 J=1,NUT
      Z=(J-1)*C(J)*XSQ(I)**(J-2)
   28 SZ=SZ+Z
      SMW=SZ*F5
   29 PRINT 27,I,XSQ(I),Y(I),D(I),SMW,CJ(I)
   27 FORMAT(10XI3,4E15.4,E15.3)
   30 CONTINUE
      GO TO 99
      END
```

```
      PROGRAM EXPO(INPUT,OUTPUT)
      DIMENSION XSQ(50),CX(50),AVCY(50),FRED(50),DXSQ(50),DFRED(50),AREA
     1(50),P(40,10),Q(40,10),NDEL(10),LIST(10,10),LID(10),A(10,10),B(40,
     21),A2(10,1),C(10,1),TITLE(8),R(10,1),D(40,1),IEN(2),A3(10,10)
   99 READ 29,(TITLE(J),J=1,8)
   29 FORMAT(8A10)
      IF (TITLE(1).EQ.10H          )STOP
      PRINT 28,TITLE
   28 FORMAT(1H1,9X,8A10)
      READ 20,M,F1,F2,F3,F4,F5,CC,AH
   20 FORMAT(I3,F7.3,F7.4,F4.1,F6.3,E11.4,F6.2,E13.6)
      N=7
      NCOMB=9
      DO 23 J=1,M
      READ 21,CX(J),CY1,CY2,CY3,CY4,CY5,CY6
   21 FORMAT(7F7.3)
      XSQ(J)=((CX(J)-F1)*F2+F3)**2
      AVCY(J)=(CY1+CY2+CY3+CY4+CY5+CY6)/6.0
   23 FRED(J)=(AVCY(1)-AVCY(J))/F4
      MM=M-1
      DO 25 J=1,MM
      DXSQ(J)=(XSQ(J+1)+XSQ(J))/2.0
   25 DFRED(J)=FRED(J+1)-FRED(J)
      AREA(1)=DXSQ(1)*DFRED(1)
      DO 26 J=2,M
   26 AREA(J)=AREA(J-1)+DXSQ(J)*DFRED(J)
      AA=XSQ(M)*FRED(M)-AREA(M-1)
      BB=XSQ(M)-XSQ(1)
      B(1,1)=CC-AA/BB
      B(1,1)=B(1,1)/2.5
      DXSQ(1)=0.0
      DO 36 J=2,M
      K=J-1
      B(J,1)=B(K,1)+DFRED(K)
      B(J,1)=B(J,1)/2.5
   36 DXSQ(J)=XSQ(J)-XSQ(1)
      PRINT 35,(B(J,1),J=1,M)
   35 FORMAT(* CONCENTRATION VECTOR B IS,*/(10X,E10.3))
      DO 37 J=1,M
   37 P(J,1)=EXP(AH*DXSQ(J))
      NN=N-1
      DO 38 I=1,NN
      DO 38 J=1,M
      K=I+1
   38 P(J,K)=EXP(2*I*AH*DXSQ(J))
      DO 60 I=1,N
      DO 60 J=1,M
   60 Q(J,I)=P(J,I)
      DO 98 ILOOP=1,NCOMB
      GO TO (1,2,3,4,5,6,7,8,9),ILOOP
    1 DO 11 I=1,M
   11 P(I,5)=Q(I,7)
      N=5
      PRINT 41
   41 FORMAT(///10X22HCOMBINATION 1,2,4,6,12/)
      GO TO 62
    2 N=4
```

```
      PRINT 42
   42 FORMAT(///10X19HCOMBINATION 1,2,4,6/)
      GO TO 62
    3 DO 13 I=1,M
      P(I,3)=Q(I,4)
   13 P(I,4)=Q(I,7)
      N=4
      PRINT 43
   43 FORMAT(///10X20HCOMBINATION 1,2,6,12/)
      GO TO 62
    4 DO 14 I=1,M
   14 P(I,3)=Q(I,4)
      N=3
      PRINT 44
   44 FORMAT(///10X17HCOMBINATION 1,2,6/)
      GO TO 62
    5 K=J+1
      NN=N-1
      DO 15 I=1,M
      DO 15 J=1,NN
   15 P(I,J)=Q(I,K)
      N=6
      PRINT 45
   45 FORMAT(///10X25HCOMBINATION 2,4,6,8,10,12/)
      GO TO 62
    6 DO 16 I=1,M
      P(I,1)=Q(I,2)
      P(I,2)=Q(I,3)
      P(I,3)=Q(I,4)
   16 P(I,4)=Q(I,7)
      N=4
      PRINT 46
   46 FORMAT(///10X20HCOMBINATION 2,4,6,12/)
      GO TO 62
    7 DO 17 I=1,M
      P(I,1)=Q(I,2)
      P(I,2)=Q(I,3)
   17 P(I,3)=Q(I,4)
      N=3
      PRINT 47
   47 FORMAT(///10X17HCOMBINATION 2,4,6/)
      GO TO 62
    8 DO 18 I=1,M
      P(I,1)=Q(I,2)
      P(I,2)=Q(I,4)
   18 P(I,3)=Q(I,7)
      N=3
      PRINT 48
   48 FORMAT(///10X18HCOMBINATION 2,6,12/)
   10 GO TO 62
    9 DO 19 I=1,M
      P(I,1)=Q(I,2)
   19 P(I,2)=Q(I,4)
      N=2
      PRINT 49
   49 FORMAT(///10X15HCOMBINATION 2,6/)
   62 CONTINUE
      NUT=N+1
```

```
      ENCODE(20,64,IEN)N
   64 FORMAT(4H(10X,I1,6HE12.4))
      PRINT IEN,((P(I,J),J=1,N),I=1,M)
      CALL MATRIX(23,M,N,N,P,40,P,40,A,10)
      PRINT 72
   72 FORMAT(///10X20HP TRANSPOSE P MATRIX/)
      ENCODE(20,70,IEN)N
   70 FORMAT(4H(10X,I1,6HE14.6))
      PRINT IEN,((A(J,I),I=1,N),J=1,N)
      CALL MATRIX(23,M,N,1,P,40,B,40,A2,10)
      PRINT 71,(A2(J,1),J=1,N)
   71 FORMAT(* P TRANSPOSE B VECTOR A2 IS,*/(10X,E11.4))
      NUT=N+1
      DO 80 J=1,N
   80 A(J,NUT)=A2(J,1)
      ENCODE(20,81,IEN)NUT
   81 FORMAT(4H(10X,I1,6HE14.6))
      PRINT IEN,((A(J,I),I=1,NUT),J=1,N)
      NCOL=N+1
      CALL MATRIX(10,N,NCOL,0,A,10,DET)
      PRINT 90,DET,(A(J,NUT),J=1,N)
   90 FORMAT(* DETERMINANT OF NXN SECTION OF A IS*E11.4/*0SOLUTION C IS*
     1,/(10X,F10.4))
      DO 91 J=1,N
   91 C(J,1)=A(J,NUT)
      CALL MATRIX(20,M,N,1,P,40,C,10,R,10)
      CALL MATRIX(22,M,1,0,R,40,B,40,D,40)
      PRINT 92,(D(J,1),J=1,M)
   92 FORMAT(* SOLUTION DIFFERENCE IS,*/(10X,E10.2))
   98 CONTINUE
      GO TO 99
      END
```

II PROGRAM EXPO

The computer program EXPO was designed to solve, for each sedimentation equilibrium experiment, a set of over-determined linear equations of the type shown in equation 4(3). The data required is the same as from program SEDEQ except for the additional value $AH = \frac{6000\ (1 - \bar{v}\rho)\ \omega^2}{2RT}$ assuming that the monomer molecular weight is 6,000 (See Chapter 4, section III). The concentration vector B(I, 1), and the matrix (P(I, J)) of the $e^{iH(x^2 - x_m^2)}$ values for a particular self-association model are set up. The computer library program MATRIX is then called to solve the set of over-determined linear equations for the meniscus concentrations of each of the species assumed present in the particular self-association model. A number of possible self-association models is tested.

REFERENCES

1. R. Hamlin, R.C. Lord and A. Rich, Science, 148, 1734 (1965)
2. P.J. Debye, J. Phys. Colloid Chem., 51, 18 (1947); 53, 1 (1949)
3. M.E. Lamm and D.M. Neville Jr., J. Phys. Chem., 69, 3872 (1965)
4. P.O.P. Ts'o, I.S. Melvin and A.C. Olson, J. Am. Chem. Soc., 85, 1289 (1963)
5. L.W. Nichol, Aust. J. Sci., 27, 342 (1965)
6. D.C. Shaw, Aust. J. Sci., 28, 11 (1965)
7. J.M. Creeth and L.W. Nichol, Biochem. J., 77, 230 (1960)
8. C. Frieden, The Enzymes, Volume 7, Edited by P.D. Boyer, H. Lardy and K. Myrback, N.Y., Academic Press (1963)
9. M.S. Doscher and F.M. Richards, J. Biol. Chem., 238, 2399 (1963)
10. J. Monod, J.-P. Changeux and F. Jacob, J. Mol. Biol., 6, 306 (1963)
11. J. Monod, J. Wyman and J.-P. Changeux, J. Mol. Biol., 12, 88 (1965)
12. W. Kauzmann, Advan. Protein Chem., 14, 33 (1959)
13. M.S.N. Rao and G. Kegeles, J. Am. Chem. Soc., 80, 5724 (1958)
14. R.J. Goldberg, J. Phys. Chem., 57, 194 (1953)
15. G.A. Gilbert, Disc. Faraday Soc., 20, 68 (1955)
16. G.A. Gilbert and R.C.Ll. Jenkins, Nature, 177, 853 (1956)
17. R.F. Steiner, Arch. Biochem. Biophys., 39, 333 (1952)
18. R.F. Steiner, Arch. Biochem. Biophys., 44, 120 (1953)
19. P.D. Jeffrey, Ph.D. Thesis, University of Adelaide (1964)
20. E.T. Adams Jr., Ph.D. Thesis, University of Wisconsin(1962)
21. E.T. Adams Jr. and H. Fujita, Ultracentrifugal Analysis in Theory and Experiment, p.119, Edited by J.W. Williams, N.Y., Academic Press (1963)
22. E.T. Adams Jr. and J.W. Williams, J. Am. Chem. Soc., 86, 3454 (1964)
23. E.T. Adams Jr., Biochemistry 4, 1646 (1965)

24. E.T. Adams Jr. and D.L. Filmer, Biochemistry, 5, 2971 (1966)

25. E.T. Adams Jr., Biochemistry, 6, 1864 (1967)

26. E.T. Adams Jr. and M.S. Lewis, Biochemistry, 7, 1044 (1968)

27. E.T. Adams Jr., Fractions, No. 3 (1967)

28. P. Desnuelle and M. Rovery, Advan. Protein Chem., 16, 139 (1961)

29. D. Van Hoang, M. Rovery, A. Guidoni and P. Desnuelle, Biochim. Biophys. Acta, 69, 186 (1963)

30. F. Sanger, Proc. Chem. Soc., 1963, 77 (1963)

31. J.R. Knowles, J. Theoret. Biol., 9, 213 (1965)

32. C. Niemann, Science, 143, 1287 (1964)

33. F.J. Kezdy and M.L. Bender, Biochemistry, 4, 104 (1965)

34. T. Inagami and J.M. Sturtevant, Biochemistry, 4, 1340 (1965)

35. P.S. Sarfare, G. Kegeles and S.J. Kwon-Rhee, Biochemistry, 5, 1389 (1966)

36. K. Morimoto and G. Kegeles, Biochemistry, 6, 3007 (1967)

37. G.W. Schwert, J. Biol. Chem., 179, 655 (1949)

38. G.W. Schwert and S. Kaufman, J. Biol. Chem., 190, 807 (1951)

39. E.L. Smith, D.M. Brown and M. Laskowski, J. Biol. Chem., 191, 639 (1951)

40. E.L. Smith and D.M. Brown, J. Biol. Chem., 195, 525 (1952)

41. J.A. Gladner and H. Neurath, J. Biol. Chem., 206, 911 (1954)

42. W.J. Dreyer, R.D. Wade and H. Neurath, Arch. Biochem. Biophys., 59, 145 (1955)

43. V. Massey, W.F. Harrington and B.S. Hartley, Disc. Faraday Soc., 20, 24 (1955)

44. I. Tinoco Jr., Arch. Biochem. Biophys., 68, 362 (1957)

45. M.S.N. Rao and G. Kegeles, J. Am. Chem. Soc., 80, 5724 (1958)

46. R.F. Steiner, Arch. Biochem. Biophys., 53, 457 (1954)

47. R. Egan, H.O. Michel and R. Schlueter, Federation Proc., 14, 206 (1955)

48. E. Fredericq, Arch. Biochem. Biophys., 65, 218 (1956)

49. P.D. Jeffrey and J.H. Coates, Biochemistry, 5, 489, 3820 (1966)

50. F. Sanger, E.O.P. Thompson and R. Kitai, Biochem. J., 59, 509 (1955)

51. F. Tietze and H. Neurath, J. Am. Chem. Soc., 75, 1758 (1953)

52. K. Marcker, Acta Chem. Scand., 14, 194 (1960)

53. E. Fredericq and H. Neurath, J. Am. Chem. Soc., 72, 2684 (1950)

54. H.L. Crespi, R.A. Uphaus and J.J. Katz, J. Phys. Chem., 60, 1190 (1956)

55. D.W. Kupke and K. Linderstrøm-Lang, Biochim. Biophys. Acta, 13, 153 (1954)

56. J.L. Oncley, E. Ellenbogen, D. Gitlin and F.R.N. Gurd, J. Phys. Chem., 56, 85 (1952)

57. P. Doty and G.E. Myers, Disc. Faraday Soc., 13, 51 (1953)

58. L.W. Cunningham, R.L. Fischer and C.S. Vestling, J. Am. Chem. Soc., 77, 5703 (1955)

59. E. Fredericq, Arch. Biochem. Biophys., 65, 218 (1956)

60. K. Kakiuchi, J. Phys. Chem., 69, 1829 (1965)

61. M.J. Adams, T.L. Blundell, E.J. and G.G. Dodson, M. Vijayan, E.N. Baker, M.M. Harding, D.C. Hodgkin, B. Rimmer, S. Sheat, Nature, 224, 491 (1969)

62. E.F. Cassassa and H. Eisenberg, J. Phys. Chem., 65, 427 (1961)

63. H.K. Schachman, Ultracentrifugation in Biochemistry, p. 201, N.Y., Academic Press (1959)

64. K.E. Van Holde and R.L. Baldwin, J. Phys. Chem., 62, 734 (1958)

65. A. Tiselius, Z. Phys. Chem., 124, 449 (1926)

66. D.A. Albright and J.W. Williams, Biochemistry, 7, 67, (1968)

67. M. Derechin, Biochemistry, 7, 3253 (1968); 8, 921 (1969); 8, 927 (1969)

68. D.E. Roark and D.A. Yphantis, Ann. N.Y. Acad. Sci., 164, 245 (1969)

69. P.W. Chun and S.J. Kim, Biochemistry, 9, 1957 (1970)

70. H.K. Schachman, Ultracentrifugation in Biochemistry, p. 90, N.Y., Academic Press (1959)

71. G.A. Gilbert, Proc. Roy. Soc., A250, 377 (1959)

72. D.J. Cox, Arch, Biochem. Biophys., 129, 106 (1969)

73. A.E. Anderson and R.A. Albety, J. Phys. Chem., 52, 1345 (1948)

74. B. Jirgensons, Die Makromol. Chem., 91. 74 (1966)

75. M.Z. Atassi and S.K. Gandhi, Die Naturwissenschaften, 10, 259 (1965)

76. H.B. Halsall, Nature, 215, 880 (1967)

77. L. Mandelkern and P.J. Flory, J. Chem. Phys., 20, 212 (1952)

78. L. Mandelkern, W.R. Krigbaum, H.A. Scheraga and P.J. Flory, J. Chem. Phys., 20, 1392 (1952)

79. H.R. Mahler and E.H. Cordes, Biological Chemistry, p. 75, N.Y. and London, Harper and Row

80. P.G. Squire and C.H. Li, J. Am. Chem. Soc., 85, 3521 (1961)

81. A.J. Sophianopoulos, C.K. Rhodes, D.N. Holcomb and K.E. Van Holde, J. Biol. Chem., 237, 1107 (1962)

82. J.W. Williams, K.E. Van Holde, R.L. Baldwin and H. Fujita, Chem. Rev., 58, 715 (1958)

83. M.R. Bruzzesi, E. Chiancone and E. Antonini, Biochemistry, 4, 1796 (1965)

84. G.E. Perlman and L.G. Longsworth, J. Am. Chem. Soc., 70, 2719 (1948)

85. H.S. Harned and B.B. Owen, The Physical Chemistry of Electrolytic Solutions, p.361, N.Y., Reinhold Pub. Co. (1964)

86. D.J. Winzor and H.A. Scheraga, Biochemistry, 2, 1263 (1963)

87. R. Egan, H.O. Michel and R. Schlueter, Arch. Biochem. Biophys., 66, 354, 366 (1957)

88. B.H.J. Hofstee, J. Biol. Chem., 238, 3235 (1963)

89. C.H. Chervenka, J. Biol. Chem., 237, 2105 (1962)

90. C.J. Martin and A.R. Frazier, J. Biol. Chem., 238, 3268 (1963)

91. C.W. Wu and M. Laskowski, Biochim. Biophys. Acta, 19, 110 (1956)

92. B.F. Erlanger and F. Edel, Biochemistry, 3, 346 (1964)

93. B.F. Erlanger, A.G. Cooper and A.J. Bendich, Biochemistry, 3, 1880 (1964)

94. H. Weiner, W.N. White, D.G. Hoare and D.E. Koshland, Jr., J. Am. Chem. Soc., 88, 3851 (1966)

95. D.C. Teller, T.A. Horbett, E.G. Richards and H.K. Schachman, Ann. N.Y. Acad. Sci., 164, 66 (1969)

96. M.E. Magar, J. Theoret. Biol., 27, 127 (1970)

97. G. Kegeles, L. Rhodes and J.L. Bethune, Proc. Nat. Acad. Sci., 58, 45 (1967)

98. L.F. TenEyck and W. Kauzmann, Proc. Nat. Acad. Sci., 58, 888 (1967)

99. R. Josephs and W.F. Harrington, Proc. Nat. Acad. Sci., 58, 1587 (1967)

100. A. Polson, Biochem. J., 104, 410 (1967)

101. F.E. LaBar, Proc. Nat. Acad. Sci., 54, 31 (1965)

102. T. Svedberg and K.O. Pederson, The Ultracentrifuge, Clarendon Press Inc., Oxford (1940)

103. J. Schlichtkrull, Acta Chem. Scand., 10, 1455 (1956)

104. D.B. Millar, V. Frattali and G.E. Willick, Biochemistry, 8, 2416 (1969)

105. R.F. Steiner, J. Theoret. Biol., 28, 155 (1970)

106. J.E. Snoke and H. Neurath, J. Biol. Chem., 182, 577 (1950)

107. R. Cecil and A.G. Ogston, J. Sci. Instr., 28, 253 (1951)

108. Handbook of Chemistry and Physics, Chemical Rubber Publishing Company, Cleveland Ohio (1959)

109. L.J. Gosting and M.S. Morris, J. Am. Chem. Soc., 71, 1998 (1949)

110. International Critical Tables, II, 343, McGraw-Hill N.Y. (1927)

111. Sephadex in Gel Filtration, Pharmacia, Uppsala Sweden

112. Instrumentation Specialties Co. Inc., Lincoln Nebraska

113. Model E Ultracentrifuge Instruction Manual, Beckman Instruments Inc., Spinco Division, California

114. E.G. Richards and H.K. Schachman, J. Phys. Chem., 63, 1578 (1959)

115. D.A. Yphantis, Biochemistry, 3, 297 (1964)

116. S.R. Erlander and G.E. Babcock, Biochim. Biophys. Acta., 50, 205 (1961)

117. Optical Measuring Tools Ltd., Maidenhead Berkshire

118. Model 6400, Control Data Corporation, Minneapolis Minnesota

119. J.B.T. Aten and A.J. Schouten, J. Sci. Instr., 38, 325 (1961)

120. R. Moore, R.S. Ledley, M. Belson and J.D. Jacobsen, Science, 152, 1509 (1966)

121. J.J. Bartulovich and W.H. Ward, Anal. Biochem., 11, 42 (1965)

122. A.T. Ansevin, Anal. Biochem., 19, 498 (1967)

123. G.D. Dew, J. Sci. Instr., 41, 160 (1964)

124. R.H. Haschemeyer and W.F. Bowers, Biochemistry, 9, 435 (1970)

125. B. Noble, Applied Linear Algebra, Prentiss-Hall (1969)

126. E.T. Adams, Proc. Nat. Acad. Sci., 51, 509 (1964)

127. J. Roth, P. Gorden and I. Pastan, Proc. Nat. Acad. Sci., 61, 138 (1968)

128. B.H. Frank and A.J. Veros, Biochem. Biophys. Res. Com., 32, 155 (1968)

129. K.E. Van Holde and G.P. Rossetti, Biochemistry, 6, 2189 (1967)

130. K.E. Van Holde, G.P. Rossetti and R.D. Dyson, Ann. N.Y. Acad. Sci., 164, 279 (1969)

131. K.E. Van Holde and G.P. Rossetti, Biochem. Biophys. Res. Comm., 26, 717 (1967)

132. J.C. Nichol, J. Biol. Chem., 243, 4065 (1968)

133. D.K. Hancock and J.W. Williams, Biochemistry, 8, 2598 (1969)

Addenda

1. The two species plot was first suggested by Sophianopoulos and Van Holde [J. Biol. Chem., 239, 2516 (1964)], not by Roark and Yphantis as stated on page 20, paragraph 2, line 4.

2. The theory developed in Chapter 2 is strictly applicable to two-component systems. However it has been shown, by the workers listed below, that the sedimentation equilibrium equations in a multi-component system could be reduced to equations formally the same as those for two component systems:

A. Vrij, Ph.D. dissertation, Utrecht (1959)

A. Vrij and J.Th.G. Overbeek, J. Colloid Interface Sci., 17, 570 (1962)

E.F. Cassassa and H. Eisenberg, Advan. Protein Chem., 19, 287 (1964).